National Library of Canada
Acquisitions and Bibliographic Services Branch
395 Wellington Street
Ottawa, Ontario
K1A 0N4

Bibliothèque nationale du Canada
Direction des acquisitions et des services bibliographiques
395, rue Wellington
Ottawa (Ontario)
K1A 0N4

Your file Votre référence
Our file Notre référence

NOTICE

The quality of this microform is heavily dependent upon the quality of the original thesis submitted for microfilming. Every effort has been made to ensure the highest quality of reproduction possible.

If pages are missing, contact the university which granted the degree.

Some pages may have indistinct print especially if the original pages were typed with a poor typewriter ribbon or if the university sent us an inferior photocopy.

Reproduction in full or in part of this microform is governed by the Canadian Copyright Act, R.S.C. 1970, c. C-30, and subsequent amendments.

AVIS

La qualité de cette microforme dépend grandement de la qualité de la thèse soumise au microfilmage. Nous avons tout fait pour assurer une qualité supérieure de reproduction.

S'il manque des pages, veuillez communiquer avec l'université qui a conféré le grade.

La qualité d'impression de certaines pages peut laisser à désirer, surtout si les pages originales ont été dactylographiées à l'aide d'un ruban usé ou si l'université nous a fait parvenir une photocopie de qualité inférieure.

La reproduction, même partielle, de cette microforme est soumise à la Loi canadienne sur le droit d'auteur, SRC 1970, c. C-30, et ses amendements subséquents.

Canada

University of Alberta

Characterization of the Electrophysiological Response to Serotonin in an Identified Neuron from *Helisoma tivolvis*

BY

Christopher J. Price ©

A thesis submitted to the Faculty of Graduate Studies and Research in partial fulfillment of the requirements for the degree of Doctor of Philosophy.

Department of Zoology

Edmonton, Alberta
Spring, 1994

National Library of Canada
Acquisitions and Bibliographic Services Branch
395 Wellington Street
Ottawa, Ontario
K1A 0N4

Bibliothèque nationale du Canada
Direction des acquisitions et des services bibliographiques
395, rue Wellington
Ottawa (Ontario)
K1A 0N4

The author has granted an irrevocable non-exclusive licence allowing the National Library of Canada to reproduce, loan, distribute or sell copies of his/her thesis by any means and in any form or format, making this thesis available to interested persons.

L'auteur a accordé une licence irrévocable et non exclusive permettant à la Bibliothèque nationale du Canada de reproduire, prêter, distribuer ou vendre des copies de sa thèse de quelque manière et sous quelque forme que ce soit pour mettre des exemplaires de cette thèse à la disposition des personnes intéressées.

The author retains ownership of the copyright in his/her thesis. Neither the thesis nor substantial extracts from it may be printed or otherwise reproduced without his/her permission.

L'auteur conserve la propriété du droit d'auteur qui protège sa thèse. Ni la thèse ni des extraits substantiels de celle-ci ne doivent être imprimés ou autrement reproduits sans son autorisation.

ISBN 0-612-11332-9

Canada

UNIVERSITY OF ALBERTA

RELEASE FORM

NAME OF AUTHOR: Christopher J. Price

TITLE OF THESIS: Characterization of the Electrophysiological Response to Serotonin in an Identified Neuron from *Helisoma trivolvis*

DEGREE: Doctor of Philosophy

YEAR THIS DEGREE GRANTED: 1994

Permission is hereby granted to the University of Alberta Library to reproduce single copies of this thesis and to lend or sell such copies for private, scholarly or scientific research purposes only.

The author reserves all other publication and other rights in association with the copyright in the thesis, and except as hereinbefore provided neither the thesis nor any substantial portion thereof may be printed or otherwise reproduced in any material form whatever without the author's prior written permission.

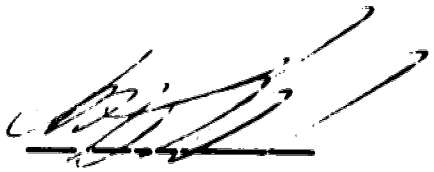

Christopher J.Price
#303-11104 84 Avenue
Edmonton, Alberta
Canada T6G 2R4

December 30/ 1993

UNIVERSITY OF ALBERTA

FACULTY OF GRADUATE STUDIES AND RESEARCH

The undersigned certify that they have read, and recommend to the Faculty of Graduate Studies and Research for acceptance, a thesis entitled: **Characterization of the Electrophysiological Response to Serotonin in an Identified Neuron From *Helisoma trivolvis*** submitted by **Christopher J. Price** in partial fulfillment of the requirements for the degree of **Doctor of Philosophy**.

Dr. J.I. Goldberg (Supervisor)

Dr. W.F. Colmers (Committee Member)

Dr. W.J. Gallin (Committee Member)

Dr. A.N. Spencer (Committee Member)

Dr. A.G.M. Bulloch (External Examiner)

Dr. N.E. Stacey (Examination Chairman)

December 23/1993

Abstract

The neurotransmitter serotonin (5-HT) regulates the embryonic development of the identified *Helisoma* neuron B19 and modulates its electrical activity in the adult animal. In both of these responses, membrane depolarization is thought to play a critical role. To examine how 5-HT leads to depolarization of neuron B19, electrophysiological experiments were conducted to characterize the ion channels, receptors and second messengers that produce the response. To achieve this, neuron B19s were isolated in cell culture and examined with whole-cell and single channel patch clamp recordings.

Current clamp and voltage clamp experiments indicated that 5-HT-dependent depolarization of neuron B19 is mediated through the activation of a maintained inward current. Ion replacement experiments indicated that sodium was the physiological carrier of the current, however, the reversal potential of approximately -30 mV suggested that the current conducted cations non-specifically. While calcium carried a small portion of the current, reduction of extracellular calcium concentrations actually resulted in a large increase in current amplitude.

cAMP analogues, phosphodiesterase inhibitors and kinase inhibitors were employed to determine the role of cyclic nucleotides in mediating the response. These experiments indicated that 5-HT normally induces the production of cyclic nucleotides in neuron B19 through a G-protein coupled receptor, followed by activation of the ion current. This current activation was not dependent upon phosphorylation, rather it occurred through direct gating of a small conductance ion channel by either cAMP or cGMP. The sensitivity of the whole-cell current to calcium ions and the direct activation by cyclic nucleotides of the ion channel suggests that it is probably related to the cyclic nucleotide-gated ion channels of vertebrates. Pharmacological experiments revealed that the neuron B19 5-HT receptor is most similar to a 5-HT receptor coupled to the activation of adenylate cyclase from *Drosophila*, dro1. Since the regenerative neurite outgrowth of neuron B19 is inhibited by 5-HT in a depolarization dependent fashion, the 5-HT response characterized in this thesis may play a critical role in the regulating the embryonic development of this identified neuron.

ACKNOWLEDGEMENTS

During my graduate studies, several people and organizations provided me with scholarly, financial and moral support and deserve to be recognized. First I would like to thank my supervisor Dr. Jeff Goldberg, who had the chutzpah to lure me from the then Dean of Graduate Studies and give me the opportunity to learn electrophysiology. From Jeff I will be able to take with me a lot of insight that will be useful to me in my future career, as well as a strong friendship.

I would also like to thank the members of my supervisory committee who were very influential in shaping the final outcome and therefore the success of my project. Its members included: Dr. A.N. Spencer, who in addition to his supervisory role, also loaned me a number of very important pieces of equipment; Drs. W.F Colmers and W.J. Gallin. I would also like to thank the external examiner for my dissertation, Dr. A.G.M. Bulloch, for his helpful input into the final version of the thesis and to Dr. N.E. Stacey for his very useful edit of my thesis.

In addition to these people I would also like to thank the following individuals. Dr. Nikita Gregoriev, for sharing with me his knowledge of all things electrical and for his overall friendliness. Dr. S.K. Malhotra for giving my wife a job and keeping an eye out for papers I should read. I would especially like to thank Dr. John Chang, whose reservoir of knowledge of second messenger systems seems as boundless as his hospitality and friendliness.

Regarding financial support, this was provided by a number of sources deserving of recognition. Both the Department of Zoology, through teaching assistantships, and the Natural Sciences and Engineering Research Council of Canada, through a Post Graduate fellowship, provided me with direct financial support. Moreover, both the Department of Zoology and the Faculty of Graduate Studies and Research provided support for me to attend scientific conferences at New Orleans and Anaheim.

Finally I would like to thank the various arms of my family for their support. Firstly I would like to thank my mother, Maureen, who despite being a single parent still managed, my sister Angela for helping her manage, and my brother Damian. I would also like to thank my wife's family, especially her mother and father, Margaret and John Leeuw, for having confidence in me, as well as her sister and brother-in-law Diane and John Pollard for their confidence in me and for the use of their sanity saving retreat in the mountains. Finally I would like to thank my wife, Karen, who in addition to providing emotional support for me during my studies and being a hiking, scuba and travel buddy, also read and edited the thesis.

Table of Contents

Page

I) Introduction 1

i) Molluscan neurons as models of nervous system function 1

ii) Serotonin in the molluscan nervous system 2

iii) Electrophysiological actions of 5-HT in molluscan neurons 4

iv) Neurotransmitter regulation of neuronal development 7

v) Serotonin and neuron B19 11

vi) Objectives 15

II) Materials and Methods 17

i) Animals 17

ii) Salines and Solutions 17

iii) Isolation of neuron B19 18

iv) Primary cultures of embryonic cells 20

v) Electrophysiological recordings 21

vi) Data analysis 25

Figures 26

III) Electrophysiological characterization of 5-HT's action on neuron B19 29

i) 5-HT-dependent depolarization of neuron B19 29

ii) 5-HT activates a sodium current in neuron B19 30

iii) Calcium sensitivity of 5-HT-dependent inward current 33

iv) An additional electrophysiological effect of 5-HT on neuron B19 34

Figures 35

IV) Cyclic nucleotides mediate activation of 5-HT-dependent inward current 45

i) G-protein involvement in activation of 5-HT-dependent inward current 45

ii) cAMP activation of inward current in neuron B19 47

iii) Phosphodiesterase inhibition potentiates 5-HT-dependent inward current 48

iv) Protein kinase inhibition does not influence the activities of 5-HT on neuron B19 51

Figures 53

V) Single channel analysis of 5-HT-dependent inward current 65

i) 5-HT activates a small amplitude single channel current in cell-attached membrane patches 65

ii) Inside-out patch recordings 67

iii) Unitary current/voltage relationships for the cAMP activated channel 70

iv) cGMP activates the same channel as cAMP 71

Figures 73

VI) Pharmacology of the neuron B19 5-HT receptor 88

i) Dose-response relationship for 5-HT activation of inward current 88

ii) Agonists at the neuron B19 5-HT receptor 89

iii) Examination of the activities of 5-HT receptor antagonists on 5-HT activation of inward current: Apparent antagonism 92

Figures 96

VII) Excitable properties of embryonic *Helisoma* neurons 116

i) Embryonic neurons are electrically excitable 116

ii) Voltage-gated calcium currents in embryonic neurons 119

iii) Electrophysiological responsiveness of embryonic neurons to 5-HT 120

Figures 122

VIII) Discussion 134

i) Neuron B19 5-HT/cyclic nucleotide response: comparison to similar molluscan responses 134

ii) Comparison with vertebrate cyclic nucleotide-gated ion channels 140

iii) Pharmacology of the neuron B19 5-HT receptor 144

iv) The neuron B19 5-HT response and its role in the biology of neuron B19 150

IX) Literature Cited 156

List of Figures

Figure II-1: Neuron B19 in cell culture 27

Figure II-2: Embryonic *Helisoma* cell with neuronal morphology 28

Figure III-1: 5-HT depolarizes neuron B19 35

Figure III-2: Bath-applied 5-HT decreases neuron B19 input resistance 36

Figure III-3: 5-HT activates an inward current in neuron B19 37

Figure III-4: Current/Voltage (I/V) relationship for 5-HT activated inward current in neuron B19 39

Figure III-5: 5-HT-activated inward current is sodium dependent 40

Figure III-6: Current/Voltage relationship for the 5-HT response under sodium-free conditons 41

Figure III-7: Low calcium recording conditions potentiate 5-HT-activated sodium current 42

Figure III-8: Current/voltage relationship for 5-HT-activated sodium current recorded in low-calcium conditions 43

Figure III-9: Sodium-insensitive action of 5-HT on neuron B19 44

Figure IV-1: G-protein involvement in activation of 5-HT-dependent inward current 53

Figure IV-2: The adenylate cyclase activator forskolin induces the transient activation of a sodium current in neuron B19 54

Figure IV-3: 8-bromo cAMP activation of inward current 55

Figure IV-4: Sodium-dependency of cAMP-activated inward current 56

Figure IV-5: IBMX potentiation of 5-HT-dependent inward current 57

Figure IV-6: IBMX-induced current is significantly increased if preceded by 5-HT exposure 58

Figure IV-7: IBMX potentiates the same current as that activated by 5-HT 59

Figure IV-8: IBMX-potentiation of 5-HT-dependent inward current was still apparent in zero sodium conditions 60

Figure IV-9: Sodium and calcium sensitivity of IBMX-potentiated inward current 61

Figure IV-10: Graph summarizing the ionic dependency of IBMX-potentiated current in neuron B19 62

Figure IV-11: Protein kinase inhibitor H7 does not prevent activation of 5-HT-dependent inward current 63

Figure IV-12: Both components of the 5-HT response do not appear to involve protein kinase activity 64

Figure V-1: 5-HT activates a small conductance ion channel in neuron B19 73

Figure V-2: A small amplitude current is conducted through the 5-HT-dependent ion channel 74

Figure V-3: 8-bromo cAMP activates a small amplitude ion current 76

Figure V-4: cAMP activates ion channels in inside-out patches 77

Figure V-5: Inside-out patches contain several cAMP-dependent ion channels 78

Figure V-6: Activation of ion channels by cAMP is dose-dependent 80

Figure V-7: Dose-dependent decrease in the total closed time 81

Figure V-8: cAMP-activated channels conduct better in the inward direction when recorded in divalent cation containing saline 82

Figure V-9: Outward currents are enhanced under divalent cation-free conditions 83

Figure V-10: Unitary current/voltage (i/V) relationship for the cAMP-dependent ion channel 84

Figure V-11: cGMP activation of ion channels 86

Figure V-12: i/V relationship for cGMP-activated ion channel 87

Figure VI-1: Dose-response relationship for 5-HT activation of inward current 96

Figure VI-2: Hill plot for 5-HT activation of inward current 97

Figure VI-3: Chemical structures of compounds having agonist activities at the neuron B19 5-HT receptor 98

Figure VI-4: Tryptamine activation of inward current 99

Figure VI-5: 5-Carboxyamidotryptamine (5-CT) activation of inward current 100

Figure VI-6: 5-methoxytryptamine (5-MOT) activation of inward current 101

Figure VI-7: α-methyl serotonin (αm-5-HT) activation of inward current 103

Figure VI-8: Dose-response curves for activation of inward current by indolylalkylamines 104

Figure VI-9: Mixed agonist/antagonist activity of methysergide 105

Figure VI-10: Methysergide dose-response curves 106

Figure VI-11: Apparent antagonism of 5-HT-dependent inward current 107

Figure VI-12: Mianserin and cyproheptadine inhibition of voltage-gated ion currents 109

Figure VI-13: Dose-response relationships for antagonism of 5-HT-dependent inward current and voltage-gated sodium current 110

Figure VI-14: Antagonism of inward current induced by IBMX 111

Figure VI-15: Cyproheptadine inhibition of neuron B19 steady-state currents 112

Figure VI-16: Cyproheptadine inhibition of voltage-gated currents in *Aplysia* sensory neurons 113

Figure VI-17: Cyproheptadine inhibition of *Lymnaea* voltage-gated currents 114

Figure VI-18: Cyproheptadine inhibits action potential firing in *Aplysia* sensory neurons 115

Figure VII-1: Whole-cell voltage clamp currents of embryonic *Helisoma* neurons 122

Figure VII-2: Comparison of the amplitudes of voltage-gated currents recorded from embryonic neurons in cell culture for between one and three days 123

Figure VII-3: I/V relationship for embryonic voltage-gated inward current 124

Figure VII-4: I/V relationship for embryonic steady-state outward current 125

Figure VII-5: I/V relationship for embryonic transient outward current 126

Figure VII-6: Excitable states of embryonic neurons 128

Figure VII-7: Anode-break responses of embryonic cells 129

Figure VII-8: Current amplitudes vs. excitable states of embryonic neurons 130

Figure VII-9: Voltage-gated calcium current 131

Figure VII-10: Voltage-gated currents obtained from perforated patch recordings 132

Figure VII-11: Possible responses of embryonic neurons to 5-HT 133

I) Introduction

The biogenic amine serotonin (5-HT) has long been known to function as a neurotransmitter in the nervous systems of molluscs. Moreover, much of the original evidence supporting the hypothesis that 5-HT is a neurotransmitter arose from studies of molluscs (Paupardin-Tritsch and Gerschenfeld, 1973). As a result, a tremendous amount of research on molluscan systems has examined the roles that 5-HT plays in behavior, learning and memory. Furthermore, the cellular mechanisms through which 5-HT serves these functions have been elucidated. More recently, evidence shows that 5-HT acts as a factor regulating the development of the nervous system of *Helisoma trivolvis* (Goldberg and Kater, 1989). A hypothetical mechanism describing how 5-HT exerts this action, may represent one way neurotransmitters regulate nervous system development in both molluscs and other animals (Mattson and Kater, 1987; Mattson and Hauser, 1991). The study presented herein examines the signal transduction pathway for 5-HT in an identified neuron from *Helisoma*, whose neuronal development and activity in the adult is influenced by 5-HT.

i) Molluscan neurons as models of nervous system function

Molluscan neurons have been and continue to be useful experimental models for many aspects of how nervous systems function at both the cellular and behavioral levels. Early research into the ionic basis and generation of action potentials made use of the large size of preparations, such as the squid giant axon (Hodgkin and Huxley, 1952) and molluscan neuronal cell bodies (Tauc, 1962a and b), which facilitated the application of electrophysiological recording techniques. The uniquely large presynaptic and postsynaptic elements of the giant synapse in the squid stellate ganglion made this preparation extremely useful for examining the voltage and calcium dependency of synaptic transmission (Katz and Miledi, 1967; Llinas and Nicholson, 1975; Llinas et al., 1976). The size of the presynaptic terminal made possible the insertion of electrodes for

recording electrophysiological events and for the iontophoretic injection of chemicals directly into the presynaptic terminal. The ability to introduce both recording and iontophoresis electrodes into the large cell bodies of molluscan neurons made them ideal for examining the transduction of neurotransmitter signals (Castellucci et al., 1980 and 1982). This allowed both the recording of the electrophysiological response to the neurotransmitter and the introduction of substances into the intracellular environment to test for the involvement of second messenger systems in the transduction process.

In addition to large size, another major advantage of molluscan neurons is that many have the property of identifiability. Individual neurons can be reliably identified in a given experimental preparation due to characteristic cell body locations, pigmentation and electrical activity. Identifiability is extremely useful, since it permits the researcher to examine the electrophysiological properties of particular neurons and determine with precision their synaptic interactions. As well, the neurotransmitters they contain and are sensitive to can be analyzed. With this information one can then see how all these factors interact to produce behaviors.

The ability to identify neurons coupled with the relative simplicity of the molluscan brain facilitates the study of more complex aspects of nervous system function, such as those associated with learning and memory (Kandel and Schwartz, 1982). Since it is possible to locate the same neurons from preparation to preparation, it is also possible to determine how their stereotyped properties are altered by experience. The factors leading to these changes can then be examined and their importance in the learning process tested.

ii) Serotonin in the molluscan nervous system

The utility of molluscan neurons as models for nervous system function is demonstrated through studies of the activities of 5-HT. 5-HT

plays a number of important roles in the molluscan nervous system. The neuronal control of feeding is a well studied example of such a role. In gastropods, rhythmic contractions of the buccal mass musculature are responsible for feeding (Kater, 1974; Cohen et al., 1978). The buccal ganglia contain the motoneurons and interneurons that innervate the buccal musculature and coordinate the basic feeding rhythm (Kater, 1974). The cerebral ganglia of many gastropods possess a bilaterally symmetrical pair of giant serotonergic neurons (GSN: Gelperin, 1981; Granzow and Rowell, 1981). These neurons send axons to the buccal ganglia where they modulate the activity of a number of the neurons involved in generating the feeding rhythm (Paupardin-Tritsch and Gerschenfeld, 1973; Cottrell and Macon, 1974; Granzow and Kater, 1977; Gadotti et al., 1986). GSN axons also extend to the periphery where they directly modulate the contractile activity of the buccal musculature (Weiss et al., 1978).

The nature of GSN influence on buccal ganglion neuronal activity has been studied in a variety of species. In *Aplysia*, *Limax* and *Pleurobranchaea*, stimulation of the GSN excites a variety of neurons. This leads to a general increase in the frequency of the patterned motor output of active buccal ganglia, but does not initiate sustained activity in inactive ganglia (Gillette and Davis, 1977; Weiss et al., 1978; Gelperin, 1981; Kupfermann and Weiss, 1981). Therefore, 5-HT is thought to play a modulatory role by accelerating the feeding motor output (Kupfermann and Weiss, 1981). However, in *Helisoma* and *Tritonia*, in addition to being able to modulate the output of an active feeding rhythm, GSN activity can initiate the rhythm in inactive preparations (Granzow and Kater, 1977; Bulloch and Dorsett, 1979).

In addition to being involved in the regulation of basic behaviors such as feeding, 5-HT is also important at higher levels of nervous system function such as learning and memory. Studies of the sea hare *Aplysia*, suggest that 5-HT serves as one of the messengers that mediates both short-term and long-term sensitization of the defensive gill and siphon

withdrawal reflexes (Kandel and Schwartz, 1982). When a noxious stimulus, such as electrical shock to the tail, is applied to an *Aplysia*, the gill withdrawal response to weak tactile stimulation of the siphon is enhanced (Kandel and Schwartz, 1982). The 5-HT involvement arises from activation, by the noxious stimulus, of a group of serotonergic interneurons that synapse onto the presynaptic terminals of the siphon mechanosensory neurons. These sensory neurons excite the motoneurons that control gill withdrawal. 5-HT causes presynaptic facilitation of neurotransmitter release from the siphon sensory neurons, resulting in a larger EPSP in the follower neuron (Kandel et al., 1981).

Depending on the number, timing and intensity of noxious stimuli delivered, sensitization can last from several minutes to several weeks (Kandel and Schwartz, 1982). The immediate result of 5-HT exposure to the sensory neuron terminals is the cAMP-mediated closure of a class of potassium channels that are normally open at the resting membrane potential (Klein et al, 1982; Siegelbaum et al., 1982). This leads to a lengthening of the repolarization phase of the sensory neuron action potential, which will enhance the influx of calcium into the presynaptic terminal. The end result is the enhanced release of neurotransmitter from the sensory neuron presynaptic terminals onto the siphon-withdrawal motoneurons (Kandel and Schwartz, 1982; Blumenfeld et al., 1990). Over the long-term, morphological changes occur whereby the number and size of transmitter release sites in the sensory neuron terminals are increased (Bailey and Chen, 1983). Furthermore, prolonged exposure to 5-HT leads to the activation of cAMP response elements that results in the expression of new gene products involved in producing long-term changes in synaptic strength (Kaang et al., 1993).

iii) Electrophysiological actions of 5-HT in molluscan neurons

Several studies have examined mechanisms through which 5-HT influences the electrical activities of molluscan neurons. From these studies it is apparent that 5-HT has a multitude of electrophysiological

actions. Nowhere is this better demonstrated than in one of the first studies examining 5-HT activities in molluscan neurons. Using neurons from *Aplysia* and the snail *Helix*, Gerschenfeld and Paupardin-Tritsch (1974a and b) identified six different electrophysiological responses to 5-HT, three depolarizing and three hyperpolarizing. Moreover, at least four of these responses were mediated through pharmacologically separate receptors.

The first 5-HT response Gerschenfeld and Paupardin-Tritsch described was a rapidly activating and short lived depolarization seen following iontophoretic application of 5-HT to certain neurons. Repeated application of 5-HT resulted in a marked desensitization of the response. Sodium-free recording conditions reduced this response, while the pharmacological agents tubocurarine, LSD, tryptamine, 7-methyltryptamine and bufotenine were also effective at reducing this response. Because of its ion selectivity, rapid kinetics, susceptability to desensitization and pharmacological blockage by tubocurarine this response, labelled the A-response, resembles 5-HT responses in vertebrate neurons that were later found to be mediated by the 5-HT3 receptor-ion channel complex (Maricq et al., 1991).

The second depolarizing effect seen following iontophoretic application of 5-HT was a more slowly activating depolarization which did not display marked desensitization with repeated 5-HT application. Like the A-response this response was reduced by elimination of sodium ions, however, it was not blocked by tubocurarine, tryptamine, LSD or 7-methyltryptamine. Only bufotenine was found to be effective at pharmacologically blocking this response. Such responses were labelled A'-responses. Recently, responses similar to A' responses have been observed in the identified *Aplysia* buccal ganglia neurons B15 and B16 (Taussig et al., 1989; Kirk et al., 1988). Interestingly, in both these latter studies, the cAMP analogue 8-bromo cAMP could induce the activation of this response.

The third depolarizing response seen was rather atypical in nature. The amplitude of the depolarization decreased in size when the membrane potential was brought to more negative potentials, and became a hyperpolarization at membrane potentials more negative than -75 mV, the potassium equilibrium potential. Associated with this response was a substantial increase in cell input resistance, which together with the response having a reversal potential of -75 mV indicated that this response was due to the closure of a potassium channel that is normally open at resting membrane potentials. This response, labelled the α-response, resembles the response that was later refered to by Kandel's group as the S-current.

5-HT application also resulted in membrane hyperpolarization in some neurons. The B-response involved a long lasting hyperpolarization following 5-HT iontophoresis. The reversal potential for the B-response was near -75 mV and was shifted to positive potentials by increasing external potassium concentrations, indicating the B-response was mediated by the opening of a potassium channel. This response was blockable with LSD, bufotenine and 5-methyoxygramine.

The second hyperpolarizing influence of 5-HT occurred only in *Helix* neurons. It involved a hyperpolarization that had a reversal potential of -55 mV and was sensitive to substitution of external chloride ions with sulfate ions. Therefore this action of 5-HT appeared to involve the opening of a chloride channel. This response was labelled the C-response and could be pharmacologically inhibited by tubocurarine, LSD and neostigmine.

The final hyperpolarizing response described by Gerschenfeld and Paupardin-Tritsch was also atypical. They found that the amplitude of the observed hyperpolarization decreased when the membrane potential was depolarized, and had a reversal potential of between -15 and -38 mV. The reversal potential was influenced by altering either the external potassium or sodium concentration. Like the α-response, an increase in

cell input resistance was associated with this response . Therefore this response, labelled the β-response, was likely due to the closure of an ion channel that conducted both sodium and potassium ions.

Since this early study by Gerschenfeld and Paupardin-Tritsch, several other electrophysiolgical effects of 5-HT on molluscan neurons have been identified. Moreover, the importance of second messenger systems in mediating some of these actions has become apparent. In the identified *Aplysia* neuron R15, 5-HT has two distinct actions (Lotshaw et al., 1986; Levitan and Levitan, 1988). At low concentrations 5-HT led to an increase in the size of an inwardly rectifying potassium current. This resulted in enhancement of the interburst interval in this endogenously bursting neuron. At higher concentrations, Levitan and Levitan (1988) also noted that 5-HT potentiated a low voltage-activated calcium current, that activated at -70 mV and resulted in an enhancement of the depolarizing phase of the burst. This could change the pattern of activity from a bursting pattern to one of constant spiking activity. Both actions of 5-HT were mimicked by forskolin activation of adenylate cyclase or by application of 8-bromo cAMP and involved protein phosphorylation.

5-HT has also been shown to influence calcium currents in other molluscan preparations. In identified neurons from the viscero-abdominal ganglionic mass of *Helix*, Paupardin-Tritsch et al. (1986) showed that 5-HT enhanced the size of high voltage-activated calcium currents. This response was mimicked either by injection of cGMP into the cell soma or by phorbol ester activation of protein kinase C, suggesting two separate second messenger systems converge upon the same substrate. The net result of calcium current enhancement was an increase in the width of action potentials.

iv) Neurotransmitter regulation of neuronal development

Neurotransmitters have a well defined function in synaptic transmission. However several recent lines of evidence have indicated

these substances are equally as important in the development of the nervous system, acting as factors regulating neuronal development. The form that this regulation takes covers many aspects of neuronal development including triggering neuronal differentiation, maintenance of an environment permissive for the extension of neuronal processes, and signalling to the developing processes the arrival at the appropriate area where synapse formation is to occur (Mattson and Hauser, 1991; Whitaker-Azmitia, 1991; Lauder, 1993).

The idea that neurotransmitters may act as factors that stimulate neuroblasts to cease dividing and differentiate into neurons arose mainly from the results of experiments by Lauder and her colleagues (1982). In the developing rat brain 5-HT is expressed very early in Raphe neurons of the brain stem, prior to the incorporation of these cells into neuronal circuits. The developing Raphe neurons extend both ascending and descending processes. The arrival of these processes at other regions of the brain often coincided with the cessation of neuroblast proliferation in that region. This observation prompted the hypothesis that 5-HT released by the Raphe projections caused the cessation of neuroblast proliferation and thus differentiation in the target area. To test this hypothesis p-chlorophenylalanine was used to deplete endogenous 5-HT concentrations. This resulted in a continuation of neuroblast proliferation beyond the normal time frame, thereby supporting the idea of a developmental role for 5-HT as a differentiation factor.

Evidence that neurotransmitters can either directly or indirectly facilitate the extension of neuronal processes is provided from a number of sources. In cultures of cerebellar granule cells and serum-containing cultures of chick tectal neurons, GABA exposure enhanced the ability of these cells to extend processes (Hansen et al., 1987; Michler-Stuke and Wolff, 1987). Similarly, exposure to the glutamate receptor agonist N-methyl-D-aspartate (NMDA) can facilitate process extension in short-term cultures of rat cerebellar granule cells (Rashid and Cambray-Deakin, 1992). While these studies suggest that the neurotransmitters

themselves were acting as trophic factors to facilitate process extension, evidence that neurotransmitters can also stimulate the release of growth factors from glial cells has recently been obtained. In rat brain 5-HT causes astrocytes to release a growth factor, S-100, which supports the development of serotonergic neurons (Whitaker-Azmitia, 1992).

One role to which neurotransmitters seem well suited is in signalling a neuron's developing dendritic region that it should stop growing and establish normal synaptic contacts with presynaptic partners. Several studies provide strong support in favor of this hypothesis. In cultures of chick tectal neurons, GABA exposure inhibited the otherwise vigorous process elaboration seen under serum-free conditions (Michler-Stuke and Wolff, 1987). Similarly, in cultured rat cortical neurons activation of 5-HT_{1A} receptors inhibited process length and the extent of neurite branching (Sikich et al., 1990). While in *in vivo* studies, injection of low concentrations of the 5-HT agonist 5-methoxytryptamine into pregnant rats resulted in decreased numbers of serotonergic nerve terminals in the offspring (Shemer et al., 1991).

Studies have also shown dopamine to inhibit process extension. In avian retinal neurons, an interesting situation exists where dopamine D_1 receptor activation inhibits process extension. However this receptor is transiently expressed only during retinal development (Lankford et al., 1987). In *Drosophila* DfDdc mutants, which are incapable of synthesizing 5-HT or dopamine, the branching of serotonergic neurons that innervate the gut was greatly increased (Budnik et al., 1989). When mutant larvae were fed dopamine, but not 5-HT, normal branching was restored. This confirmed dopamine was an important factor regulating neurite branching.

Studies of glutamate inhibition of neurite outgrowth in hippocampal pyramidal neurons have been particularly useful in elucidating a mechanism through which dendritic outgrowth may be regulated (Matteson and Hauser, 1991). When two day old cultured hippocampal

pyramidal neurons were exposed to low doses of glutamate, kainic acid or quisqualic acid, Mattson and his colleagues (1988a) found the rate of dendritic outgrowth was reduced. At intermediate doses dendrites began to retract, while only at higher doses did axonal outgrowth become inhibited. The highest doses were found to be cytotoxic. Co-cultures of entorhinal cortex explants and hippocampal pyramidal cells were then made to test what effect a natural glutamate source would have on dendritic outgrowth. It was found that pyramidal cells that contacted entorhinal cortex axons possessed less elaborate dendritic arbors than those that occurred at a distance (Mattson et al., 1988c).

In examining the intracellular mechanism responsible for these actions on pyramidal neurons, it was found that glutamate application resulted in an increase in intracellular calcium concentrations, as measured with the calcium sensitive dye fura-2 (Mattson et al., 1988b). Moreover, it was possible to prevent both the dendritic regression and cytotoxicity of glutamate by incubating cultures with cobalt and mimic the effects with the calcium ionophore A23187 (Mattson et al., 1988a). Phorbol-12-myristate-13-acetate activation of protein kinase C could also mimic these actions of glutamate (Mattson et al., 1988b). Taken together it was concluded that glutamate activation of a non-NMDA receptor caused calcium influx and protein kinase C stimulation that resulted in inhibition of dendrite outgrowth.

In addition to glutamate, fibroblast growth factor (FGF) exerts a regulatory influence on pyramidal cell dendritic arborization. When cultures were incubated with FGF for several hours it was found that the sensitivity of neurons to glutamate was significantly decreased and dendrites continued growing (Mattson et al., 1989). This effect of FGF was dependent on both gene transcription and protein synthesis. Therefore, these results indicate that in hippocampal pyramidal neurons the state of dendritic outgrowth is controlled by the net effect of the factors that the dendritic arbor is exposed to. If the dendritic arbor is stable, glutamate would be expected to be the dominant factor, while if it

is in a state permissive for growth FGF would be expected to be dominant (Mattson et al., 1989; Mattson and Hauser, 1991).

v) Serotonin and neuron B19

Molluscan neurons have been instrumental in furthering the concept of neurotransmitters functioning as regulators of neuronal development. Experiments by Kater and colleagues using identified neurons from the pond snail *Helisoma trivolvis* provide *in vitro* and *in vivo* evidence that 5-HT serves to regulate growth cone motility and the state of neurite outgrowth of specific identified neurons. Moreover, experiments into the mechanism underlying these actions have been central to the development of a model concerning the regulation of growth cone activity by calcium.

Neuron B19 is an identified neuron, bilaterally paired in the *Helisoma* buccal ganglia (Kater, 1974). In the snail, neuron B19 innervates the supralateral radula tensor muscle, which is involved in protraction of the odontophore during the feeding rhythm (Kater, 1974). Neuron B19 receives synaptic inputs from a variety of sources, including mechanosensory neurons and several interneurons, which coordinate the rhythmic firing of the motoneurons responsible for protraction and retraction of the buccal mass and radula (Kater and Rowell, 1973; Kater, 1974; Murphy, 1991). Neuron B19 also receives serotonergic input from the metacerebral giant cell (C1) of the cerebral ganglia (Granzow and Kater, 1977; Gadotti et al., 1986). Stimulation of neuron C1 results in the slow depolarization of neuron B19 and an increase in the frequency of its rhythmic motor output. Experiments examining this input indicate that it persists in high extracellular calcium and therefore is likely a monosynaptic input. Furthermore, the synaptic communication between neurons C1 and B19 is weakened after 5-HT levels in the snail are lowered by treatment with 5,7-dihydroxytryptamine (Gadotti et al., 1986).

Individual B19s can be removed from buccal ganglia and placed in cell culture. Under the appropriate cell culture conditions B19 will regenerate new neuritic processes, each of which is tipped by a growth cone. When isolated B19s are exposed to 5-HT, the filopodia of the growth cones retract and the neurites cease growing (Haydon et al., 1984). This action was selective for specific responsive neurons such as B19, P1 and P5, but not for other non-responsive neurons such as B4 and B5 (Haydon et al., 1987; McCobb et al., 1988). Moreover, focal application of 5-HT to an individual neuron B19 growth cone only resulted in filopodial retraction in that specific growth cone, even if additional growth cones emanated from the same neuron (Haydon et al., 1985).

To test that this outgrowth inhibition activity was not just a culture artifact Murrain et al. (1990) examined the ability of 5-HT to influence neurite regeneration following axotomy *in vivo*. Consistant with the cell culture studies, the normal profuse regeneration of neuron B19 following axotomy was significantly reduced with 5-HT exposure, while the regeneration of neuron B5 proceeded.

Initial experiments investigating the mechanism through which 5-HT inhibits growth cone motility and neurite outgrowth revealed that action potential generation in neuron B19 also caused filopodial retraction (Cohan and Kater, 1986). To examine the linkage between these two stimuli, McCobb and Kater (1988) performed experiments testing the ability of 5-HT to initiate action potential activity in neuron B19. Using extracellular patch recordings, they found that 5-HT caused an increase in action potential activity in neuron B19 but not in neuron B5. Furthermore, the inhibition of growth cone motility by 5-HT in neuron B19 was blocked if the cell membrane potential was artificially hyperpolarized. Taken together, these results suggest membrane depolarization is a critical step in 5-HT-induced inhibition of neurite outgrowth.

Further support for this hypothesis came from experiments examining the combined effects of 5-HT and acetylcholine (ACh). When Ach was applied alone to neuron B19, no change in outgrowth was observed. However, when 5-HT and ACh were applied in tandem, the inhibitory actions of 5-HT were blocked (McCobb et al., 1988). Neuron B19 possesses tubocurarine sensitive ACh receptors (Haydon and Zoran, 1989) that control a chloride conductance. The decrease in input resistance accompanying the activation of these receptors results in a shunting effect that prevents the 5-HT-induced depolarization of neuron B19 and inhibition of growth cone motility and neurite outgrowth (McCobb et al., 1988).

Further study of the mechanism underlying 5-HT's actions on neuron B19 revealed that calcium ions play a critical role. Through the use of fura-2, it was observed that both 5-HT and action potentials cause an increase in intracellular calcium concentration in neuron B19 (Cohan et al., 1987). Moreover, increasing intracellular calcium concentration with the calcium ionophore A23187 was sufficient to cause inhibition of growth cone motility and neurite outgrowth (Mattson and Kater, 1987). In addition, the inorganic calcium channel blocker lanthanum prevented inhibition of growth cone motility and neurite outgrowth due to 5-HT (Mattson and Kater, 1987). Therefore, it was concluded that 5-HT-induced excitation of neuron B19 resulting in the influx of calcium ions through voltage-gated calcium channels, are the initial events in the mechanism that lead to inhibition of growth cone motility and neurite outgrowth. Although it is not entirely known how increased intracellular calcium leads to inhibition of neurite outgrowth, experiments using the calmodulin antagonist CGS 9343B strongly suggested the involvement of calcium-calmodulin dependent protein kinase (Polak et al., 1991).

An additional element that has been implicated in the mechanism underlying 5-HT's actions on neuron B19 is cAMP. Growth cone motility and neurite outgrowth were inhibited by increasing intracellular cAMP concentrations, through treatment with either the adenylate cyclase

activator forskolin or the cAMP analogue dibutyrl cAMP (Mattson et al., 1988d). It has not been determined if 5-HT leads to an increase in intracellular cAMP concentrations in neuron B19. Furthermore it remains to be seen at what stage of the 5-HT response, if any, cAMP acts.

The previously mentioned studies all involved the use of regenerating adult neurons to examine the effects of 5-HT on neurite outgrowth. To test if the model that has arisen from these studies can be extended to developing neurons, Goldberg and Kater (1989) examined the effects of transiently depleting 5-HT levels during embryonic development. Embryos treated with 5,7-dihydroxytryptamine survived and were allowed to grow until they were large enough to be examined electrophysiologically. In these snails, neuron B19 possessed morphological anomalies and had formed abnormally strong electrical synapses. Previous cell culture studies had reported that for *Helisoma* neurons to form electrical synapses, the neurites of the coupling cells must both be actively growing (Hadley and Kater, 1983). Moreover, 5-HT prevented the formation of electrical synapses between neurons B19 and B5, which normally form in cell culture (Haydon et al., 1987). Therefore, in the *in vivo* experiments of Goldberg and Kater (1989), it appeared that the lack of an inhibitory, serotonergic influence on neuron B19 neurite outgrowth during embryogenesis resulted in the enhanced formation of electrical synapses. Taken together, these studies support the hypothesis that 5-HT acts as a regulator of neuronal development in *Helisoma*.

Studies using primary cultures of dispersed embryonic cells have further examined this hypothesis. 5-HT application to primary cultures resulted in inhibition of neurite outgrowth in approximately 50% of the neuronal population (Goldberg et al., 1990). Further, a large portion of the neuronal population also responded to 5-HT with an elevation of intracellular calcium concentration. It seems likely that this neurite

outgrowth response was mediated through a similar mechanism as seen in the adult cells.

vi) Objectives

The neurotransmitter 5-HT plays two major roles in the biology of the identified buccal ganglion neuron B19. For both roles membrane depolarization is an important element. However, little is known about the electrophysiological response of neuron B19 to 5-HT. Therefore in the thesis to follow a study designed to examine the mechanism underlying 5-HT-dependent depolarization of neuron B19 is presented. Specifically, the ion channels responsible for depolarization of neuron B19, the role, if any, of second messenger systems in mediating 5-HT's activity and the pharmacological description of the 5-HT receptor initiating the process will be addressed. The results obtained in the study outlined above could prove important in two major ways. Firstly, they will identify receptors and ion channels that may be important during neuronal development. Secondly, they will provide details on a 5-HT response in an identified neuron that is associated with the control of a fundamental behavior.

In this study electrophysiological recordings from cultured neurons B19 were carried out using the patch clamp recording technique. This technique was particularly useful, since it allowed for the recording of both macroscopic whole cell currents and single channel currents with the same amplifier. Moreover, both the whole-cell and inside-out single channel recording configurations allowed for the introduction of substances to the intracellular surface of the membrane. This approach was particularly useful for studying the involvement of second messengers in mediating 5-HT's actions.

In addition to studying the mechanism responsible for 5-HT-dependent depolarization of neuron B19, a second study was performed examining the excitable characteristics of embryonic *Helisoma* neurons. Whole-cell and perforated patch configurations of the patch clamp recording

technique were used to obtain voltage clamp and current clamp recordings from cells in primary cultures of dispersed embryonic cells possessing neuronal morphologies. The presence of voltage-gated sodium, potassium and calcium currents, as well as the ability of these cells to generate action potentials were tested. These experiments will indicate whether the model describing the inhibitory actions of 5-HT on neurite outgrowth in regenerating adult *Helisoma* neurons can be applied to developing neurons.

II) Materials and Methods

i) Animals

The snails used in this study were members of a laboratory colony of the freshwater snail, *Helisoma trivolvis* (Class Gastropoda, Subclass Pulmonata, Order Basommatophora, Family Planorbidae). Snails were housed in 54 L aquaria, which contained an oyster shell substratum and aerating aquarium filters. Fresh water maintained at 24° to 27°C was continuously supplied to aquaria in a flow through manner. Snails were maintained under a 12 hr light/dark photoperiod and fed a diet of trout chow (Vextra) and lettuce.

For the studies involving the adult neuron B19, snails that served as neuron donors were selected from their aquaria on the morning of dissection. Snails used were generally between 8 and 15 mm in vertical shell diameter. Snails with clear, as opposed to opaque and chalky shells were preferred. Neuron isolation from snails with these characteristics had higher success rates.

In the studies involving cultured embryonic cells, the egg masses that contained the embryos were usually collected the day of dissociation. This reduced the occurrence of fungal contamination of the cultures. Embryos used for dissociation were at a stage of development where they had undergone between 20 and 30% of their embryonic development, stage E20-30. This conforms to the period of embryogenesis in which the nervous system is first starting to develop and the first evidence of 5-HT expression is observed (Goldberg and Kater, 1989; McKenny and Goldberg, 1989).

ii) Salines and solutions

Several types of salines were used during the course of this study, as well as a variety of chemical compounds. *Helisoma* saline consisted of:

51 mM NaCl, 1.7 mM KCl, 4.1 mM $CaCl_2$, 1.5 mM $MgCl_2$, 5 mM Hepes; pH 7.3-7.4. Antibiotic saline (ABS) contained, in addition, 150 μg/ml Gentamicin. Defined medium (DM) consisted of: 50% Liebowitz medium; (Gibco special order, containing no salts) supplemented with 40 mM NaCl, 1.7 mM KCl, 4.1 mM $CaCl_2$, 1.5 mM $MgCl_2$, 5mM Hepes, 50 μg/ml Gentamicin and 0.015% glutamine; pH 7.3-7.4.

Two different electrode solutions were used for electrophysiological recordings. The basic whole-cell recording electrode solution consisted of: 54.4 mM K-aspartate, 2 mM EGTA, 2 mM $MgCl_2$, 5 mM Hepes, 5 mM dextrose, 5 mM ATP and 1 mM GTP; pH 7.3-7.4. For single channel recordings electrodes contained 90 mM NaCl and 5 mM Hepes.

Chemical compounds obtained from Sigma (St. Louis) include: CsCl, trizma base, choline chloride, N-methyl D-glucamine, K-asp, Gentamicin, amphotericin B, glutamine, EGTA, Hepes, ATP, GTP, cAMP, tryptamine, cGMP, 5-HT, IBMX, poly-L-lysine, dibutyrl cAMP and 8-bromo cAMP. KCl, $CaCl_2$, NaCl and $MgCl_2$ were obtained from BDH Chemicals (Toronto). The following compounds were obtained from Research Biochemicals Inc. (Natick, Ma.): α-methyl serotonin, 5-carboxamidotryptamine, 5-methoxytryptamine, mianserin, cyproheptadine, 8-hydroxy DPAT, mesulergine, MDL 7222, H7,LY-53857, pipenerone. Calbiochem (San Diego) was the source for: GTPγS, H7 and H89.

iii) Isolation of neuron B19

The method used for isolation of the identified neuron B19 basically follows that described by Haydon et al. (1985). Snails were removed from their shells and placed in a solution consisting of 25% Listerine and 75% artificial pond water (0.025% Instant Ocean; Mentor, Ohio), for 15 min. This treatment served to both anesthetize and sterilize the snails for subsequent dissection. Once in Listerine (Warner-Lambert, Scarborough), snails were transfered to a sterile, laminar flow hood

(Forma) where all subsequent procedures took place. On removal from the Listerine solution, snails were blotted clean of mucous with sterile cotton and Kim-wipes and then placed on a silicone rubber (General Electric) dissection pad bathed with sterile, antibiotic containing, *Helisoma* saline.

For dissection, snails were pinned ventral-side-down to the dissection pad. An incision was made in the head region of the snail to expose the buccal mass and the circumesophageal ganglia that form the central nervous system ("brain") of the snail. The esophagus was cut near its entrance with the stomach, resected anteriorly and pinned, exposing the paired buccal ganglia. Buccal ganglia were freed from their connections with the brain by cutting the paired cerebro-buccal connectives. They were then removed from the snail along with attached pieces of lateral muscle, buccal mass and esophagus, which facilitated pinning out the ganglia for subsequent isolation of neuron B19. Following their removal, the ganglia were placed in a 0.2% trypsin solution for 15 min and then transfered to fresh ABS for at least an additional 45 min before neuron B19 isolation.

To isolate neuron B19, buccal ganglia were pinned dorsal-side-up to a silicone rubber pad bathed with high osmolarity DM, where 1 ml of 4 times saline was used to fortify every 10 mls of DM, increasing the osmolarity of the medium. Neuron B19 was then visually identified as the middle neuron in a trio of large neurons lined up across the equator of the ganglion. The inter-buccal commissure and the nerve trunks leading to the attached lateral muscles were then crushed with fine forceps. The ganglionic sheath was slit in the region between neurons B19 and B5 using an electrolytically sharpened tungsten needle, and the B19 cell body was gently pushed out the slit. The neuron B19 cell body was then drawn with suction into the mouth of a micropipette, whose position was controlled with a micromanipulator (Prior). The micropipette had been previously cut to obtain a tip diameter of approximately 100-200 μm. The micropipette was attached to a micrometer syringe (Canlab,

Mississauga) via tygon tubing and the whole apparatus filled with the high osmolarity DM. Using repetitive cycles of positive and negative pressure, neuron B19's axons were gently stretched until they broke, freeing the cell from the ganglia. Neuron B19 was then transferred to a poly-L-lysine coated 35 mm culture dish (Falcon 3001) that contained two mls of conditioned medium (CM; see below). The cell was then placed onto a small poly-L-lysine coated piece of cover glass (Fisher; Nepean, Ont.). In early experiments, cells were placed directly onto the floor of the culture dish.

Cultured *Helisoma* neurons require conditioning factors for their proper growth and maintenance (Wong et al., 1984). CM for neuron B19 cultures was prepared by incubating four brains in two mls of DM, for 48 to 96 hours. This incubation occurred directly in the 35 mm culture dishes used for the cultures. The cover glass pieces were added at the start of the incubation period. Alternatively, for the embryo cultures to be described later, CM was prepared by incubating, in bulk, two brains/ml of DM in 75 mm glass petri dishes (Pyrex).

iv) Primary cultures of embryonic cells

To prepare cultures of embryonic cells, embryos at the appropriate stage of development were dissociated following the method of Goldberg et al. (1988). Between eight and 15 embryo-containing egg masses were placed in a 35% ethanol/ABS solution for two min, followed by two consecutive ABS washes of two and 10 min. Embryos were then isolated from their egg mass by poking a hole in each egg chamber with a 27 gauge needle and sucking the embryo out of the chamber with a pasteur pipette. All the embryos were collected and placed in a 0.2% trypsin solution for 45 min, followed by a 15 min treatment in a 0.1% trypsin inhibitor solution. Embryos were then transfered to DM for 10 min prior to dissociation.

Dissociation involved placing the embryos into a three ml syringe that was equipped with a piece of 62 μm nylon mesh (Small Parts Inc.) covering the tip. The syringe was then back-filled with two mls of CM and the syringe plunger inserted. The embryos were mechanically dissociated by forcing the embryos repeatedly through the mesh with the syringe plunger approximately 10 times. 0.5 mls of the resulting cell suspension was then plated in a single drop on the surface of a poly-L-lysine coated 35 mm petri dish and allowed to settle over night. The following morning each culture dish was supplemented with 1.5 mls of DM.

v) Electrophysiological recordings

Neuron B19: Neuron B19 recordings were performed on the day following neuron isolation. Neurons possessing either an encircling veil of lammelopodia or neurites were used for recordings (Figure II-1) Both types of cells possessed normal electrophysiological properties and there were no qualitative differences in the response to 5-HT seen. However, cells possessing neurites tended to give larger amplitude responses to 5-HT. Therefore, where comparisons were necessary between various experimental treatments, an attempt was made to use cells with similar states of neurite expression. Cells which showed no evidence of membrane elaboration were not used since they generally demonstrated poor expression of voltage-gated ion currents and often were poorly attached to the substratum. For whole-cell recordings, the cell-containing coverslip was transferred to a recording chamber (Warner Instruments; Hamden, CT) that allowed for rapid changes in the perfusing solution. Perfusion inflow was gravity powered, while outflow was controlled by the building vacuum system. In some early experiments recordings were made using cells plated directly on the 35 mm culture dish. For single channel recordings cells were either recorded from directly in the culture dish, or alternatively, if cells were cultured onto cover glass, these were transfered to new 35 mm petri dishes containing saline. Owing to the small size of the single channel events recorded, the excess noise associated with the use of a perfusion system made it impractical.

Therefore, for inside-out patch recordings bath exchange was crudely performed by hand using a pasteur pipette.

Saline was the basic bath recording solution for both whole-cell and single channel recordings. In a few experiments, DM served as the bathing solution. With inside-out patch recordings calcium was excluded from the bathing saline. Sodium-free saline was obtained by direct molar substitution of Tris for NaCl, correcting the pH with HCl. In some experiments choline chloride was used as a substitute for sodium. However, this chemical appeared to activate the Ach receptor-mediated conductance in neuron B19, resulting in a significant decrease in membrane input resistance (F. Bahls, personal communication). Therefore, only voltage clamp recordings could be unambiguously used in experiments involving choline containing saline. In experiments using low-calcium or divalent-free salines, the missing ions were not compensated.

The activity of several chemical substances were examined in this study. Solutions of 5-HT, 5-HT agonists and antagonists, and agents examining the role of second messenger systems were prepared fresh daily. Two methods of application were used in experiments. When the Warner recording chamber was used the compound was dissolved directly in the appropriate perfusing saline and perfused through the recording chamber. Alternatively in recordings using 35 mm petri dishes substances were generally bath applied. Here a concentrated drop, typically 10 µl, was added at a distance from the cell to yield the desired final concentration in 2 mls of solution.

Electrodes used for whole-cell recordings were fashioned either from borosilicate glass (WPI: 1B150F; OD=1.5 mm) or from lead glass (WPI: PG61165-4; OD=1.65 mm). For single channel electrodes, only the borosilicate glass was used. Electrodes were pulled on either a Narishigi PB-7 vertical puller (Tokyo) or a Flaming Brown P-87 horizontal puller (Sutter Instruments; Novato, Calif.). Electrodes were generally coated

with dental wax (Modern Materials) near the tip, to lower electrode capacitance and therefore noise pickup, and heat polished with an MF-83 microforge (Narishigi; Tokyo). When filled with the basic whole-cell recording solution, electrodes had resistances of between 1 and 5 MΩ. The opening of single channel electrodes needed to be quite small to obtain stable recordings. When filled with 90 mM NaCl and 5 mM Hepes, resistances were between 10 and 30 MΩ. All electrode solutions were filtered through 0.22 μm filter units (Nalgene; Rochester, NY) before use.

Embryonic Neurons: Whole-cell recordings were performed within the first three days of culture on cells that possessed neuron-like morphologies: spherical cell bodies and neuritic processes (Figure II-2). DM was used as the bathing solution in experiments where total whole-cell currents were recorded. The electrode solution used was identical to that used in the neuron B19 experiments, with the exception of ATP and GTP being absent. Electrodes were pulled from borosilicate glass and after heat polishing and filling, gave resistances of between 10 and 20 MΩ. In order to record calcium currents, choline chloride subsitituted saline served as the bathing solution, while CsCl substituted for K-aspartate in the electrode solution.

In addition to conventional whole-cell recordings, perforated patch recordings were also used on embryonic neurons. In perforated patch recordings an antibiotic, such as amphotericin B or nystatin, is included in the electrode solution. Upon giga-ohm seal formation, the pore-forming antibiotic molecules insert into the membrane creating an electrical connection between the intracellular environment and the interior of the pipette (Horn and Marty, 1988). Under these conditions only monovalent ions pass between the pipette and the interior of the cell. Large intracellular regulatory factors remain in the cell and do not diffuse into the pipette. Here, amphotericin B was used following the technique of Rae et al. (1991). 240 μg/ml amphotericin was dissolved in dimethyl sulfoxide, mixed with 60 mM K-aspartate or KCl, and sonicated to form the antibiotic solution. To fill pipettes, the pipette tip was dipped briefly

in antibiotic-free pipette solution to fill a small portion of the electrode tip. The electrode was then backfilled with the antibiotic containing solution. The electrode was then quickly brought to the cell membrane, the seal formed and the electrode capacitance electronically cancelled with the patch clamp amplifier. Membrane patches were allowed to permeablize for several minutes until the capacitive transients that occur during the onset and offset of voltage pulses stopped increasing in amplitude. This capacitive current indicated access to the intracellular environment was achieved.

In experiments on both neuron B19 and embryonic cells, recordings were made using a Dagan 3900 (Minneapolis) integrating patch clamp amplifier. Cells were viewed with a Nikon Diaphot inverted microscope under phase-contrast optics. The microscope, recording chamber, head stage and micromanipulator were all located within a Faraday cage. Standard whole-cell and single channel recording procedures were followed (Hamill et al., 1981). However series resistance compensation was never used in recordings because the small size of the currents did not warrant its use. Therefore the instability associated with its use was avoided. Whole-cell recordings were filtered at 2 KHz and single channel recordings at 0.5 KHz via the 4 pole Bessel filter internal to the amplifier. Whole-cell recordings were performed in the mixed RC recording mode, where a resistor, in parallel with the feed back capacitor, continuously discharges the capacitor to avoid it becoming saturated. Single channel recordings employed the full integrating recording mode, which gave significantly lower noise levels.

The setting of membrane potentials, delivery of stimuli and acquisition of responses involved the use of Indec Fastlab DA/AD hardware and software and was controlled by an 80386 computer (Indec; Sunnyvale, Calif.). Whole-cell responses to the application of chemical substances were recorded onto chart paper using a Gould RS3200 chart recorder (Cleveland, Ohio). Single channel events were recorded onto video tape

through a PCM-2 VCR interface (Medical Systems Corp.) for offline analysis.

vi) Data analysis

In whole-cell recording experiments designed to obtain current/voltage (I/V) relationships, current responses to changes in membrane potential were recorded using the Fastlab data acquisition program Acquire. The responses were then measured using the Fastlab data analysis program Read. Data was then exported to various commercial programs for statistical analysis (Statview) and the creation of graphs (Cricket Graph). Chart records of responses to chemical substances were measured manually.

Single channel records were analyzed using the Pclamp (Axon Instruments) suite of programs. VCR recordings were digitized at 5 KHz using the Fetchex program. Digitized records were then further filtered at 200 Hz, via a digital Gaussian filter. Measurements of unitary current amplitude, channel open-time and closed-time were made using the Fetchan program. Fetchan employs a 50% threshold crossing criterion to determine channel openings. Baseline levels were manually determined and were immediately manually adjusted if drifting was noticed. The pSTAT program was used to generate histograms and perform curve-fitting functions.

For the presentation of electrophysiological recordings, traces were scanned at 300 dots per inch resolution directly into the graphics program Superpaint (Aldus), using a Scanman 32 hand scanner (Logitech). In Superpaint, recording artifacts were deleted from the traces. In the textual presentation of data, mean values are given as: $x \pm$ standard error of the mean. Similarily, error bars on histograms refer to the standard error of the mean. In instances where t-tests were employed to test for significance differences, an asterisk (*) will denote significance at the 95% confidence interval.

Figure II-1: Neuron B19 in cell culture. In this study of neuron B19, cells suitable for recordings possessed either a veil of lamellapodia surrounding the cell body (Upper cell) or neurites (Lower cell). Both situations gave qualitatively similar responses to 5-HT. Scale bar corresponds to approximately 25 μm for the upper photo and 50 μm for the lower.

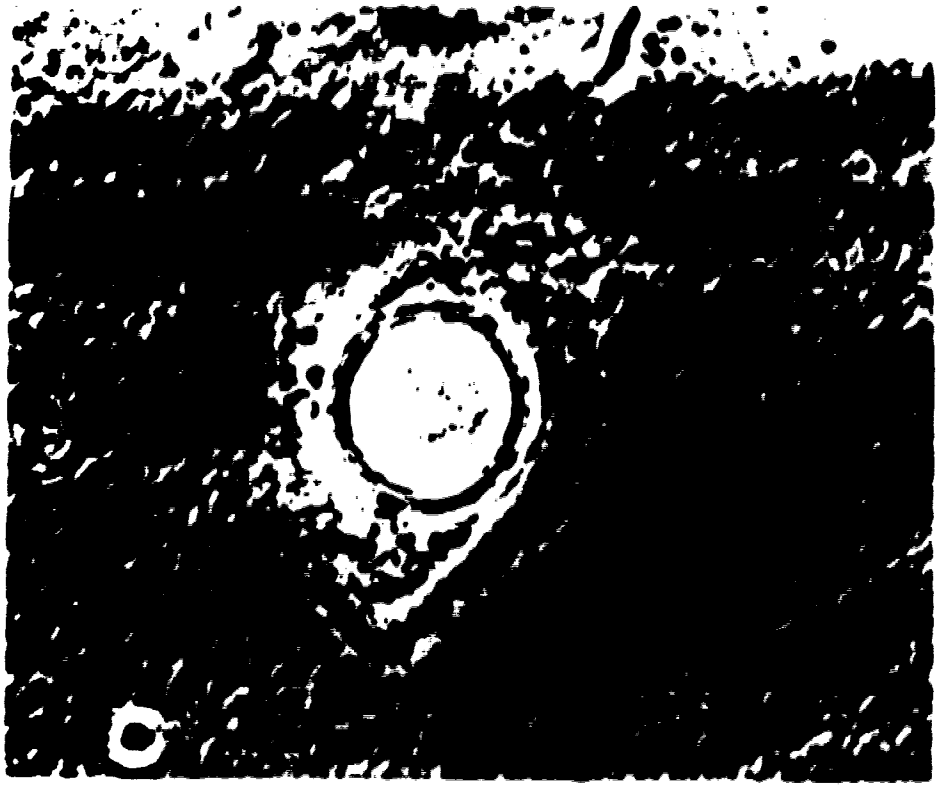

Figure II-2: Embryonic *Helisoma* cell with neuronal morphology. Cells selected for electrophysiological recording in primary cultures of dissociated *Helisoma* embryos (indicated by the arrow) possessed spherical cell bodies and one or more neuritic processes. Whole-cell recordings generally supported the identification of these cells as neurons, as they generally possessed a full complement of voltage-gated ion channels. Scale bar indicates approximately 25 μm

III) Electrophysiological characterization of 5-HT's action on neuron B19

At least two separate studies have previously examined the effect of 5-HT on the membrane potential of neuron B19. Gadotti et al. (1986) demonstrated that stimulation of the serotonergic neuron C1 resulted in the slow depolarization of neuron B19 through a monosynaptic pathway. Moreover, McCobb and Kater (1988) demonstrated that 5-HT induced spiking activity in these cells, using extracellular patch recordings from cell bodies of cultured neurons B19. However no studies to date have examined the specific ionic currents that are responsible for 5-HT-dependent depolarization of neuron B19. Therefore, the section to follow describes the results of whole-cell current and voltage clamp experiments which were designed to examine the current underlying 5-HT-dependent depolarization of neuron B19, with emphasis on the current's ionic and voltage dependency.

i) 5-HT- dependent depolarization of neuron B19

Current clamp recordings from cultured neurons B19 revealed that exposure of the neuron to 25 μM 5-HT resulted in robust membrane depolarization and initiation of spiking activity, which is consistant with the above reports (Figure III-1). The depolarization induced by 5-HT was characteristically long lasting, persisting for as long as 5-HT was present in the bathing solution. For example, in one instance a cell remained depolarized and spiking for four hours. Depolarization was reversible upon washing 5-HT from the bathing solution.

To determine if membrane conductance changes accompanied 5-HT-dependent depolarization, experiments were performed in which hyperpolarizing current pulses were delivered to neuron B19 before and during exposure to 5-HT. The membrane potential following 5-HT

application was artificially hyperpolarized to its original level to avoid introduction of voltage-dependent variables associated with recording at a depolarized membrane potential. Generally, a decrease in the amplitude of voltage responses to current injection was seen following exposure to 5-HT (Figure III-2). This is indicative of an increase in membrane conductance resulting from the opening of ion channels, and makes it unlikely that a change in ionic pump activity was responsible. On average, a 17.5 ± 3.7 % (n=8) decrease in amplitude of the voltage response to a 200 pA hyperpolarizing current pulse was observed. Paired t-test comparison revealed this to be a statistically significant decrease in conductance (p=0.0073).

ii) 5-HT activates a sodium current in neuron B19

To directly examine the ion current responsible for 5-HT-dependent depolarization of neuron B19, voltage clamp recordings were performed. Rapid bath exchange for 25 μM 5-HT-containing saline resulted in an inward shift in holding current that was generally associated with an increase in baseline current noise (Figure III-3). 5-HT-activation of inward current was typically slow in onset, taking several seconds for the final steady-state level to be reached. The steady-state amplitude of the inward shift in current, recorded from a holding potential of -70 mV, averaged 112 ± 7.7 pA (n=40, range: 40 to 268 pA). Like 5-HT-dependent depolarization, the current recorded in voltage clamp persisted in the continued presence of 5-HT. Upon exchange for 5-HT-free saline, the holding current slowly returned towards its pre-5-HT level. Typically this recovery was characterized by a fast and slow phase (Figure III-3).

The maintained nature of the 5-HT-dependent inward current has several experimental advantages associated with it. One advantage is that the current, when activated, will become a part of the cell's steady-state current. This facilitated the determination of current/voltage (I/V) relationship for the 5-HT-dependent inward current, using a variation of the slow voltage ramp. To obtain I/V curves a staircase protocol was

used where the B19 holding potential was stepped successively in 10 mV, 1 s long increments, from -100 mV to -10 mV before and after activation of the inward current by 5-HT (Figure III-4, inset). This range of voltage was chosen to limit possible complications arising from the activation of voltage-gated currents at more positive holding potentials. The holding current level was measured at the end of each 1 s step to obtain the steady-state I/V relationship (Figure III-4, top panel). Subtraction of the before curve from the curve after 5-HT activation yielded a difference curve equivalent to the I/V curve for the 5-HT-dependent inward current. This experimental method was particularly valuable in light of the observation that the neuron B19 5-HT response appears to slowly desensitize. When neuron B19 was repeatedly exposed to 5-HT, with intermediating wash periods, the amplitude of each subsequent 5-HT-dependent inward current decreased. This was surprising since the current maintained a constant amplitude once a steady-state level was attained in response to a single, long duration application. Therefore, I/V curves were reliably obtained from single cells with a single application of 5-HT using the staircase protocol.

As seen in Figure III-4 (bottom panel), the I/V curve obtained for the 5-HT-dependent inward current possesses some interesting characteristics. Firstly, the current remained inward across most of the range of hyperpolarized potentials and reversed direction at approximately -20 mV. Currents conducted through ion channels that do not discriminate well between different cations, such as the nicotinic acetylcholine receptor channel current, typically have reversal potentials near 0 mV. This result suggested that the current activated by 5-HT was also carried through an ion channel that conducted cations in a non-specific manner.

Secondly, at approximately -40 mV the I/V curve for 5-HT-dependent inward current departed from its predicted trajectory, and shifted temporarily in the inward direction. This voltage corresponds to a region of negative slope that was seen in the steady-state I/V curve for neuron B19. This indicates that the current responsible for the negative slope

region in neuron B19 is potentiated by 5-HT. This result has two possible explanations: 1) there are two separate currents that are influenced by 5-HT, one seen at hyperpolarized membrane potentials that is activated by 5-HT, and one, a voltage-sensitive current responsible for the negative slope region, that is potentiated by 5-HT; 2) alternatively, a single current with some voltage dependent properties could be responsible for both phenomena.

To examine more directly the ion selectivity of 5-HT-dependent inward current, ion substitution experiments were performed. In initial experiments, potassium currents were inhibited by replacing potassium aspartate in the electrode solution with N-methyl-D-glucamine. Moreover, cells lacking neurites were chosen for recordings to facilitate adequate diffusion of the electrode solution throughout the cell. Under these conditions 25 μM 5-HT still activated inward current (mean amplitude 49.1 ± 10.6 pA, n=6). Coupled with the previous finding that a general increase in membrane conductance occurs with 5-HT exposure, it was decided that the sodium dependency of the current be examined. Tris substitution for sodium in the perfusing saline resulted in a marked decrease in the amplitude of 5-HT-dependent inward current recorded at a holding potential of -70 mV (Figure III-5, upper trace). Moreover, re-introduction of sodium-containing saline, following an appropriate wash interval, restored the ability of B19 to conduct inward current following 5-HT application (Figure III-5, lower trace). Therefore, sodium is likely the major carrier of 5-HT-dependent inward current.

Staircase experiments were also performed to better examine the effects of 5-HT on steady-state current under sodium-free conditions (Figure III-6). The difference current obtained in the absence of sodium indicated that the 5-HT-dependent inward current was greatly reduced across the hyperpolarizing range of potentials. Moreover, the difference current reversal potential was shifted in the hyperpolarized direction. Furthermore, the difference current demonstrated outward rectification, as current conducted better in the outward direction at more positive

potentials. These results are consistent with the hypothesis that 5-HT-dependent inward current normally conducts sodium ions at the membrane potentials where it is active, but demonstrates little overall selectivity for cations.

Calcium sensitivity of 5-HT-dependent inward current

In addition to examining the sodium dependency of 5-HT-dependent inward current, experiments were also carried out to test for calcium-dependency of the current. To accomplish this, recordings were done under low-calcium conditions (approximately 100 μM). Extracellular calcium was not completely eliminated because of deleterious effects on cell stability. Rather surprisingly when neuron B19 was exposed to 25 μM 5-HT in low calcium conditions at a holding potential of -70 mV very large inward currents were seen in response (Figure III-7, upper trace). On average, inward currents recorded in low calcium conditions, at a holding potential of -70 mV, were 339.9 ± 53 pA in amplitude (range: 66.8 to 695 pA; n=13). In comparison to currents recorded under normal calcium conditions, t-test analysis indicated that this was a significant increase in amplitude (Figure III-7, bottom panel; p=0.0001).

In order to determine that an additional 5-HT-dependent current was not being uncovered by the low calcium recording conditions, staircase experiments were also carried out. The resulting steady-state I/V curves obtained were similar to those obtained under normal recording conditions, and possessed a negative slope region (Figure III-8, top panel). In addition the calculated difference current was similar in shape to that seen under normal recording conditions (Figure III-8, bottom panel). The only obvious difference noted was that the negative slope region was shifted approximately 10 mV in the hyperpolarizing direction. This hyperpolarizing shift would be expected for a voltage sensing ion channel as a result of the decreased membrane surface charge associated with low-calcium conditions (Hille, 1992). Therefore, calcium appears to play a

significant inhibitory role in the conduction and/or activation of the neuron B19 5-HT-dependent inward current.

iv) An additional electrophysiological effect of 5-HT on neuron B19

In several early current clamp experiments examining the effects of 5-HT on neuron B19, it was observed that in addition to the sodium-sensitive action, a sodium-insensitive action was apparent. Initial evidence for this sodium-insensitive activity was that an increase in input resistance was occasionally observed following 5-HT application (data not presented). To examine the nature of this action a variation of the staircase protocol was used, where the membrane potential was stepped between -110 mV and -50 mV in 2 mV increments. This provided a steady-state I/V curve for the membrane potentials surrounding the potassium equilibrium potential. Difference currents obtained in sodium-free conditions, with choline substituting for sodium, described a 5-HT-dependent current that was outwardly directed at very hyperpolarized potentials and reversed direction at approximately -85 mV (Figure III-9). The combined findings of an increase in input resistance and a current that reversed direction near -90 mV, the approximate reversal potential for potassium ions under these recording conditions, suggested that closure of a potassium channel may be a component of the response to 5-HT. This would work in parallel with the sodium-sensitive response to depolarize neuron B19. Experiments were conducted in the summer of 1991 to confirm that potassium and not chloride was the primary ion conducted in this component of the 5-HT response. Unfortunately, this component was no longer observed from this time forward, and thus could not be studied further. It is not known why this component stopped being expressed by neuron B19. Therefore, no further discussion of this response will be provided.

Figure III-1: 5-HT depolarizes neuron B19. Current clamp recording of neuron B19 demonstrating the robust, maintained depolarization induced by bath application of 5-HT (25 μM final concentration; Vm maintained near -60 mV). Individual action potentials cannot be resolved in the trace owing to the slow chart recorder speed used. Depolarization was completely reversible upon washing out the 5-HT. A version of this figure has been published previously (Price and Goldberg, 1993).

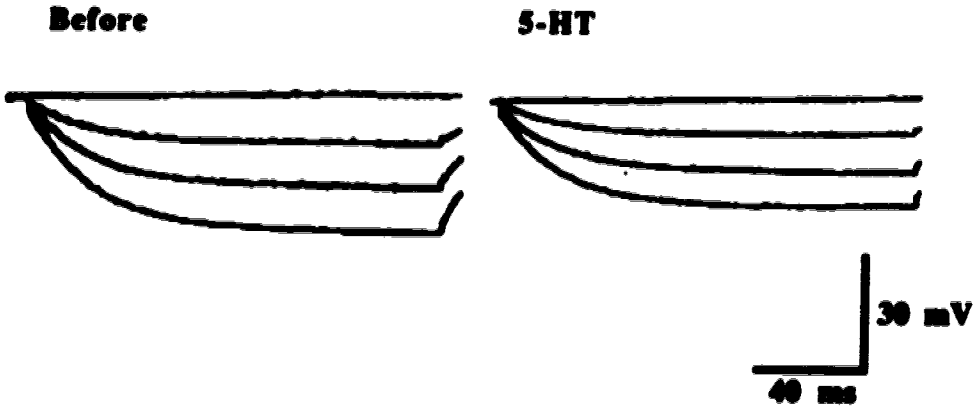

Figure III-2: Bath-applied 5-HT decreases neuron B19 input resistance. Current clamp recording showing the response of neuron B19 to hyperpolarizing current pulses of amplitudes -100, -200 and -300 pA delivered before and during exposure to 25 μM 5-HT. Note the decreased amplitude of the voltage responses during 5-HT exposure. In both instances the membrane potential was hyperpolarized to -90 mV. A version of this figure has been published previously (Price and Goldberg, 1993).

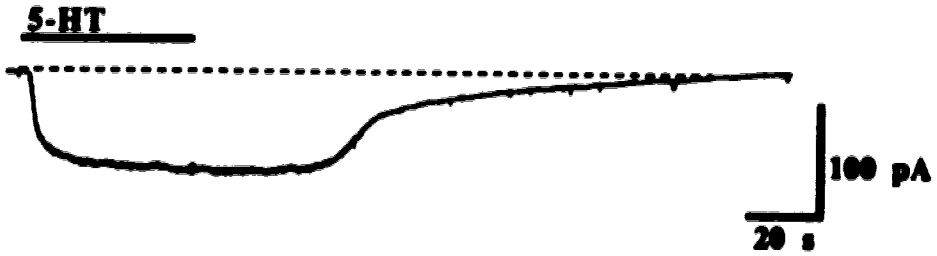

Figure III-3: 5-HT activates an inward current in neuron B19. Voltage clamp recording from neuron B19, showing that rapid exchange for 25 μM 5-HT containing saline resulted in a maintained inward shift in holding current. The holding current slowly returned to its original level upon exchange for 5-HT-free saline. Bar indicates duration of 5-HT exposure, while the dotted line represents the basal current level. Holding potential was -70 mV.

Figure III-4: Current/Voltage (I/V) relationship for 5-HT-activated inward current in neuron B19. **Top panel:** Representative example of an experiment where the membrane potential was incremented 10 mV every 1 s, between -100 and -10 mV, before, (open symbols) and during (closed symbols) exposure to 25 μM 5-HT. Inset graphically portraits the stimulus protocol. Current value used for plotting was measured at the end of each voltage step. Note the negative slope region occurring between -40 mV and -30 mV. **Bottom panel:** Mean difference current obtained by subtraction of the before curve from the 5-HT curve (n=7). The difference current remained inward across most of the hyperpolarized range of potentials and reversed direction near -20 mV. Note that the current within the negative slope region was also increased with 5-HT exposure.

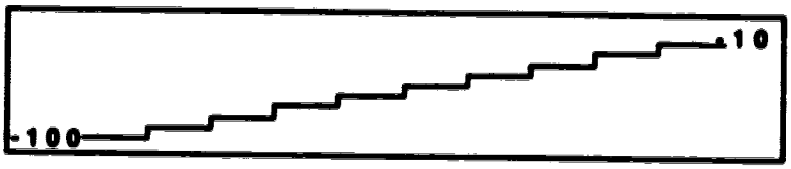
10
-100

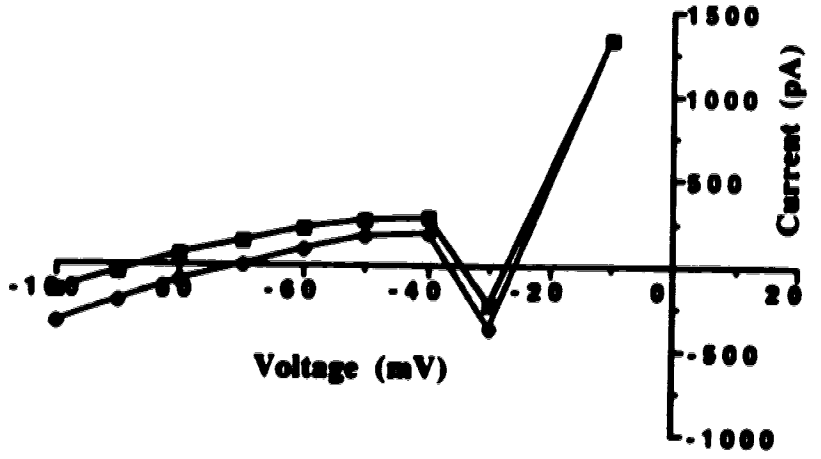
1500
1000
500
-500
-1000
Current (pA)
-60
-40
-20
0
20
Voltage (mV)

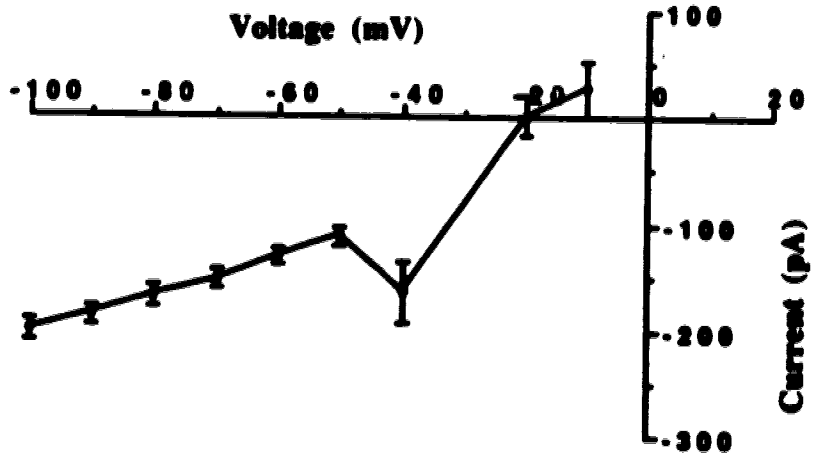
Voltage (mV)
100
-100
-200
-300
Current (pA)
-100
-80
-60
-40
0
20

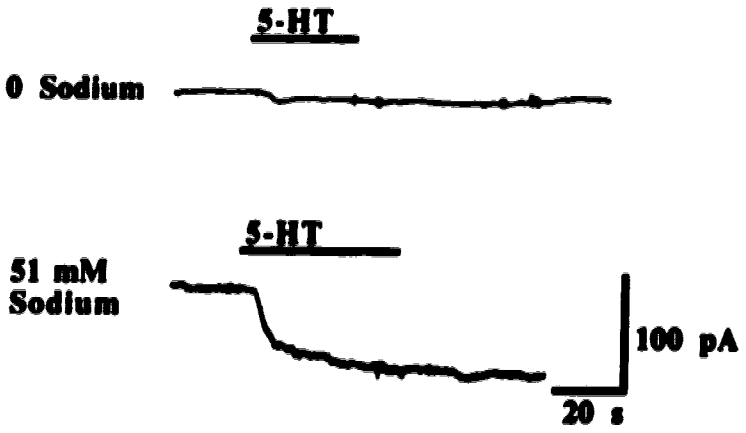

Figure III-5: 5-HT-activated inward current is sodium dependent. Neuron B19 was exposed to 25 μM 5-HT under sodium-free (upper trace) and then following a wash interval, under 100% sodium-containing conditions (lower trace). Bars indicate the duration of exposure to 5-HT; holding potential was -70 mV in both instances.

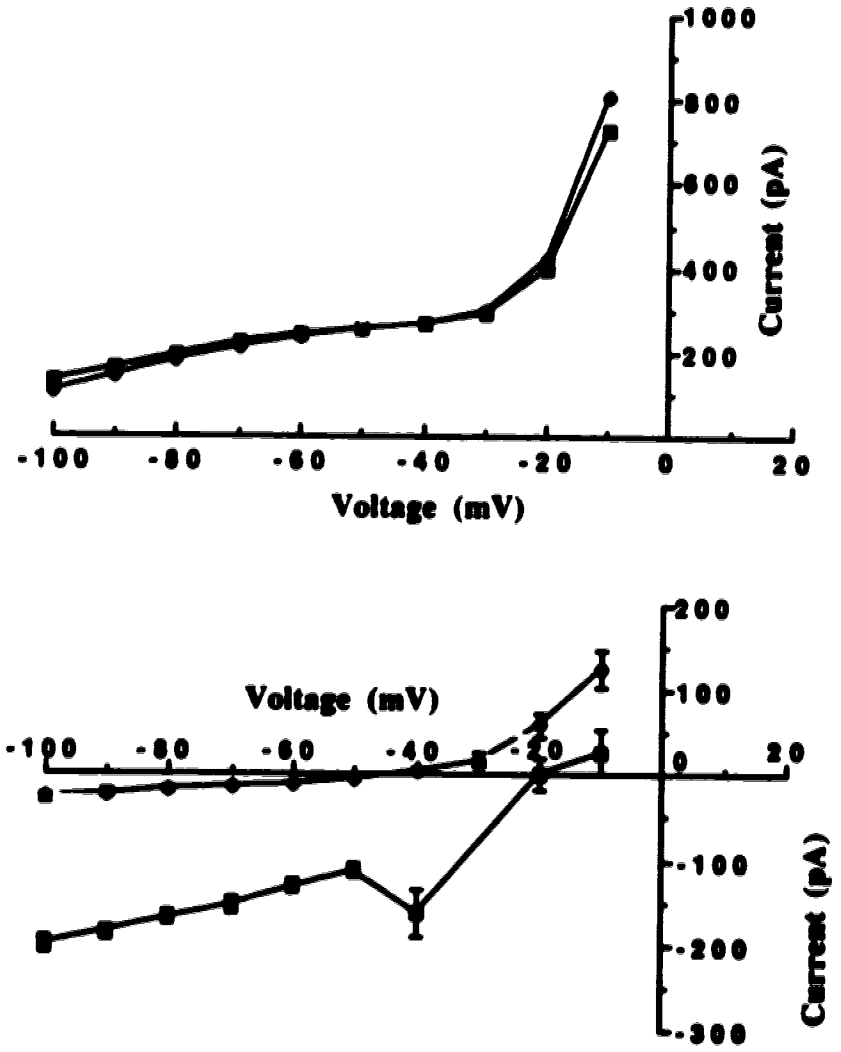

Figure III-6: Current/voltage relationship for the 5-HT response under sodium-free conditions. **Top panel:** Representative experiment where stair cases were delivered before (open symbols) and during (closed symbols) exposure to 25 μM 5-HT for a neuron B19 in tris-substituted saline. Note the lack of a negative slope region. **Bottom panel:** Mean difference current for 7 cells exposed to 5-HT in tris-substituted saline (closed symbols). Mean difference current under 100% sodium conditions (open symbols) is included for comparison. Note the hyperpolarizing shift in the reversal potential and the outward rectification under sodium-free conditions.

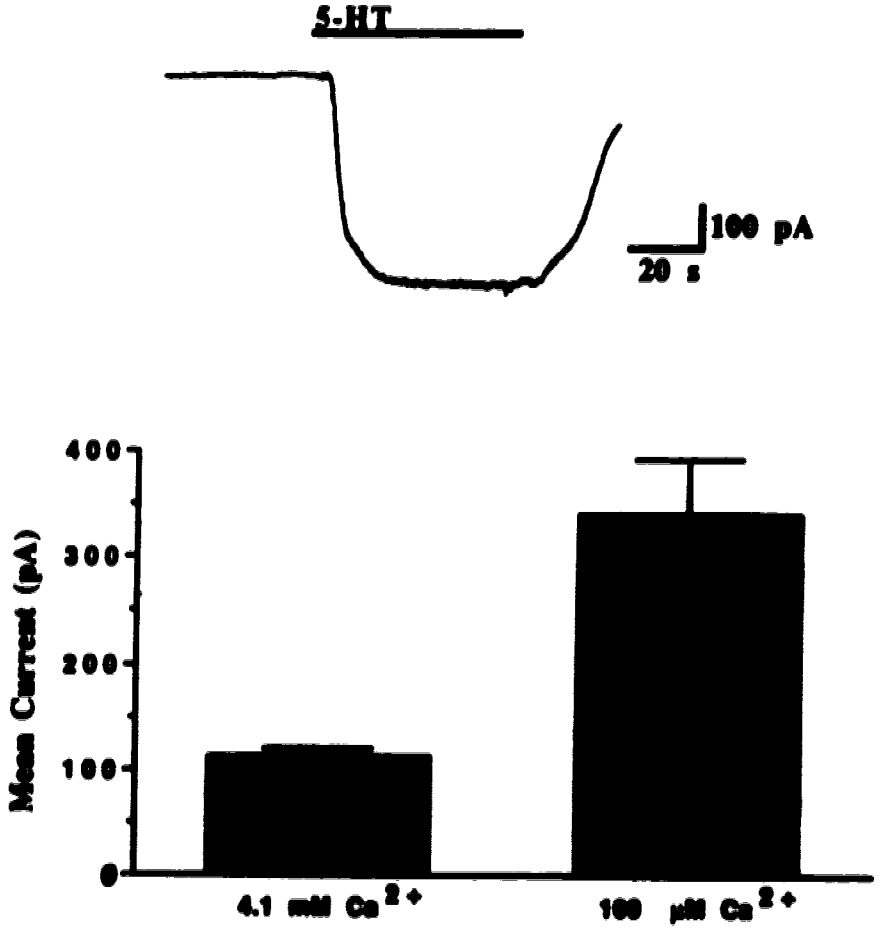

Figure III-7: Low calcium recording conditions potentiate 5-HT-activated sodium current. Upper trace: Bath exchange for 25 μM 5-HT in low-calcium saline resulted in a very large inward shift in holding current. Bar indicates duration of 5-HT exposure; holding potential -70 mV. Bottom panel: Summary comparison of the amplitude of 5-HT-activated current in normal 4.1 mM calcium saline (n=40) and low, approximately 100 μM calcium saline (n=11). All results were obtained with a holding potential of -70 mV.

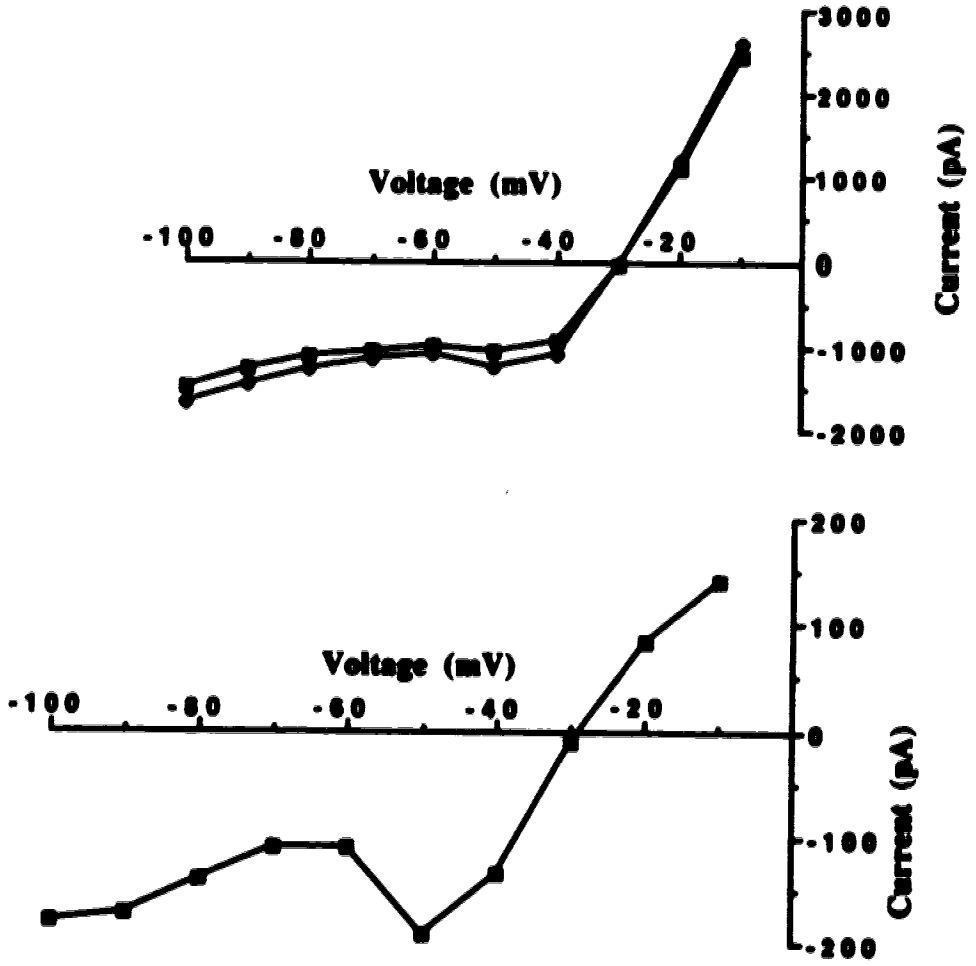

Figure III-8: Current/voltage relationship for 5-HT-activated sodium current recorded in low-calcium conditions. Top panel: Results of a single experiment where staircases were delivered before (open symbols) and during exposure to 25 μM 5-HT (closed symbols) to a neurite-lacking cell in approximately 100 μM calcium saline. Bottom panel: Difference current calculated from the above experiment. Curve was similar in shape to that obtained under normal calcium conditions, with the exception that the peak of the negative slope is shifted to -50 mV. Similar results were obtained in three process-bearing cells under these conditions, however, action potential activity made measurements in the voltage range between -50 and -40 mV impossible.

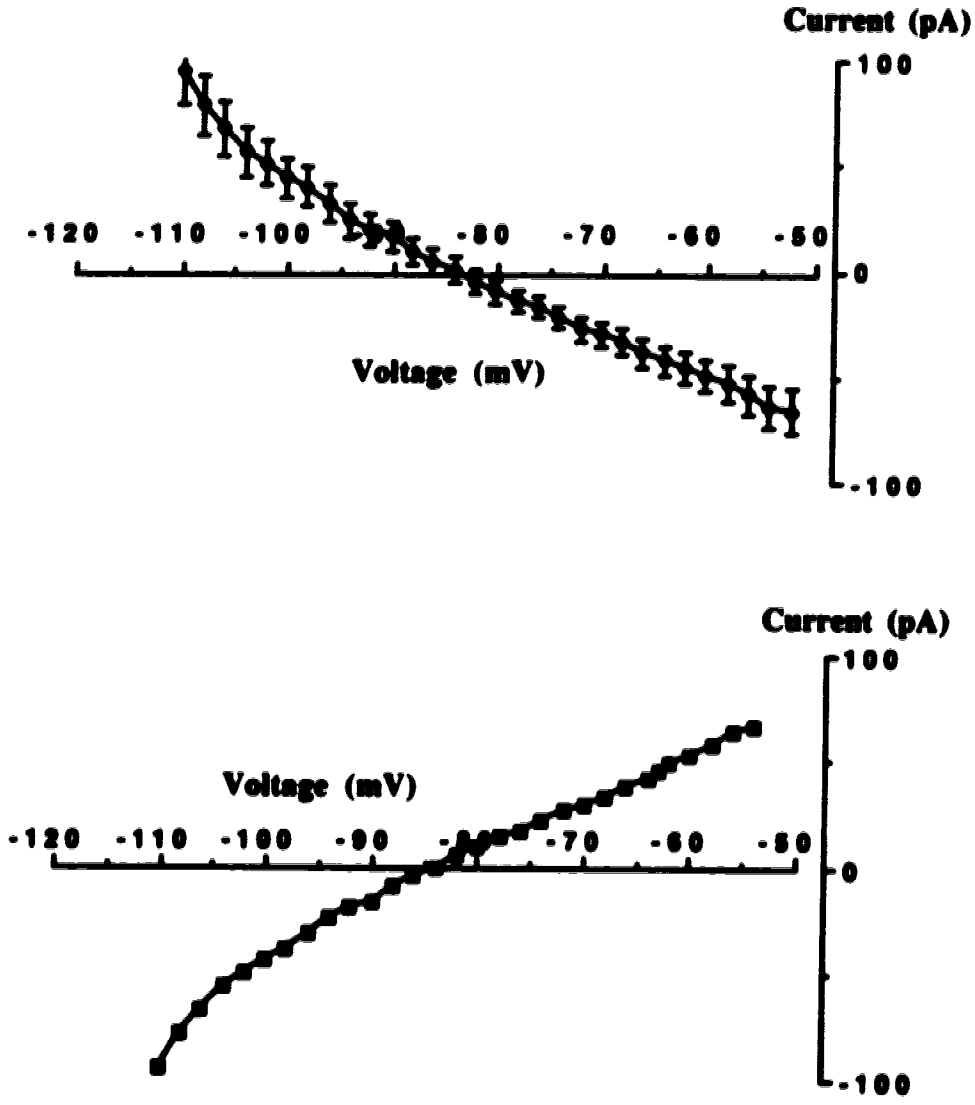

Figure III-9: Sodium-insensitive action of 5-HT on neuron B19. Upper panel: Difference current obtained through delivery of a staircase protocol for cells in sodium-free, choline saline (n=13). The holding potential was stepped between -110 and -52 mV in 2 mV increments before and during exposure to 25 μM 5-HT. The difference current obtained was outward at very hyperpolarized potentials, reversed direction near -85 mV and became outward at very positive potentials. Bottom panel: Inverse of the above I/V relationship to show how the I/V relationship for the current inhibited by 5-HT would appear. This response was not observed after the summer of 1991.

IV) Cyclic nucleotides mediate activation of 5-HT-dependent inward current

There are two general mechanisms through which a neurotransmitter can influence the activity of ion channels and, therefore, membrane potential. The neurotransmitter can bind to a receptor located on the ion channel protein and directly cause the channel to gate open and conduct ions. Generally the currents seen in these instances activate very rapidly, and desensitize rapidly in the continued presence of the neurotransmitter. Alternatively, the transmitter can bind to a receptor which stimulates the synthesis of an intracellular second messenger. The second messenger then communicates either directly or indirectly with the ion channel to influence its activity. The currents seen in this latter situation generally are slowly activating, reflecting the time needed for the various intermediating steps to occur.

In the previous results section, it was observed that the 5-HT-dependent inward current in neuron B19 did not display rapid desensitization in the continued presence of 5-HT. This characteristic is inconsistent with 5-HT directly activating an ion channel. Therefore, the possibility of a second messenger mediating 5-HT activation of inward current in neuron B19 was tested. cAMP has been shown to mimic 5-HT's actions on growth cone motility and neurite outgrowth in neuron B19 (Mattson et al., 1988D). However, no specific role for cAMP has been demonstrated in the mechanism underlying these actions. Therefore, cAMP was deemed the most likely candidate for mediating 5-HT-dependent activation of inward current in neuron B19.

i) G-Protein involvement in activation of 5-HT-dependent inward current

Neurotransmitter responses that employ second messenger mediated mechanisms are initiated by G-protein coupled receptors. To determine if the 5-HT receptor on neuron B19 is a member of this class of receptors,

experiments using the GTP analogue GTPγS were performed. GTPγS is a non-hydrolyzable form of GTP that will bind to an unstimulated heterotrimeric G-protein, and induce dissociation of its α subunit from the βγ subunit complex. The α subunit is then free to activate or inactivate second messenger formation. Because the GTPγS is not hydrolyzed, the G-protein stays in its active, dissociated state. This effectively uncouples the cell's population of receptors from the second messenger system that is normally activated by the G-protein upon receptor binding. Therefore, ligand binding to the receptor should give no additional response to that initially induced by the GTPγS.

To examine whether a G-protein coupled receptor initiates activation of 5-HT-dependent inward current, 200 μM GTPγS was included in the electrode solution. Moreover, recordings were made from neurons B19 that lacked neurites to facilitate diffusion of the GTPγS throughout the cell once the whole-cell recording configuration was obtained. Under these recording conditions two important obeervations were made (Figure IV-1). Firstly, following membrane breakthrough, the holding current drifted in the inward direction and eventually leveled off. Typically, under normal recording conditions the holding current would drift in the outward direction following membrane breakthrough as the recording improved. This inward drift likely represents the receptor independent activation of inward current by the GTPγS. Secondly, upon bath exchange for 25 μM 5-HT-containing saline very little inward current was recorded. On average, 21.8 ± 5.0 pA of inward current was recorded with GTPγS present in the electrode solution (n=6), compared to 57.3 ± 4.2 pA recorded in a subsample of seven neurite-lacking cells recorded under control conditions. T-test comparison of these two groups showed this difference to be significant (p=0.0002). These two findings provide strong evidence that a G-protein coupled receptor mediates the activation of 5-HT-dependent inward current in neuron B19.

ii) cAMP activation of inward current in neuron B19

To specifically address the hypothesis that cAMP mediates 5-HT activation of inward current, methods to artificially increase intracellular concentrations of cAMP were employed. The diterpine compound forskolin increases intracellular cAMP concentrations by activating adenylate cyclase, the enzyme responsible for cAMP synthesis. In voltage clamp recordings from B19, when the bath was exchanged for saline containing 32 μM forskolin a transient inward current was observed (Figure IV-2). This result was observed in all three cells where this was tested. Moreover, in one current clamp recording of neuron B19, forskolin induced robust depolarization (data not shown). The transient inward current was not seen in sodium-free, choline substituted recording conditions (Figure IV-2; n=2). The transient nature of the response possibly reflects the inability of forskolin, at this concentration, to generate a long term increase in cAMP levels. Therefore once the initial forskolin-induced surge in cAMP concentration was degraded by the resident phosphodiesterases, the current regressed.

Another method to increase intracellular concentrations of cAMP involved the use of membrane permeable analogues of cAMP. When voltage clamped neurons B19 were exposed to 2 mM 8-bromo cAMP (8-Br cAMP), activation of a maintained inward current was observed (Figure IV-3). On average, the inward current activated by 8-Br cAMP had an amplitude of 51.5 pA ± 8.9 pA (n=8).

When cells were exposed to 2 mM 8-Br cAMP and then subsequently exposed to 25 μM 5-HT, additional inward current was always seen (Figure IV-3, top trace). Two possible explanations for this result exist. Firstly, the membrane permeability of 8-Br cAMP may not have been sufficent to increase cAMP levels enough to fully activate the response. Secondly, the additivity seen may reflect the presence of two separate currents, one activated by 5-HT and one by cAMP. To distinquish between these two possibilities, experiments were performed in which 100

μM 8-Br cAMP was included in the electrode solution. This should effectively load the cell with 8-Br cAMP and fully activate the cAMP-dependent current. Under these conditions, bath exchange for 25 μM 5-HT failed to result in inward current activation (Figure IV-3, lower trace). Moreover, observation of the current moniter on the patch clamp amplifier showed the holding current, prior to 5-HT exposure, to be more negative than that generally observed under normal recording conditions. Taken together, these results support the hypothesis that 5-HT and 8-Br cAMP both activated the same current.

To test if the current activated by analogues of cAMP was sodium dependent, ion substitution experiments were performed. When neuron B19 was exposed to the membrane permeable analogue dibutyryl cAMP (db cAMP; 2 mM) under sodium-free, choline substituted recording conditions, a small amount of inward current was obeserved (Figure IV-4, upper trace). However, when the db cAMP was washed out and the bath was replaced with sodium-containing saline, reapplication of 2 mM db cAMP resulted in a larger current (Figure IV-4, lower trace). Paired t-test comparisons for 3 cells revealed the current recorded in sodium containing conditions to be on average 87.1 pA larger, which was a statistically significant difference (Figure IV-4, bottom panel; p=0.0123).

iii) Phosphodiesterase inhibition potentiates 5-HT-dependent inward current

A common approach for examining the involvement of cyclic nucleotides in a cellular response is by experimentally inhibiting the activity of resident phosphodiesterases. Intracellular cAMP concentrations are a reflection of the combined rate of adenylate cyclase catalyzed cAMP synthesis and the rate of phosphodiesterase catalyzed cAMP degradation. Therefore, inhibition of cyclic nucleotide breakdown should result in an accumulation of the nucleotide within the cell and potentiate any responses mediated by the nucleotide. To test for this in

neuron B19, experiments using the phosphodiesterase inhibitor, isobutyl methylxanthine (IBMX) were conducted.

In experiments designed to examine the effects of IBMX on 5-HT-dependent inward current the following protocol was employed. First, a cell was exposed to IBMX and the response recorded. Second, after a wash period sufficient to remove the previously applied IBMX, the same cell was exposed to 5-HT. After the 5-HT-induced response stabilized, the cell was then exposed to IBMX, without removal of the 5-HT. When voltage clamped neuorns B19 were exposed to 0.5 mM IBMX alone, a small amplitude inward current shift was recorded (Figure IV-5, upper trace). This inward current was maintained and averaged 55.2 ± 15.1 pA in amplitude (n=6). However, when neuron B19 was exposed to 0.5 mM IBMX following initial exposure to 25 μM 5-HT, a much larger current was observed (Figure IV-5, lower trace). The current activated by IBMX, following 5-HT stimulation, averaged 491.3 ± 117.7 pA. Figure IV-6 graphically demonstrates these results. Paired t-test comparison of the unstimulated IBMX response with the 5-HT-stimulated IBMX response indicated the observed difference to be significant (p=0.0063). Since the IBMX current was much larger after pre-stimulation with 5-HT, these results clearly demonstrate that 5-HT induces the synthesis of cyclic nucleotides in neuron B19 and these nucleotides then mediate the activation of an inward current.

To confirm that the current activated by IBMX was the same as that activated by 5-HT, staircase experiments were performed. Steady-state IV curves were obtained in the following sequence: 1) before neuron B19 was exposed to any substances; 2) during exposure to 25 μM 5-HT; 3) during exposure to 5-HT and 0.5 mM IBMX (Figure IV-7, top panel). Difference currents were then calculated for the current activated by 5-HT and the current activated by IBMX (Figure IV-7, lower panel). The IBMX difference current was similar in shape to the 5-HT difference current, being inwardly directed across the hyperpolarized range of potentials, and having a similar reversal potential.

In addition to staircase experiments, ion substitution experiments were performed on the IBMX-potentiated inward current. When 5-HT-stimulated neurons B19 were exposed to 0.5 mM IBMX under sodium-free, tris-substituted recording conditions, a fairly substantial amount of inward current was still observed (Figure IV-8). This current, recorded in four cells under these conditions, averaged 199.9 ± 47.3 pA in amplitude. While it was significantly smaller than the IBMX current recorded under normal sodium-containing conditions ($p=0.0456$), it still represented a sizable inward current.

To examine the ion that was responsible for this residual current seen under sodium-free recording conditions, experiments were performed using low calcium (approximately 100 μM), sodium-free saline. IBMX current recorded from 5-HT-stimulated neurons B19 under these conditions was very small in amplitude, averaging 45.5 ± 6.4 pA (Figure IV-9, top trace; $n=5$). Moreover, t-test comparison showed this current was significantly smaller than the IBMX current measured in normal calcium, sodium-free conditions ($p=0.0041$). Therefore, calcium ions carry a large portion of the residual current observed in the absence of sodium.

Once the response to IBMX in low calcium, sodium-free conditions was obtained in the above cells, the same cells were tested to examine their IBMX response recorded under low calcium, normal sodium conditions. This experiment was prompted by results from the previous chapter which demonstrated that low calcium conditions resulted in larger 5-HT-dependent inward currents. Following wash period to reverse the previous experiment and exchange of the bathing solution for low calcium, normal sodium saline, 5-HT-stimulated neurons B19 were exposed to 0.5 mM IBMX. The currents that resulted were the largest thus far measured, averaging 1052.3 ± 130.5 pA (Figure IV-9, lower trace). Paired t-test comparison with the IBMX currents measured under low calcium and zero sodium conditions revealed the difference seen to be significant ($p=0.0013$). These results are again consistent with the IBMX current

being the same sodium/calcium sensitive current as the one activated following 5-HT exposure.

Figure IV-10 graphically summarizes the results of ion substitution experiments and reveals some interesting characteristics of the current activated by 5-HT and potentiated by IBMX. To simplify comparisons associated with variation in response amplitudes between cells lacking and possessing neurites, only data from cells possessing neurites were used. Examination of this graph reveals an apparent contradiction. Under sodium-free conditions, a substantial amount of residual current was seen. This residual current was decreased by lowering the extracellular calcium concentration. Therefore, calcium appears to be able to permeate the channel which is activated by 5-HT through cAMP. However, under normal sodium and low calcium conditions, the IBMX current was more than two times larger than that measured under normal recording conditions. This suggests that calcium also plays a major inhibitory role in the conduction of this current.

iv) Protein kinase inhibition does not influence the activities of 5-HT on neuron B19

There are two separate mechanisms through which cyclic nucleotides can influence the activity of ion channels. In vertebrate rods and olfactory receptors, cyclic nucleotides directly gate open ion channels (Kaupp, 1991). Alternatively, there are many well documented instances describing cyclic nucleotide activation of protein kinases. The kinase then phosphorylates target ion channels, which results in their opening or closure (Hille, 1992).

To evaluate which mechanism is responsible for the activation of 5-HT-dependent inward current in neuron B19, the effects of protein kinase inhibitors were tested. Recordings were obtained from neurite-lacking cells, using an electrode solution that contained 100 μM of the relatively non-specific kinase inhibitor H7. At this concentration H7 should inhibit

the activity of most kinases in the cell. Under these conditions, bath exchange for saline containing 25 μM 5-HT still resulted in the activation of inward current (Figure IV-11). The amplitude of the current averaged 49.3 ± 7.9 pA (n=7). T-test comparison of the amplitude of the 5-HT-dependent inward current when H7 was present in the electrode with that measured from neurite-lacking cells when H7 was not present (mean: 55.8 ± 2.9 pA), revealed no significant difference (p=0.619). Furthermore, in current clamp experiments in which the electrode solution contained either 50 μM H7 or 10 μM of the more specific cAMP-dependent kinase inhibitor H89, 5-HT exposure still resulted in robust membrane depolarization (data not shown, n= 4 and 3, respectively).

Staircase experiments were also performed to determine if H7 had any effect on the shape of the 5-HT difference current. Steady-state I/V curves were obtained from cells using an H7-containing electrode solution before and during exposure to 25 μM 5-HT (Figure IV-12, top panel), and the difference current calculated (Figure IV-12, bottom panel). Examination of this current revealed that the shape was similar to that obtained in the absence of H7, however, the reversal potential for some unknown reason has shifted to more positive potentials. Nevertheless, the possibility exists that the current underlying 5-HT-dependent depolarization of neuron B19 is carried by an ion channel that is directly gated by cyclic nucleotides.

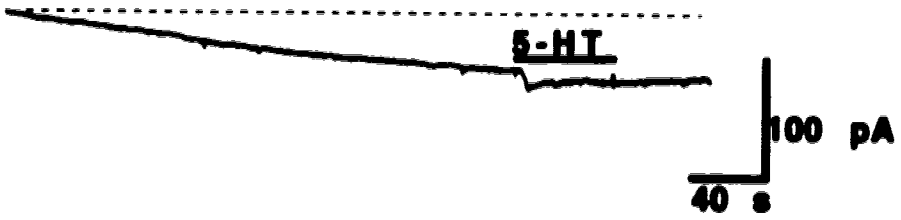

Figure IV-1: G-protein involvement in activation of 5-HT-dependent inward current. Voltage clamp recording from a neuron B19 lacking neurites in which the recording electrode contained 200 μM of the non-hydrolyzable GTP analogue GTPγS. Bath exchange for 25 μM 5-HT-containing saline resulted in only a very small amount of current activation. Note the steady inward drift of the baseline current level prior to 5-HT exposure. This likely reflects action of the current normally activated by 5-HT by the GTP analogue as the analogue diffuses from the electrode into the cell. Bar indicates the duration of 5-HT exposure, while the dotted line represents the baseline current level at the start of the recording. Holding potential was -70 mV.

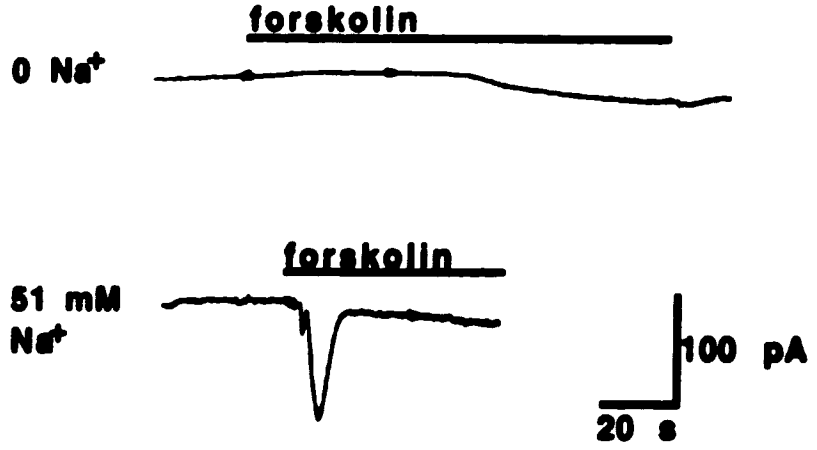

Figure IV-2: The adenylate cyclase activator forskolin induces the transient activation of a sodium current in neuron B19. Upper trace: Exposure to 32 μM forskolin under choline substituted sodium-free conditions had minimal effect on membrane holding current. Lower trace: Under normal sodium-containing conditions, 32 μM forskolin caused the transient activation of an inward current. Both upper and lower traces are from the same cell, with the experiment performed in the order of presentation. Bars indicate the duration of exposure to forskolin; holding potential was -70 mV. A version of this figure has been published previously (Price and Goldberg, 1993).

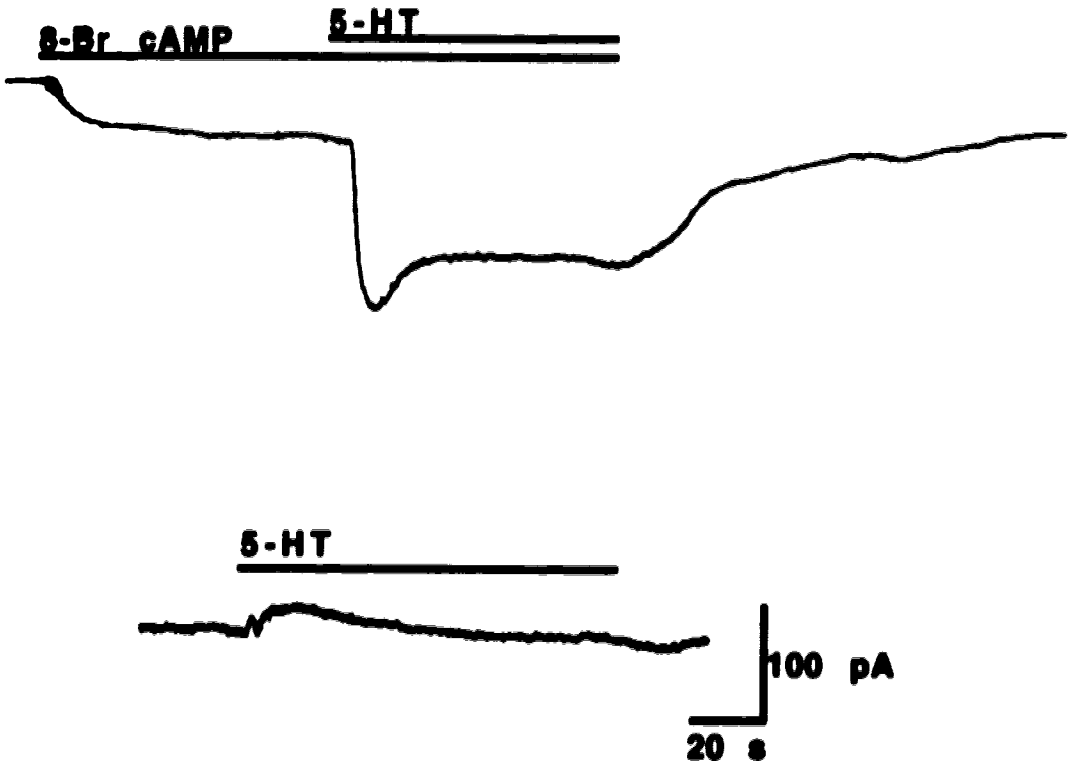

Figure IV-3: 8-Bromo cAMP activation of inward current. **Upper trace:** Bath exchange for saline containing 2 mM 8-bromo cAMP resulted in the activation of a maintained inward current. However, subsequent application of 25 μM 5-HT resulted in the activation of additional inward current. **Lower trace:** Recording from a neuron B19 cell body lacking neurites where the electrode solution contained 100 μM 8-bromo cAMP. Bath exchange for 25 μM 5-HT failed to result in inward current activation. The transient outward current is an artifact associated with the perfusion system that was occasionally observed. A version of this figure has been published previously (Price and Goldberg, 1993).

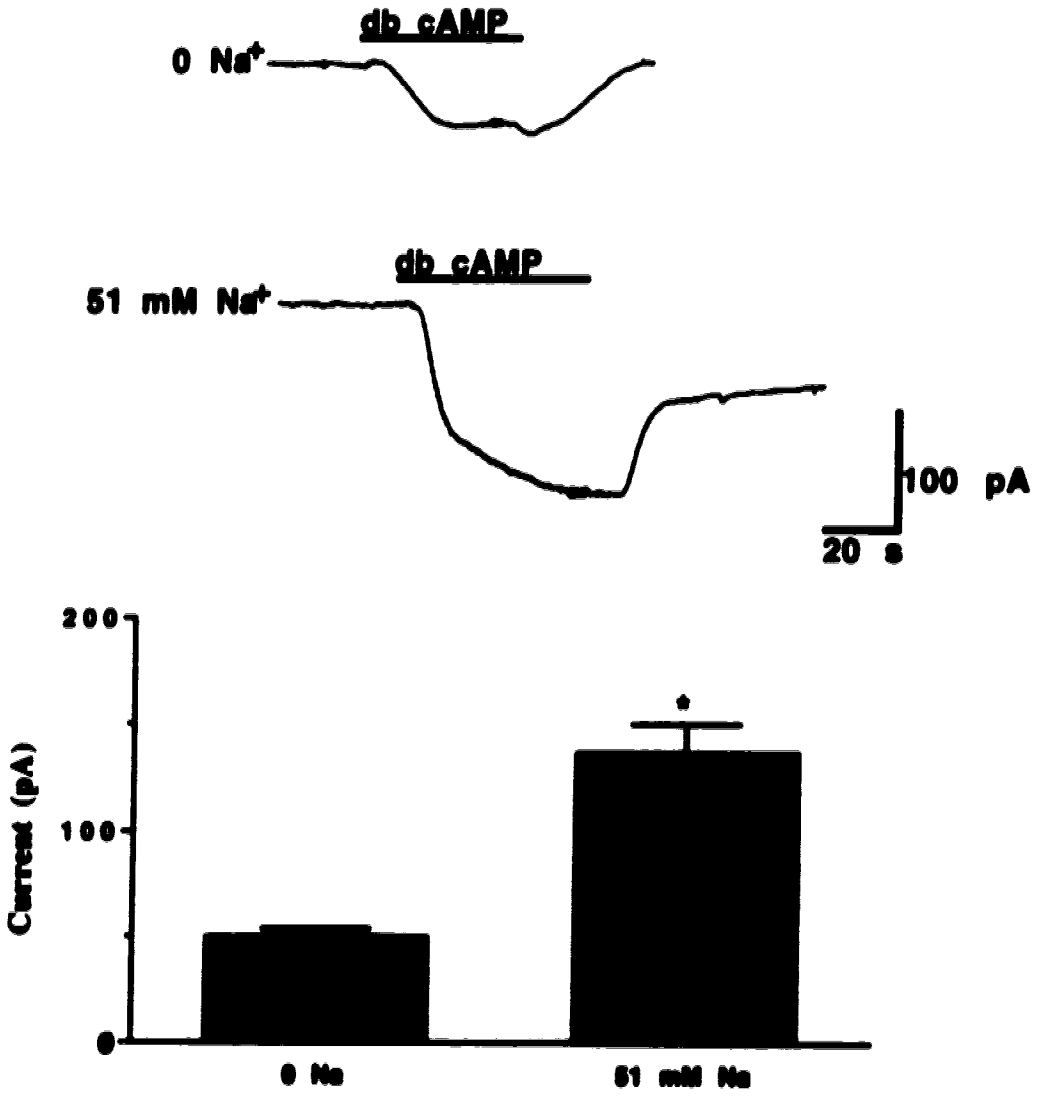

Figure IV-4: Sodium dependency of cAMP-activated inward current. Inward current induced by 2 mM db cAMP in the absence (upper trace) and the presence of (lower trace) sodium. Traces were recorded from the same cell and the experiments performed in the order of presentation. Bars indicate duration of db cAMP exposure; holding potential was -70 mV. Choline substituted for sodium in sodium-free saline. Bottom panel: Summary of the results of paired experiments as outlined above, from three cells.

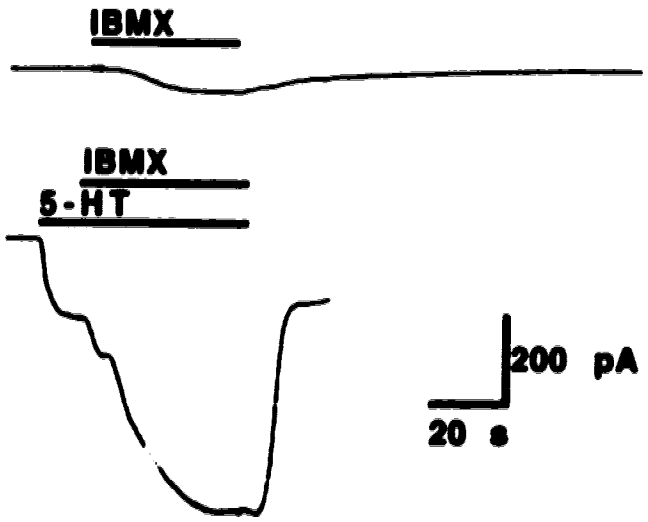

Figure IV-5: IBMX potentiation of 5-HT-dependent inward current. **Upper trace:** Bath exchange for saline containing 0.5 mM IBMX resulted in the activation of inward current. **Lower trace:** When IBMX exposure was preceded by 25 μM 5-HT exposure, the resulting IBMX-induced current was much larger in amplitude. Traces were recorded from the same cell and the experiment was carried out in the order of presentation. Bars indicate duration of IBMX and 5-HT exposure; holding potential was -70 mV. A version of this figure has been published previously (Price and Goldberg, 1993).

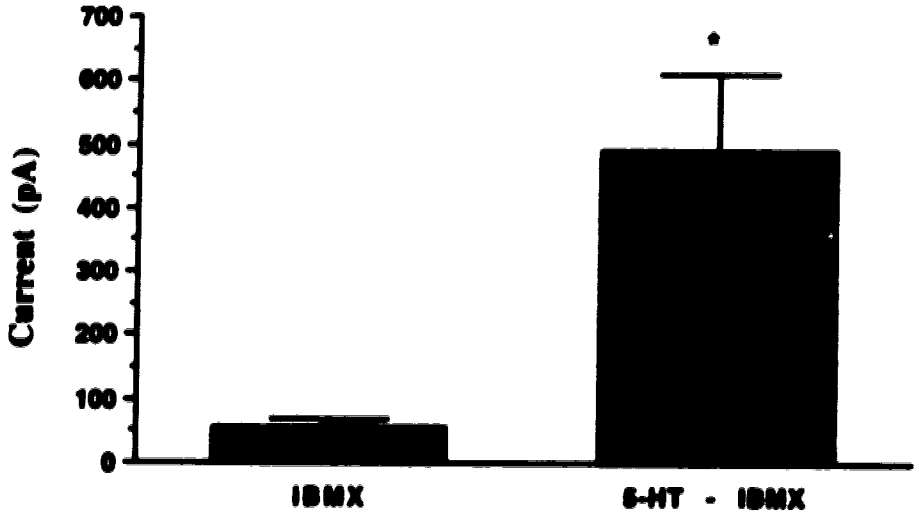

Figure IV-6: IBMX-induced current is significantly increased if preceded by 5-HT exposure. Graph summarizing the results of six paired experiments, performed as described in Figure IV-5. Paired t-test analysis revealed this difference to be significant (p=0.0063).

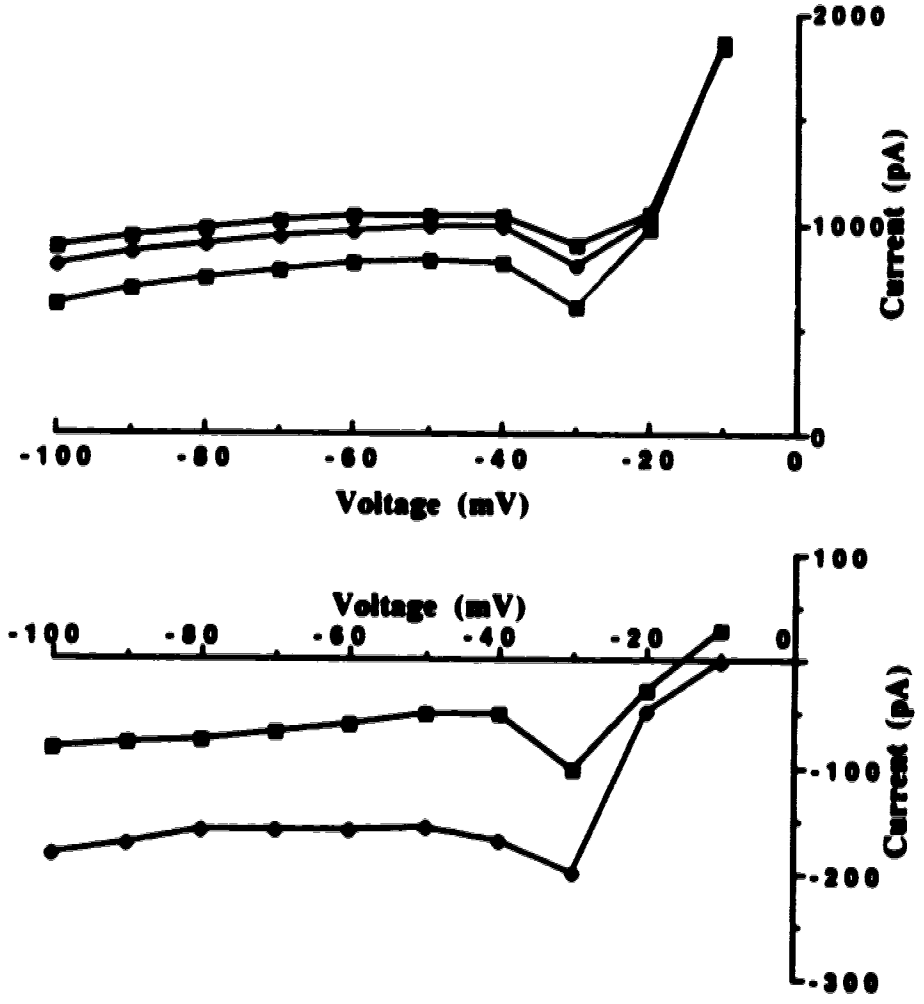

Figure IV-7: IBMX potentiates the same current as that activated by 5-HT. Top panel: Steady-state I/V curves obtained from a staircase experiment performed before exposure to 25 μM 5-HT (open symbols), during exposure to 5-HT (closed diamonds) and during exposure to 5-HT and 0.5 mM IBMX (closed squares). Lower panel: Difference current I/V curves calculated from the above experiments for 5-HT dependent (open symbols) and IBMX-potentiated (closed symbols) current. 5-HT difference current was calculated in the usual manner, while the IBMX difference current was calculated by subtracting the 5-HT staircase from the IBMX staircase. The similarity in shape of the two difference currents indicates that IBMX acts on the same current as 5-HT.

Figure IV-8: IBMX-potentiation of 5-HT-dependent inward current was still apparent in zero-sodium conditions. Exposure of neuron B19 to 25 μM 5-HT recorded in sodium-free saline resulted in a small amount of inward current. Subsequent exposure to 0.5 mM IBMX resulted in a fairly substantial amount of inward current. Bars indicate duration of 5-HT and IBMX exposure; holding potential -70 mV. The four disturbances in the recording indicate where staircase voltage stimuli were applied to the cell.

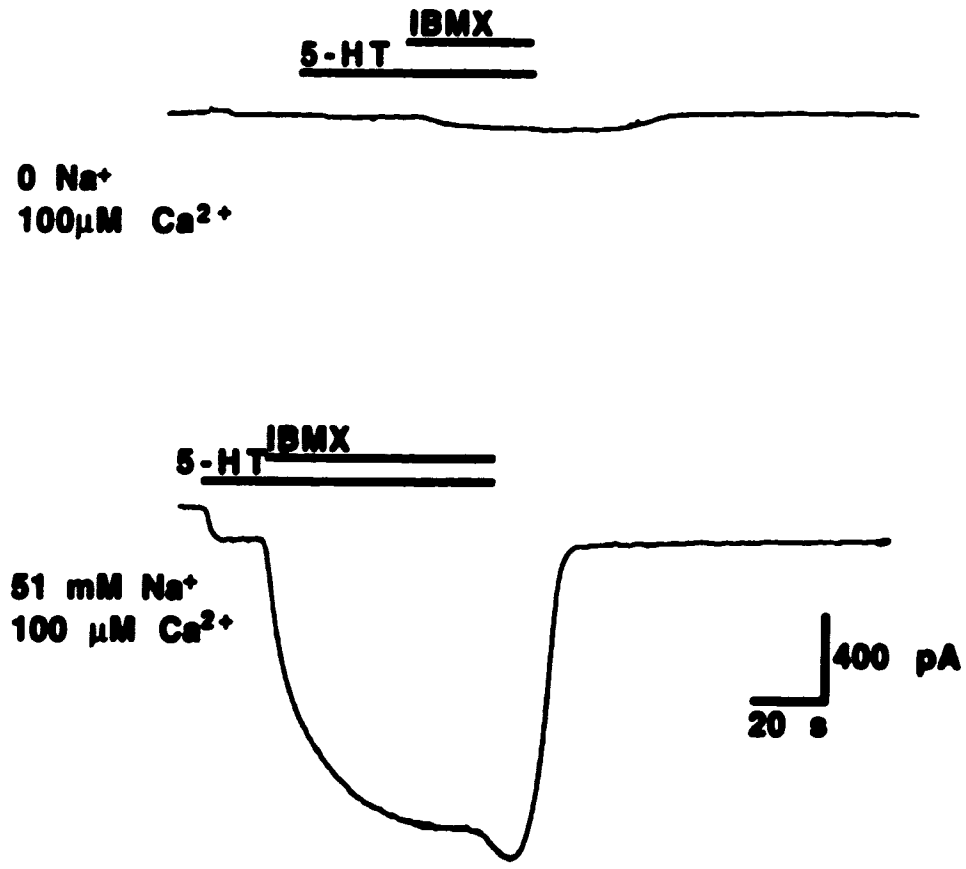

Figure IV-9: Sodium and calcium sensitivity of IBMX-potentiated inward current. **Top trace:** The 5-HT-dependent and IBMX-potentiated inward currents recorded in saline which contained zero sodium and approximately 100 μM calcium were extremely small. **Lower trace:** When the above saline was exchanged for 51 mM sodium and approximately 100 μM calcium saline, very large amplitude 5-HT and IBMX-potentiated inward currents were recorded. both traces were recorded from the same cell, and the experiment was performed in the order of presentation. Bars indicate duration of 5-HT and IBMX exposure; holding potential was -70 mV. Tris served to substitute for sodium. A version of this figure has been published previously (Price and Goldberg, 1993).

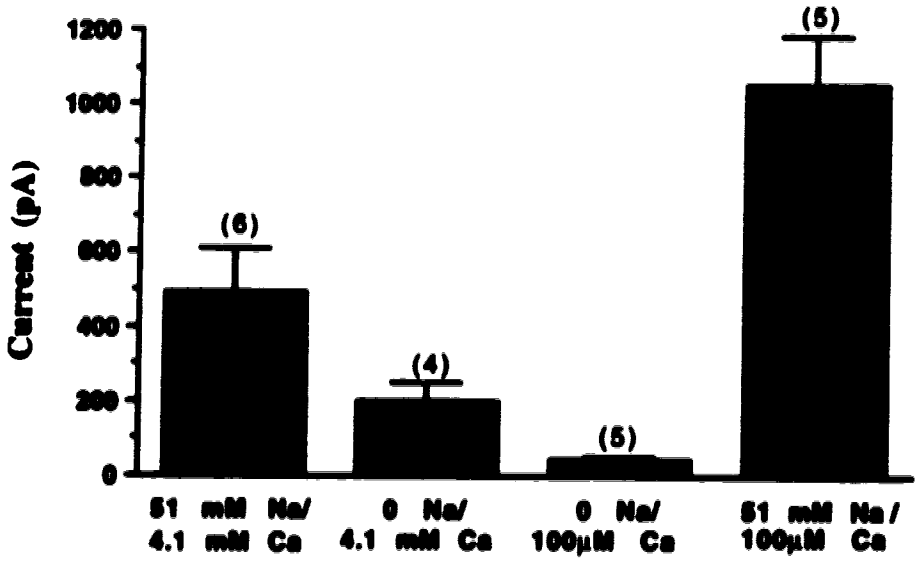

Figure IV-10: Graph summarizing the ionic dependency of IBMX-potentiated current in neuron B19. Shown are the mean amplitude of currents recorded in response to 0.5 mM IBMX following initial stimulation with 25 μM 5-HT. The 5-HT-activated current was not included in the measurments. Only cells which possessed neurite outgrowth were used in this comparison. Note that the largest IBMX-potentiated currents were recorded under low calcium conditions. Moreover, significant current was recorded under normal calcium and zero sodium conditions. Numbers appearing in brackets indicate the number of cells used in each treatment. A version of this figure has been published previously (Price and Goldberg, 1993).

Figure IV-11: Protein kinase inhibitor H7 does not prevent activation of 5-HT-dependent inward current. Bath exchange for 25 μM 5-HT-containing saline induced inward current in neuron B19 despite the electrode solution containing 100 μM H7. The cell lacked neurites to facilitate diffusion. Bars indicate duration of 5-HT exposure; holding potential was -70 mV.

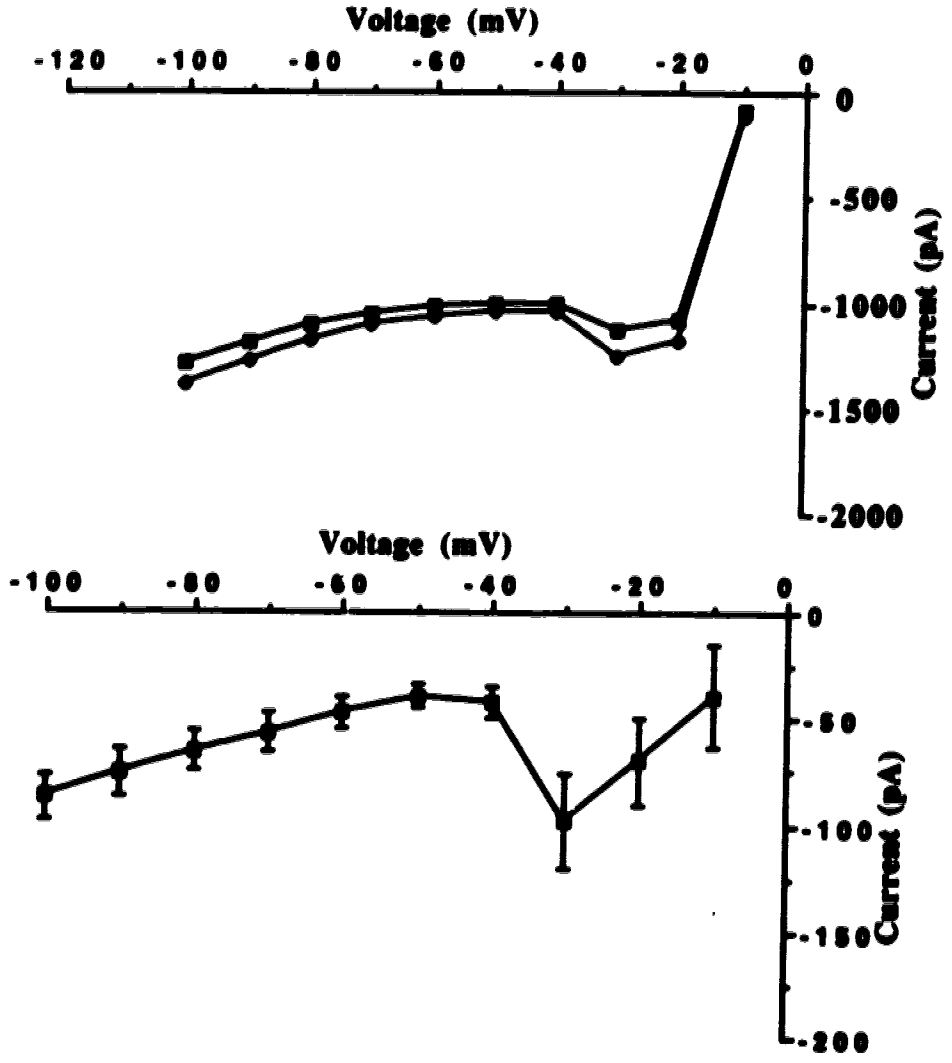

Figure IV-12: Both components of the 5-HT response do not appear to involve protein kinase activity. Top panel: steady-state I/V curves before (open symbols) and during (closed symbols) exposure to 25 μM 5-HT obtained from staircase experiments performed with an electrode solution containing 100 μM H7. Bottom panel: Mean difference current for seven cells recorded with H7 containing electrode solution. The I/V relationship obtained under H7 conditions was similar to that seen under normal conditions. The only difference noticed was a curious positive shift in the reversal potential. All cells used in these experiments lacked neurites.

V) Single channel analysis of 5-HT-dependent inward current

A major advantage of the patch clamp recording technique is that the different recording configurations provide several different experimental approaches to examine electrophysiological phenomena. From studies of whole-cell currents, several characteristics of the ion current responsible for 5-HT-dependent depolarization of neuron B19 were identified. One particularly interesting characteristic is that this current's activation does not appear to depend on phosphorylation. Single channel analysis provides an additional way to examine this hypothesis. Through the use of cell-free inside-out membrane patches, it is possible to test if a substance directly activates an ion channel. Therefore this approach was employed to test the hypothesis that cAMP directly activates the ion channel responsible for 5-HT-dependent inward current.

i) 5-HT activates a small amplitude single channel current in cell-attached membrane patches.

To initiate this study cell-attached patch recordings were obtained from neuron B19 and the response to bath applied 5-HT determined. Cell-attached patches were often quite stable and would last 15 to 30 minutes or more without visible signs of seal breakdown. Recording electrodes with very small amplitude openings tended to yield more stable recordings. With a potential of 0 or -30 mV applied to the pipette (i.e. the membrane patch allowed to follow the cell's membrane potential or hyperpolarized 30 mV from the cell's membrane potential), recordings were generally free of spontaneous channel activity. However, upon bath application of 5-HT (25 μM final concentration) an ion channel with a small amplitude current was often observed (Figure V-1). 5-HT-induced channel activity generally coincided with the appearance of action potentials in the recording (not shown). These action potentials reflect the 5-HT-dependent depolarization of the cell and were useful as indicators of when the 5-HT had actually reached and stimulated the cell. The channel openings were generally clustered into bursts of activity,

which were often interspersed with long periods of inactivity (Figure V-1). Prior to 5-HT exposure, infrequent channel openings were occasionally observed. However, of 16 patches that demonstrated robust single channel activity, in only three instances was this type of activity seen in the absence of 5-HT.

One of the features of the ion channel activated following 5-HT exposure was its small amplitude. From records of channel activity with minimal action potential activity, which facilitated the automated measurement of single channel events, amplitude histograms were generated (Figure V-2). Amplitude histograms were fit well by a single Gaussian distribution. The mean unitary current amplitudes obtained from the Gaussian distribution were in the 0.3 to 0.5 pA range. The small size of the unitary current necessitated the use of heavy filtering in both the viewing and measurement of these events (see methods). This was especially important for the automated analysis of channel events to allow unambiguous discrimination between baseline levels and open levels using the 50% threshold crossing criteria. Therefore, the unavoidable effects of heavy filtering on the underestimation of current amplitudes and on missing very fast, high frequency events must be kept in mind when interpreting these data (Colquhoun and Sigworth, 1983).

Owing to the physical nature of the cell-attached patch, the finding that bath applied 5-HT induces channel activity within the membrane patch is consistent with the hypothesis that 5-HT stimulates the formation of a diffusible second messenger which activates the channel. It is unlikely 5-HT could gain access to the extracellular surface of the membrane patch, and therefore to the 5-HT receptors, by crossing the giga-ohm seal. To determine if cAMP could mimic this activity in cell attached patches, recordings were obtained with 8-Br cAMP included in the electrode solution. Under these conditions robust single channel activity was observed that was similar to that seen with bath applied 5-HT (Figure V-3). Channel events had mean unitary amplitudes of near 0.5 pA and were clustered into bursts of openings. Similarly, when the

bath solution contained 100 or 250 μM IBMX robust channel activity was also observed in the absence of 5-HT. All together, robust channel activity in the absence of 5-HT was observed in 11 cell attached patches where 8-Br cAMP was included in the pipette or with IBMX in the bathing saline.

ii) Inside-out patch recordings

According to whole-cell recording experiments on the effects of protein kinase inhibitors, 5-HT activation of inward current does not appear to involve protein phosphorylation. This finding prompted the hypothesis that cAMP directly activates the ion channels involved. To directly test this possibility, inside-out patch recordings were obtained and cAMP was applied under conditions that did not favor phosphorylation. Several disadvantages of the cell-attached recording configuration were avoidable using cell-free membrane patches. In cell-free patch recordings the absolute value of the voltage difference across the patch clamped membrane is known. This is unlike the cell-attached patch where the unclamped membrane potential of the cell influences the potential across the membrane patch. As a result, unless the cell's membrane potential is controlled separately with additional electrodes or the cell's membrane potential is zeroed with a high potassium bathing saline, the cell's potential would remain an uncontrollable variable. Therefore, cell-free patches facilitate the determination of unitary current/voltage relationships. This advantage, coupled with the ability to apply and wash away cAMP from the intracellular surface of the membrane, made inside-out patches an attractive experimental system for examining the 5-HT-activated channel.

Recordings from inside out patches were quite stable in saline containing 0 Ca^{2+}/ 1.5 mM Mg^{2+}. Upon bath application of cAMP (100 μM final concentration), recordings generally became extremely noisy (Figure V-4). Initially this was attributed to seal damage that occurred during application of the cAMP. However, this "noise" was reversible on

washing with fresh saline. Moreover, channel activity involving individual openings of small amplitude inward current was observed following the crude washout procedure. Because no phosphate donors for phosphorylation were present, these results suggest cAMP was directly activating a population of ion channels located within the membrane patch.

Two approaches were taken to test whether the activity induced by a large dose of cAMP reflected the activation of several small amplitude cAMP-activated ion channels within the membrane patch. Firstly, in two experiments 100 μM cAMP was applied to the bath far enough from the electrode tip to ensure slow exposure of the patch to cAMP. This resulted in the gradual buildup of the noise-like activity (Figure V-5). Moreover, this activity appeared to grow in approximately 0.5 pA increments, with individual channel events clearly apparent. Secondly, experiments were performed in which membrane patches were exposed to increasing doses of cAMP. At the lowest dose of cAMP (1 μM) infrequent channel activity was generally observed (Figure V-6). At 10 μM channel activity increased, while at 100 μM cAMP, channel activity was continuous with definite multiple openings. This is strong evidence that several channels contributed to the response seen with high doses of cAMP.

Also included in Figure V-6 is a segment of the same recording made prior to patch excision, with 25 μM 5-HT present in the bath. The similarity of the single channel currents recorded in the cell-attached configuration with those measured in the inside-out configuration reinforces the idea that the channels that underlie the 5-HT-dependent inward current are the same as those that underlie the cAMP-dependent inward current.

Two additional results of the inside-out patch experiments are worth noting. Firstly, it was observed that infrequent activity of the cAMP-dependent channel could occur in the absence of cAMP. An example of such an event can be seen in the uppermost trace of Figure V-4. This

spontaneous activity suggests that channel activation is not completely dependent on cAMP, however cAMP would greatly increase the probability of channel opening. The second result concerns the frequency of success in finding channels within a given patch. Of the 31 patches tested for sensitivity to cAMP, 29 showed definite channel activity. Coupled with the finding that most patches contained multiple channels, this channel must be widely and uniformly distributed over the neuron B19 cell body surface.

The distribution of closed times is a very useful factor in the analysis of single channel records providing information on the number of kinetically different states a channel can occupy (Colquhoun and Hawkes, 1983). However, when there are multiple channels present in a patch, as occurred most often in this study, the closed time distribution is meaningless. In this situation it is impossible to determine if two adjacent openings in a record are from the same individual channel. However, the total amount of time in which there are no openings, ie. the total closed time, is a useful indicator of the probability of channel opening. With no cAMP present, channels had a low probability of opening, reflected in 95 ± 1.6% of the time no channels were open (Figure V-7). With 1 μM cAMP, a similar proportion of time showed no channel openings (96.5 ± 0.6%; p=0.1229). At 10 μM cAMP the proportion of time with no channel openings decreased to 73.5 ± 12.7% and ranged from 14.1% to 95.5%. While the difference observed was not statistically significant (p=0.1438), it does suggest that 10 μM is near the threshold dose for the response. At 100 μM cAMP there was a statistically significant decrease in the fraction of time where no channel openings were observed (33.9 ± 20.5%; p=0.0065). In fact this value is likely to be an overestimation of the actual total closed time at 100 μM cAMP, since in the majority of the records no definite baseline could be determined owing to the intense channel activity. Therefore, these records were not used in calculations. From these data it is clear that there is a steep dose-response relationship with a threshold for cAMP-dependent channel activation near the 10 μM level.

iii) Unitary current/voltage relationships for the cAMP-activated channel

To aid in comparing the neuron B19 cAMP-activated channel with ion channels from other preparations which show direct activation by cyclic nucleotides, experiments were performed to determine the channel conductance. Moreover, given the previous results with calcium ion inhibition of whole cell 5-HT responses (see chapters III and IV), the effect of divalent cations on the ability of the channel to conduct current was examined. Interestingly, studies of vertebrate cyclic nucleotide-gated ion channels indicate that divalents cations also exert inhibitory effects on the conduction of current (Kaupp, 1991).

When the potential across the membrane patch was held at negative potentials (inside negative relative to outside), single channel currents were inwardly directed. Currents decreased in amplitude with less negative voltages and were not measurable at 0 mV (Figure V-8). However, at positive potentials, one of three results was observed. In some cases there was no measurable outward current, while on other occasions, measureable outward currents of normal appearance were observed. The third result, shown in Figure V-8, was intermediate between these two extremes. In these cases definite outward currents were observed, however these were irregular in appearance when compared with the inward currents.

Magnesium ions present in the bathing solution in the above experiment may have influenced the conduction of outward current in these patches. To test this possibility the bathing solution was exchanged for divalent cation-free saline, while recording from the same membrane patch shown in Figure V-8. The outward currents now observed were more similar in appearance to the inward currents (Figure V-9). Outward currents under divalent-free conditions were significantly larger than when recorded under magnesium-containing conditions, as

determined by paired t-tests (+60 mV, p=0.0202; +90 mV, p=0.0072; n=3).

To obtain i/V curves for the cAMP-activated channel the results from a number of separate experiments were pooled and are presented in Figure V-10. The single channel conductance estimated by calculating the slope between -90 and -60 mV was 7.3 pS. In regards to the shape of the graph under magnesium-containing and divalent-free conditions, the curve became somewhat more linear and symmetrical under divalent-free conditons.

iv) cGMP-activates the same channel as cAMP

Some vertebrate cyclic nucleotide-gated channels, most notably those found in olfactory receptors, can be activated by either cAMP or cGMP (Kaupp, 1991). This raised the possibility that the neuron B19 cAMP-activated channel may also be sensitive to cGMP. When cGMP was added to inside-out neuron B19 membrane patches, a dose-dependent increase in channel activity, similar to that seen with cAMP, was observed (Figure V-11). Like cAMP the threshold concentration for activation was around 10 μM. However, this was not studied to the same extent as for cAMP.

An example of an i/V curve from a representative cGMP-activated channel is presented in Figure V-12. Like that seen for cAMP, under 0 mM Ca^{2+}/ 1.5 mM Mg^{2+} bath conditions, the unitary conductance calculated between -90 and -60 mV was small, having a value of 6.8 pS. Similarly, in magnesium-containing conditions outward currents were inhibited, and in this example unmeasureable. However, on replacement of the bath saline with a divalent cation-free saline, measureable outward currents were observed. These results therefore support the conclusion that the channel activated by cGMP is the same channel as that activated by cAMP. This finding stimulates the interesting suggestion that the cyclic nucleotide-activated ion channel of neuron B19 serves as a

convergence point for two separate second messenger systems. However, it also raises the question of which cyclic nucleotide, cAMP or cGMP, is the actual physiological second messenger mediating the 5-HT-activated response.

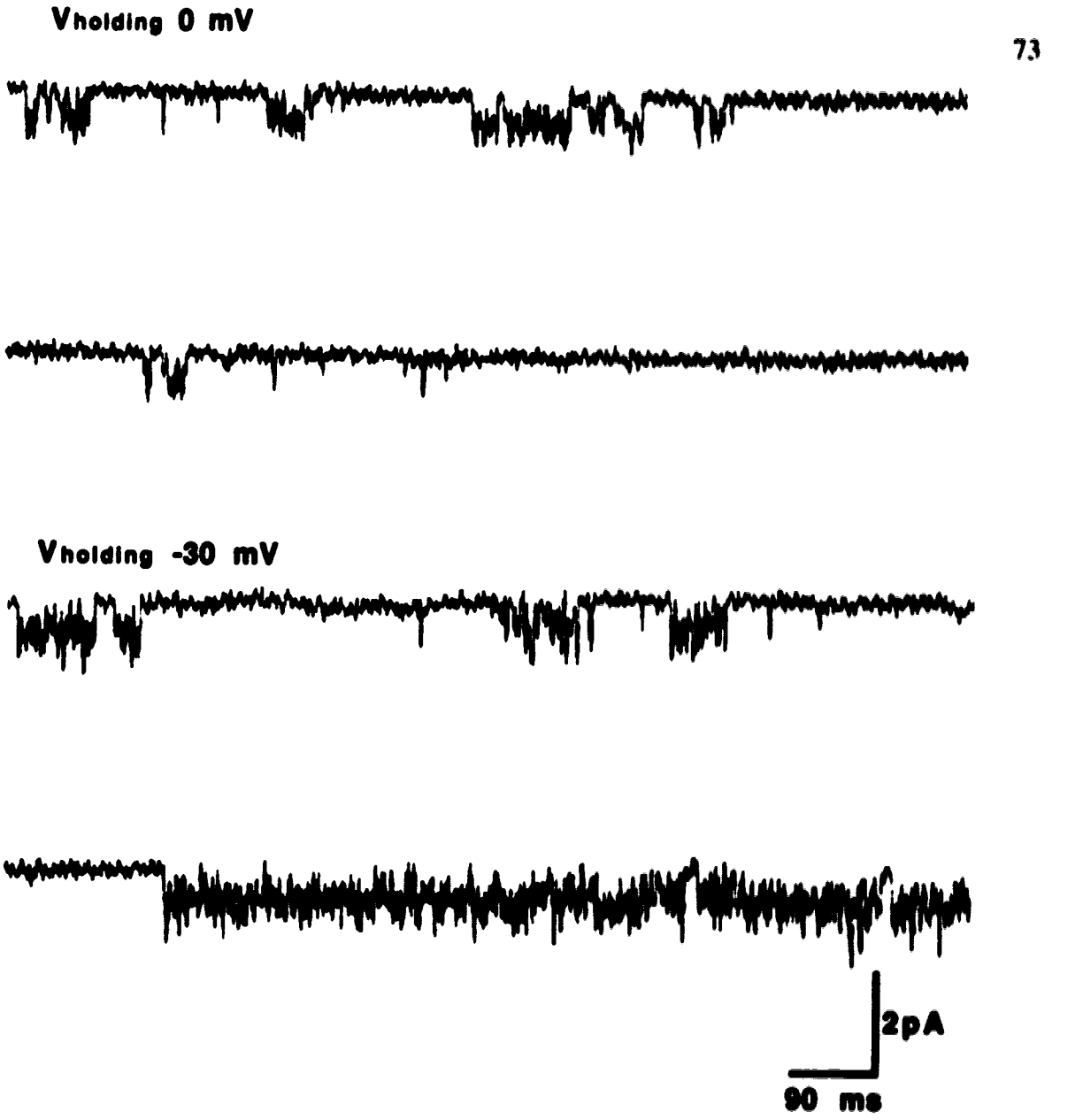

Figure V-1: 5-HT activates a small conductance ion channel in neuron B19. Bath application of 25 μM 5-HT resulted in the appearance of a small amplitude single channel current in cell-attached patch recordings. This type of activity was only infrequently observed in the absence of 5-HT (not shown). The records shown were with potentials of 0 and -30 mV applied to the electrode.

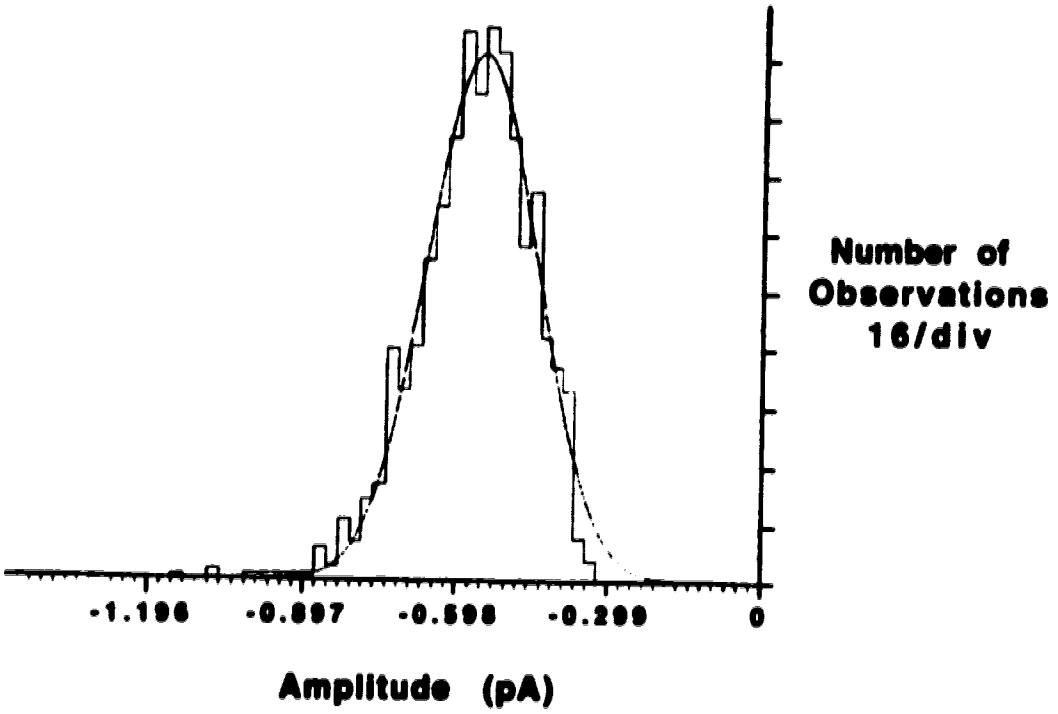

Figure V-2: A small amplitude current is conducted through the 5-HT-dependent ion channel. Amplitude histogram and Gaussian fit obtained from a cell-attached patch recording following bath application of 5-HT (25 μM final concentration). The single channel current had a mean amplitude of 0.5 pA with a holding potential of -30 mV applied to the electrode.

Figure V-3: 8-bromo cAMP activates a small amplitude ion current. **Top traces:** In a cell-attached patch recording performed using an electrode solution containing 50 μM 8-bromo cAMP, ion channel activity similar to that seen following bath application of 5-HT was recorded. -30 mV potential was applied to the electrode. **Lower panel:** Amplitude histogram and associated Gaussian fit revealed that the 8-bromo cAMP-activated single channel current was small amplitude, similar to that seen for the 5-HT-dependent channel. In this example, the mean amplitude was -0.47 pA, recorded with 0 mV applied to the electrode.

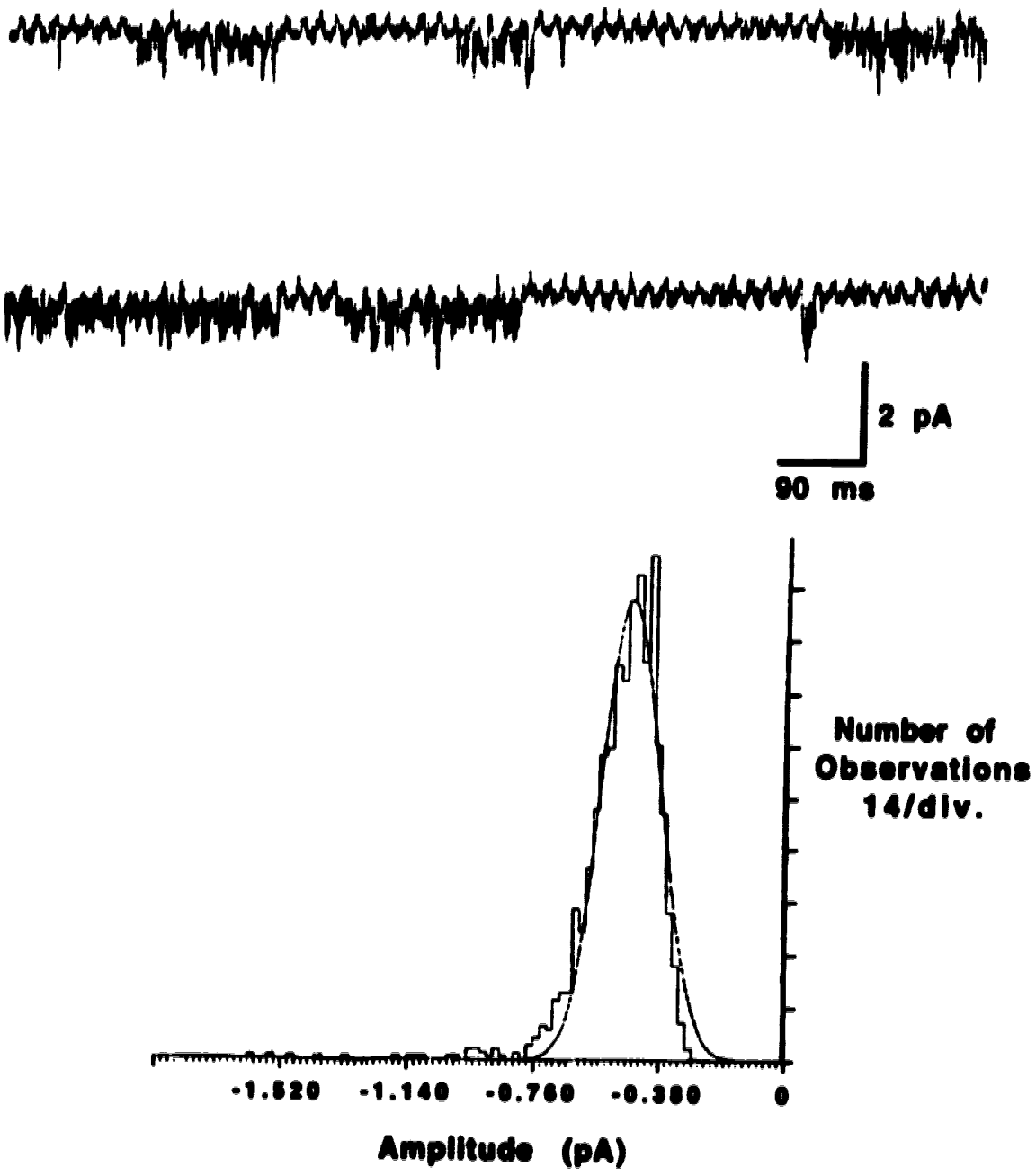
2 pA
90 ms
Number of Observations 14/div.
-1.520
-1.140
-0.760
-0.380
0
Amplitude (pA)

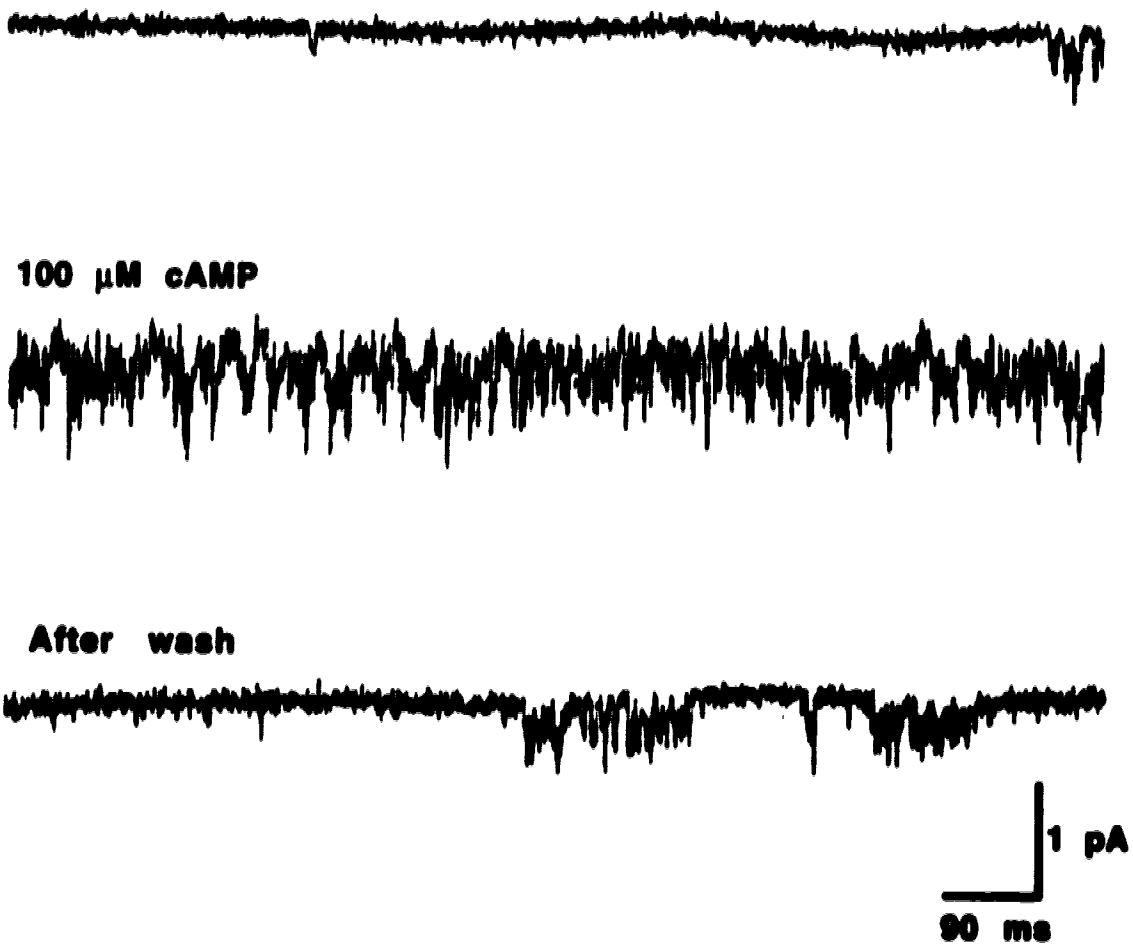

Figure V-4: cAMP activates ion channels in inside-out patches. Top trace: Inside-out patch recording obtained from neuron B19 with -60 mV potential applied to the electrode. Middle trace: Following bath application of cAMP (100 µM final concentration) a great deal of ion channel activity was recorded. Lower trace: Channel activity decreased upon washing with fresh saline.

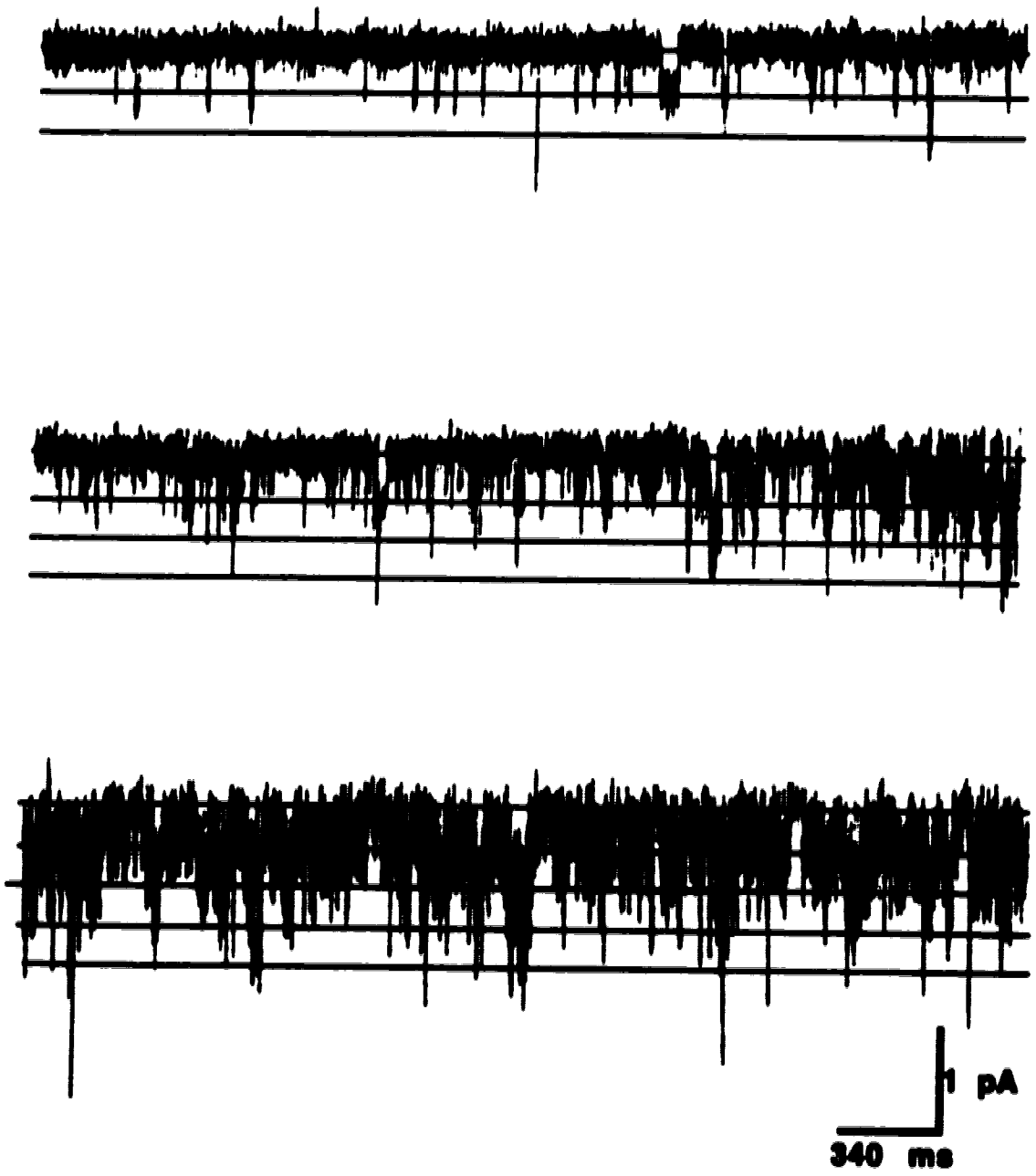

Figure V-5: Inside-out patches contain several cAMP-dependent ion channels. 100 μM cAMP was applied at a distance from an inside-out patch to allow slower activation of the cAMP-dependent ion channels. Shown are consecutive five second long recording segments where cAMP was applied just prior to the beginning of the first trace. A potential of -60 mV was applied to the electrode. Lines within the traces indicate the approximate baseline level and up to 4 open levels.

Figure V-6: Activation of ion channels by cAMP is dose-dependent. **First trace:** Cell-attached patch recording of ion channel activity with 25 μM 5-HT present in the bath. **Second trace:** Upon excision of the above patch, single channel activity was reduced. **Third to fifth traces:** Increasing doses of cAMP resulted in a dose-dependent return of channel activity. **Sixth trace:** Channel activation by cAMP was reversible upon washing with fresh saline. In all traces a potential of -60 mV was applied to the electrode.

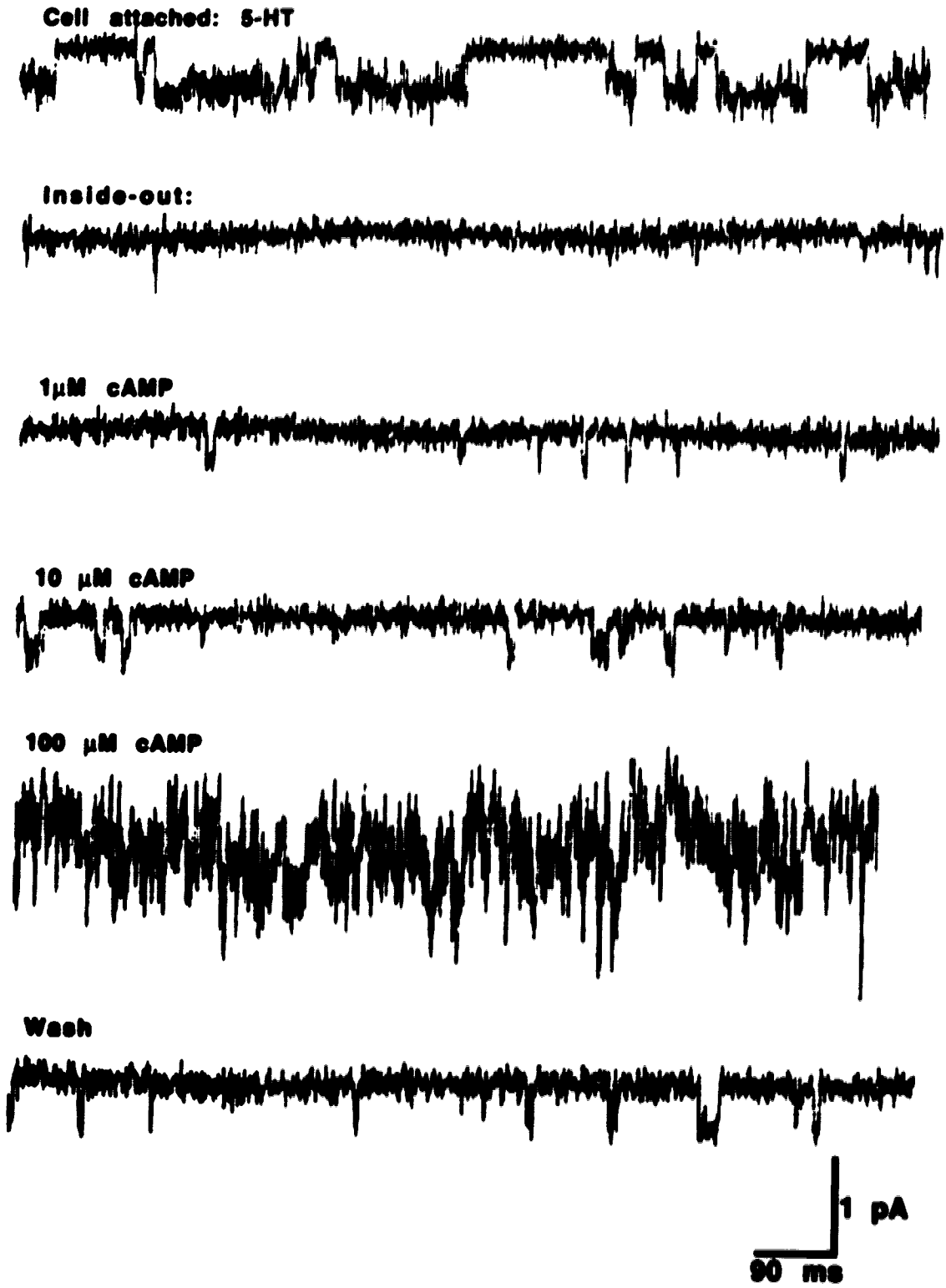
Cell attached: 5-HT
Inside-out:
1μM cAMP
10 μM cAMP
100 μM cAMP
Wash
1 pA
90 ms

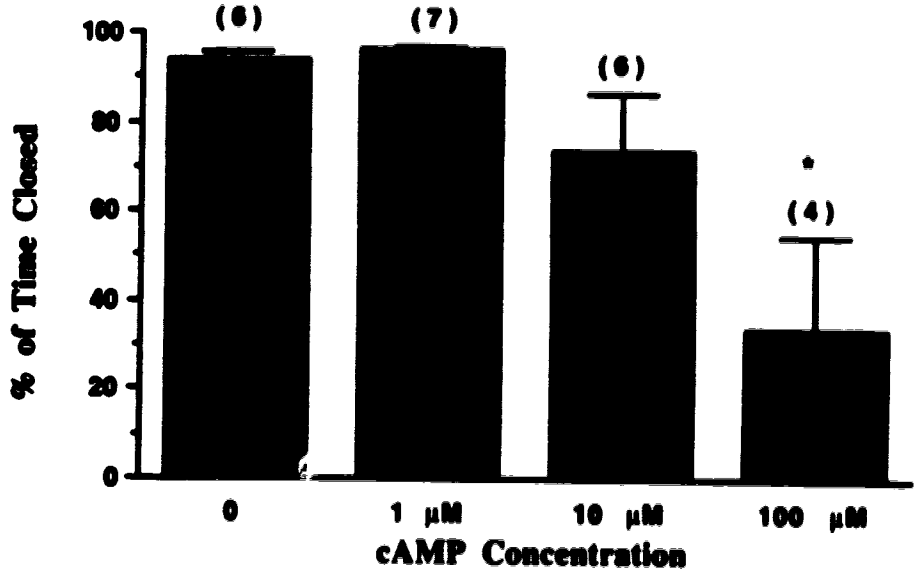

Figure V-7: Dose-dependent decrease in the total closed time. With increasing doses of cAMP less time was spent at the closed level over the duration of the recording with the threshold concentration near 10 µM. At 100 µM this difference was statistically significant. Numbers in brackets indicate the N form each concentration.

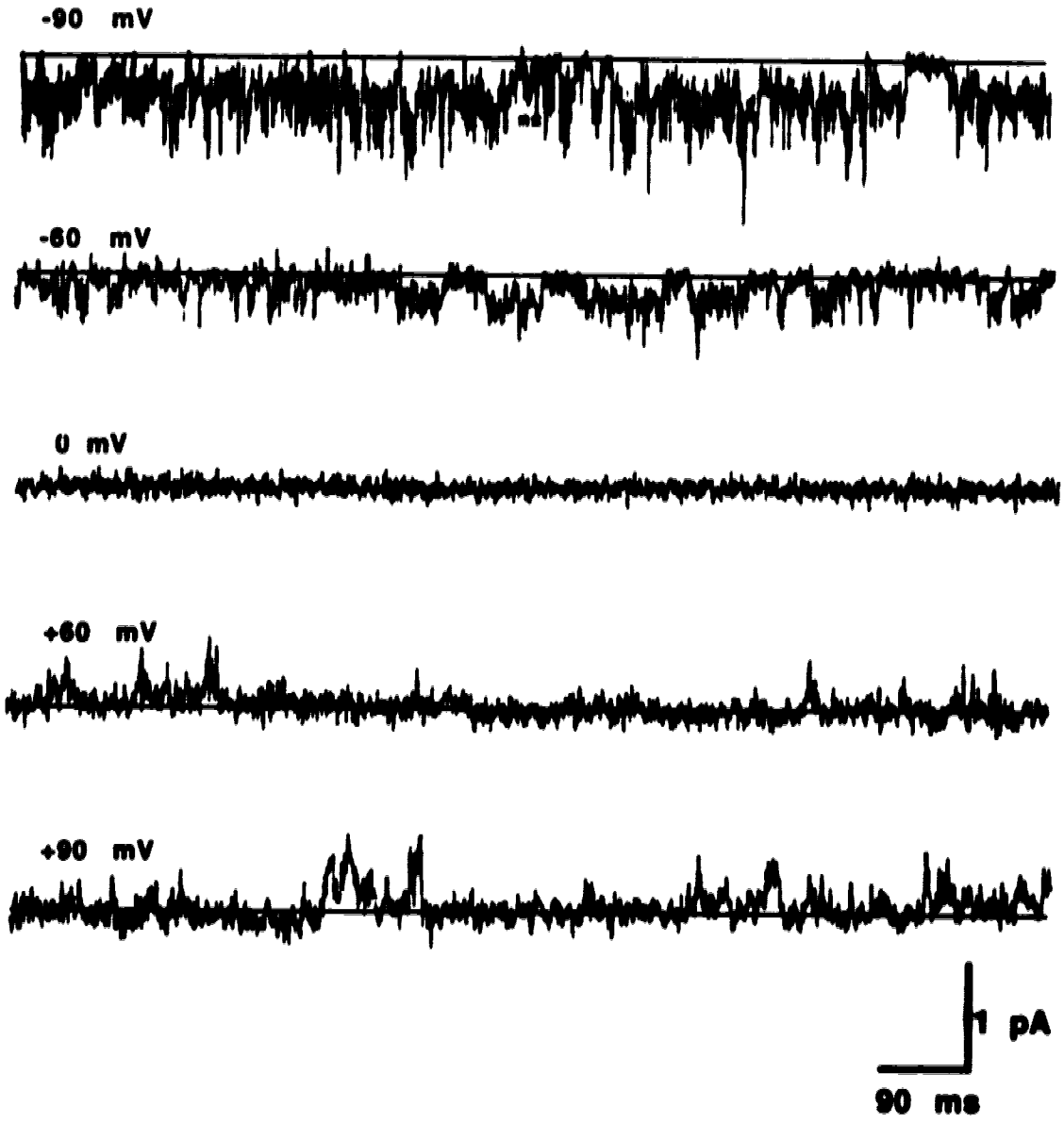

Figure V-8: cAMP-activated channels conduct better in the inward direction when recorded in divalent cation-containing saline. Traces shown were recorded at the indicated electrode potentials in 0 Ca^{2+}, 1.5 mM Mg^{2+} containing bathing saline, with 100 μM cAMP present. Note at positive potentials channel openings were less frequent and quite irregular in appearance.

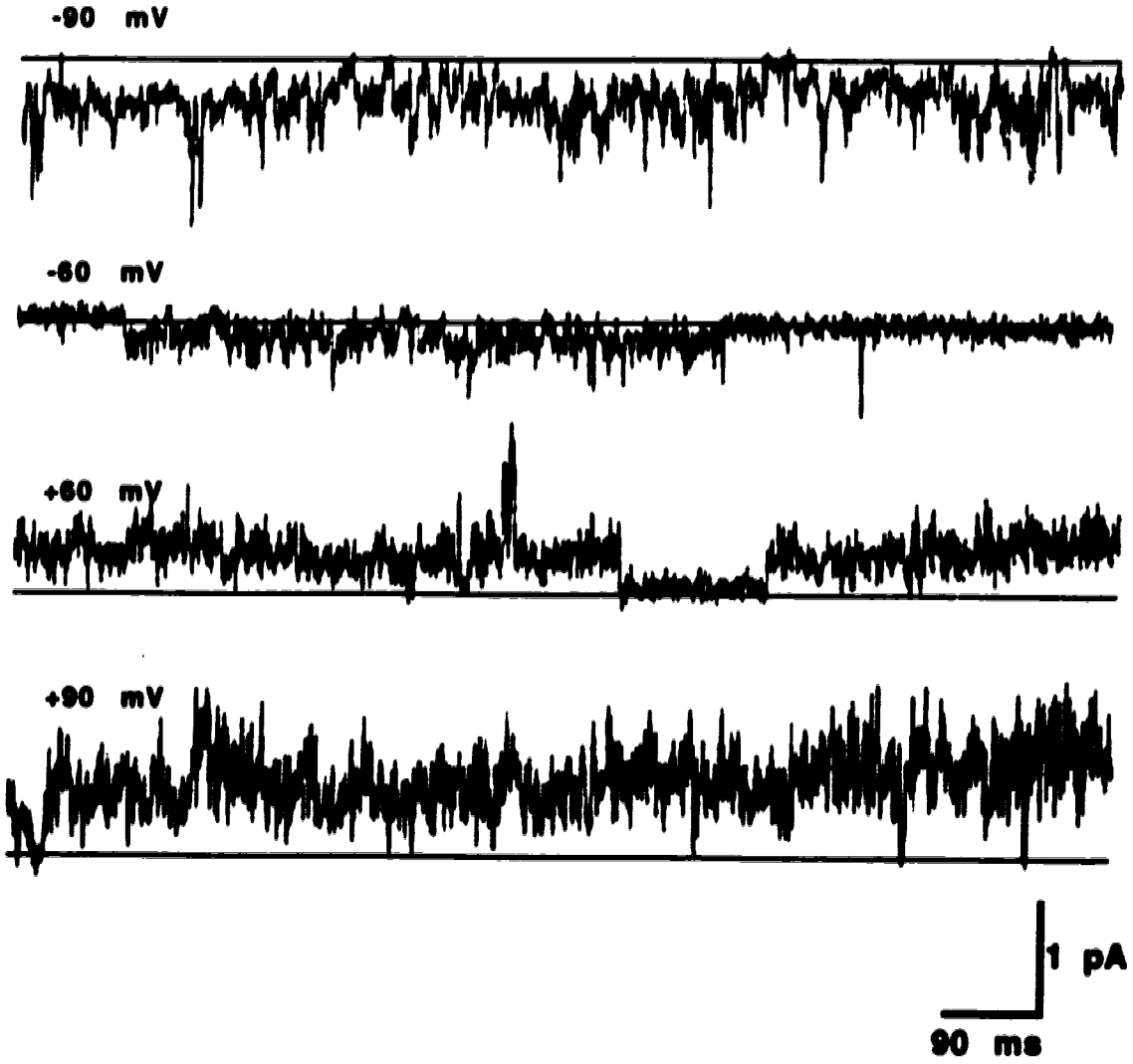

Figure V-9: Outward currents are enhanced under divalent cation-free conditions. Traces shown were recorded from inside-out patches at the indicated electrode potentials in divalent cation-free saline. Note that the activity at positive potentials is similar to that seen at negative potentials. Recordings shown are from the same membrane patch used to obtain Figure V-8. The approximate closed level is indicated in each trace.

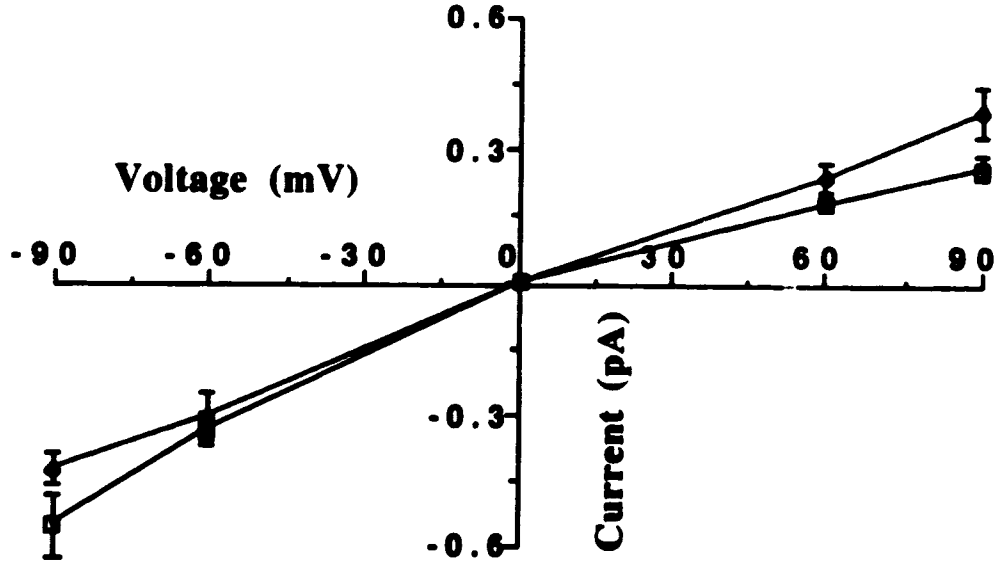

Figure V-10: Unitary current/voltage (i/V) relationship for the cAMP-dependent ion channel. Mean single channel current recorded from inside-out patches under 0 Ca^{2+}, 1.5 mM Mg^{2+} (open symbols, n=5) and divalent cation-free (closed symbols, n=5) bath conditions. Only patches in which measurable outward currents under 0 Ca^{2+}, 1.5 mM Mg^{2+} conditions were used for calculation of means. Note that under divalent cation-free conditions, the i/V relationship is more symmetrical.

Figure V-11: cGMP activation of ion channels. Inside-out patch recording revealed that upon bath application of cGMP a dose-dependent increase in ion channel activity, much like that seen with cAMP, was observed. cGMP-induced channel activity was reversible upon washing with fresh saline. Pipette potential was -60 mV.

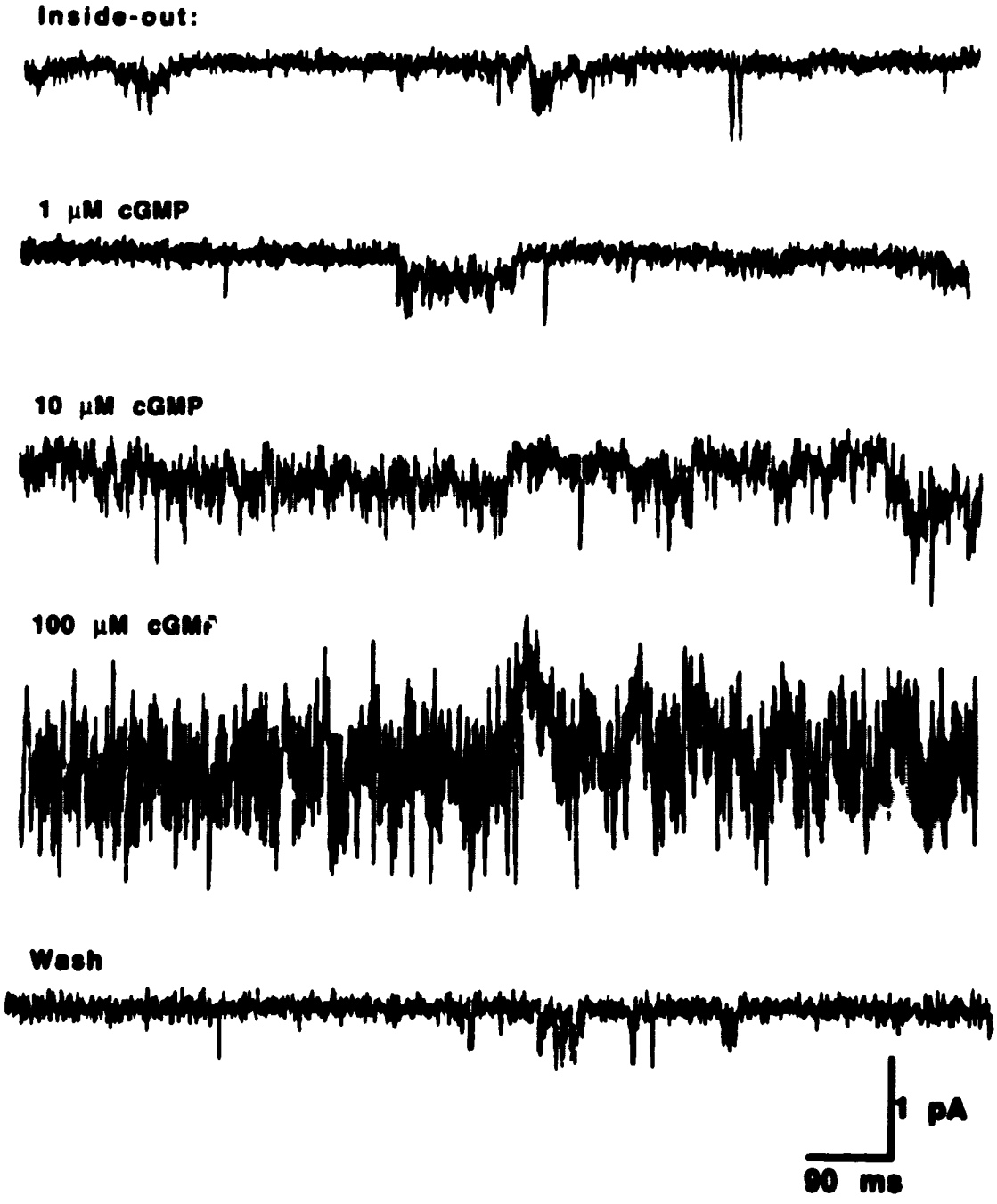
Inside-out:
1 μM cGMP
10 μM cGMP
100 μM cGMP
Wash
1 pA
90 ms

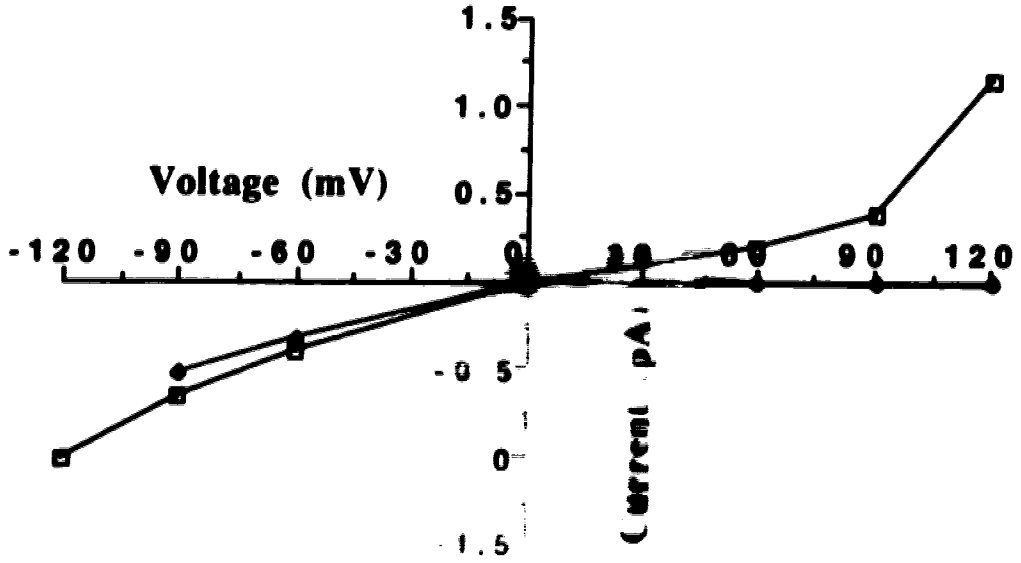

Figure V-12: i/V relationship for cGMP-activated ion channel. Unitary current measurements from a single inside-out patch recorded initially under 0 Ca^{2+}, 1.5 mM Mg^{2+} conditions (closed symbols) and then under divalent cation-free condtions (open symbols). Unitary current amplitudes at negative electrode potentials were similar to those from cAMP-activated channels. In this patch no measurable outward current was seen at positive electrode potentials under 0 Ca^{2+}, 1.5 mM Mg^{2+} conditions. However, under divalent cation-free conditions outward currents were observed.

VI) Pharmacology of the neuron B19 5-HT receptor

5-HT activation of inward current in neuron B19 appears to be mediated through a G-protein coupled receptor (see chapter IV). This results in stimulation of cyclic nucleotide synthesis and subsequent direct activation of cyclic nucleotide-gated channels (see chapter V). To gain further information on the nature of the neuron B19 5-HT receptor, a variety of drugs were tested for agonist and antagonist activities at this site. The pharmacological profile obtained would be useful for comparisons with other known 5-HT receptors. Moreover, the potential to find drugs useful for experimentally perturbing or mimicking 5-HT's actions would be beneficial in its own right.

i) Dose-response relationship for 5-HT activation of inward current

As a first step in examining the pharmacology of the neuron B19 5-HT receptor, dose-response experiments were conducted to provide information describing 5-HT's interaction with the receptor. In these experiments, the non-inactivating nature of the response to maintained 5-HT exposure was taken advantage of. Voltage-clamped neurons B19 were exposed to an increasing series of 5-HT concentrations, without intermediating wash periods. This resulted in a dose-dependent, inwardly directed shift in the holding current (Figure VI-1). Therefore, dose-response curves could be determined for individual cells.

From the summary dose-response curve shown in Figure VI-1, representing the average dose-response from 9 cells, several characteristics of 5-HT activation of inward current were revealed. Neuron B19 was quite sensitive to 5-HT, as the threshold concentration for current activation was around 1 nM. Moreover, the EC50 for current activation was between 10 and 100 nM, while maximal responses were seen at 10 μM. Therefore, the neuron B19 5-HT receptor appears to have a relatively high affinity for 5-HT.

Dose-response data were also used to generate Hill plots. The slope of a Hill plot can provide information on the number of ligand binding sites present on a receptor and examine for cooperativity in ligand-receptor binding (Cooper et al., 1978). With positive cooperativity, there are multiple binding sites for the ligand and ligand binding to one site increases the likelihood that the other site(s) becomes occupied. A slope of one indicates a single binding site is present, while a slope of two or greater indicates multiple binding sites and possible positive cooperativity. The Hill plot obtained from neuron B19 5-HT dose-response data was linear in shape and possessed a slope of 0.55 (Figure VI-2). This indicates that multiple binding sites showing positive cooperativity are unlikely to exist. However, a Hill coefficient of less than one suggests multiple binding sites demonstrating negative cooperativity may be present.

ii) Agonists at the neuron B19 5-HT receptor

Through the examination of the agonist activities of compounds that are structurally similar to 5-HT, information regarding which aspects of the 5-HT molecule are important in ligand binding and receptor activation can be revealed. Therefore, the abilities of four indolylalkylamines to activate inward current in neuron B19 were examined and compared to 5-HT's. The chemical structures of these four compounds and of 5-HT are presented in Figure VI-3. Initial experiments examined the effectiveness of a saturating dose (100-170 μM) of the agonist compared to that of 5-HT. To achieve this a protocol was used where the agonist was applied to the cell, and once the response had leveled off, the cell was exposed to a mixture of the agonist and 25 μM 5-HT. Additivity would indicate that the test compound was a less effective agonist than 5-HT. Dose-response relationships were also obtained to yield information on relative receptor affinities for these compounds.

To examine the role of the hydroxyl group located at the fifth carbon position in the activity of 5-HT, tryptamine, which lacks this group, was tested. In experiments examining the relative abilities of tryptamine and 5-HT to activate inward current, additivity was seen in five of seven cells tested (Figure VI-4). This indicates tryptamine is a less effective agonist than 5-HT. Moreover, the dose-response relationship for tryptamine was shifted to higher concentrations relative to the curve for 5-HT. The threshold for activation was between 10 and 100 nM and the EC50 was between 1 and 10 μM (Figure VI-8). Therefore, this hydroxyl group appears to be necessary for maximal receptor binding and activation.

The effect of substitution of the hydroxyl group at position five with a formamide group was also tested using the compound 5-carboxamidotryptamine. The results of this substitution were similar to those seen with tryptamine. Additivity with 5-HT exposure following initial activation by 5-carboxamidotryptamine was seen in all six cells tested (Figure VI-5). Moreover the dose-response relationship was shifted to higher concentrations, with threshold lying between 10 and 100 nM and the EC50 occurring at around 1 μM (Figure VI-8). These results again indicate the importance of the hydroxyl group in proper ligand binding and receptor activation.

Another compound investigated which involved a substitution at the five carbon hydroxyl group was 5-methoxytryptamine. Here the hydroxyl group is replaced with a methoxy group. Unlike the previous two agonists, with methoxy substitution additivity in response to 5-HT following initial exposure to 5-methoxytryptamine was small to non-existent (Figure VI-6), and was observed in only 2 of 5 cells tested. However, like the previous two compounds, the dose-response relationship demonstrated a shift to higher concentrations with the threshold for activation occurring between 10 and 100 nM and an EC50 of around 10 μM (Figure VI-8). This suggested that while an intact hydroxyl group is still required for high affinity activation of inward current, the relative effectiveness for maximal current activation is

retained if an oxygen molecule occupies the position adjacent to the fifth carbon.

While the previous three indolylalkylamines examined the importance of the fifth carbon hydroxyl group, the fourth agonist was used to investigate the importance of the ethylamine side group. α-methylation of the ethylamine side group yields the compound α-methyl-5-HT. As with tryptamine and 5-carboxamidotryptamine, additivity occurred upon 5-HT exposure following initial exposure to α-methyl-5-HT (Figure VI-7). This was seen in all four cells tested. Furthermore, the dose-response curve for α-methyl-5-HT was shifted to higher concentrations with the threshold for current activation occurring between 100 nM and 1 μM and an EC50 of around 10 μM (Figure VI-8). Therefore not only is the hydroxyl group important for proper ligand binding and receptor activation, but a sterically unencumbered ethylamine group is also important.

To test for the possibility that these indolylalkylamine agonists were activating a separate response in parallel with the 5-HT response, the above experiments were also performed in the reverse order in the same cells. When the cells were exposed to 5-HT first, followed by the agonist/5-HT mixture additivity was never seen (Figures VI-4 to 7). In fact, occasionally a reduction in the inward current was observed. This supports the idea that the agonists were activating the same response at the same receptor as 5-HT.

Another compound that displayed agonistic activity was the ergoline methysergide (see Figure VI-3 for structure). When neurons B19 were exposed to 25 μM methysergide, a small inward shift in holding current was always observed (Figure VI-9). Further exposure to a methysergide/25 μM 5-HT mixture resulted in additional inward current activation, much like that seen with the indole agonists. Overall, methysergide contributed 44.9 ± 8% (n=5) to the total current activated by methysergide and 5-HT. This was a surprising result, since

methysergide has been used as an antagonist in studies of vertebrate 5-HT receptors, with some selectivity for 5-HT2-type receptors (Glennon, 1987).

As with the indole agonists, methysergide and serotonin were added in the reverse order to determine if methysergide was acting on the same receptors as 5-HT. With initial exposure to 5-HT, followed by exposure to the 5-HT/methysergide mixture, a substantial reduction in the amplitude of the inward current by 60 ± 3.5% (n=5) was observed. Therefore methysergide appeared to act as an antagonist in this experiment. To further examine this phenomenon, dose-response experiments for both agonist and antagonist actions of methysergide were performed (Figure VI-10). Much like 5-HT, methysergide activation of inward current had an EC50 of between 10 and 100 nM. However, methysergide inhibition of inward current was only seen at high doses, with an EC 50 of between 10 and 100 μM, and complete inhibition at 1 mM. Therefore, methysergide appears to possess mixed agonist/antagonist activity at the neuron B19 5-HT receptor.

iii) Examination of the activities of 5-HT receptor antagonists on 5-HT activation of inward current: Apparent antagonism

While the study of agonist activities can give information on the nature of the ligand-receptor interaction, the study of potential antagonist drugs can lead to the discovery of compounds that are experimentally useful in studies where the effect of selectively blocking an event is analyzed. Therefore, experiments were performed to identify compounds which specifically antagonized 5-HT activation of inward current in neuron B19. Two compounds, mianserin and cyproheptadine, showed initial promise. Both compounds have been shown to possess antagonistic activities at vertebrate 5-HT2-type receptors (Glennon, 1987), while cyproheptadine has also been shown to block 5-HT-induced spike broadening in *Aplysia* sensory neurons (Mercer et al., 1991).

When neurons B19 were exposed to either cyproheptadine or mianserin following initial activation of inward current by 25 μM 5-HT, a dose-dependent decrease in the inward current was observed (Figure VI-11). Moreover, both compounds were capable of inhibiting 5-HT-dependent depolarization of neuron B19 (data not shown). However, in current clamp experiments it was observed that the neurons were no longer able to generate action potentials in the presence of these compounds. Therefore experiments were conducted that examined the effects of these compounds on voltage-gated currents. When voltage clamped cells were exposed to either 100 μM cyproheptadine or mianserin the voltage-dependent inward and outward currents were inhibited (Figure VI-12). This inhibition was reversible upon washing, which indicated the cells were not killed by exposure to the compound. Therefore, cyproheptadine and mianserin appeared to be non-selective inhibitors of voltage-gated ion channels.

With the finding that cyproheptadine and mianserin acted as non-specific inhibitors of voltage-gated currents, the possibility arose that their antagonist actions against 5-HT activation of inward current might be due to activity at the cyclic nucleotide-gated channel and not at the receptor. To further examine this possibility dose-response relationships were determined for both the inhibition of the 5-HT-dependent inward current and the voltage-gated sodium current. If there was a substantial separation in the dose-response curves for both effects, with the inhibition of 5-HT-dependent current occuring at significantly lower concentrations, a case could be made supporting the hypothesis that mianserin and cyproheptadine were indeed active at the receptor. However, results from these experiments revealed that both effects required high doses of the drugs (Figure VI-13). The EC 50 for mianserin inhibition of 5-HT-dependent inward current was between 1 and 10 μM, while for inhibition of the voltage-gated sodium current it was shifted by only approximately one log unit to higher concentrations. For cyproheptadine the EC50 for both effects was around 10 μM. Therefore

no strong conclusions could be made regarding the site of activity for cyproheptadine and mianserin inhibition of 5-HT-dependent inward current.

To examine more directly the problem of site of activity for cyproheptadine and mianserin regarding antagonism of the 5-HT response, the abilities of cyproheptadine and mianserin to inhibit the inward current activated following exposure of neuron B19 to IBMX were tested. IBMX alone can activate inward current independent of receptor activation. If these compounds are unable to inhibit this current, then support for antagonism at the 5-HT receptor would be obtained. In every instance both cyproheptadine (n=4) and mianserin (n=3) caused regression of the IBMX-stimulated current, as would be expected if their inhibitory activities were actually at the ion channel (Figure VI-14).

To test the idea cyproheptadine was acting as a non-specific ion channel blocker, experiments were performed examining the effect of cyproheptadine on the neuron B19 steady-state current. The voltage staircase protocol was used to generate steady-state I/V curves before, during and after exposure to 100 μM cyproheptadine (Figure VI-15). Cyproheptadine exposure resulted in the elimination of the negative slope current, as well as an overall decrease in the slope of the remaining segments of the steady-state I/V curve. These effects were totally reversible upon washing with cyproheptadine-free saline and were observed in all three cells tested. Therefore cyproheptadine is likely inhibiting the activity of a variety of ion channels.

In addition to these two antagonists, several other putative antagonists were also tested for activity against 5-HT-dependent inward current. Mesulergine (50 μM), MDL 7222 (100 μM), LY-53857 (100 μM) and pipenerone (100 μM), as well as the 5-HT agonist 8-hydroxy-dipropylaminotetralin (8-OH DPAT; 100 μM), all possessed the ability to cause the reduction of 5-HT-dependent inward current. Moreover, 8-OH DPAT possessed no agonist activities (n=4). However, all of these

compounds also had inhibitory effects on voltage-gated currents. Therefore these compounds were not tested any further.

Cyproheptadine has previously been used as a receptor antagonist against the 5-HT-dependent spike broadening of *Aplysia* sensory neurons (Mercer et al., 1991). Since the concentration of cyproheptadine used in that study (200 μM) was in the range that inhibited *Helisoma* voltage-gated currents, the effect of cyproheptadine on voltage-gated whole cell currents in accutely dissociated *Aplysia* sensory neurons was tested. As with *Helisoma* currents, the voltage-gated currents of *Aplysia* sensory neurons were non-specifically inhibited in a dose-dependent manner by cyproheptadine over a similar concentration range (Figure VI-16). Moreover the effects were reversible upon washing. These results were seen in all *Aplysia* cells (n=6) as well as in six unidentified acutely dissociated *Lymnaea* neurons (Figure VI-17).

In addition to looking at *Aplysia* voltage-gated currents, current clamp recordings were performed to examine the effects of cyproheptadine on the ability of sensory neurons to spike. When cells were exposed to 100 μM cyproheptadine an initial spike broadening was observed. This was followed by a steady decrease in the amplitude of the action potential and in the ability of the cell to repolarize following the depolarizing current pulse (Figure VI-18; n=7). Therefore, it must be concluded that the non-specific activities of cyproheptadine and mianserin make these substances inappropriate for use, at micromolar concentrations, as antagonists in neurobiological experiments in *Aplysia*, *Helisoma* and *Lymnaea*.

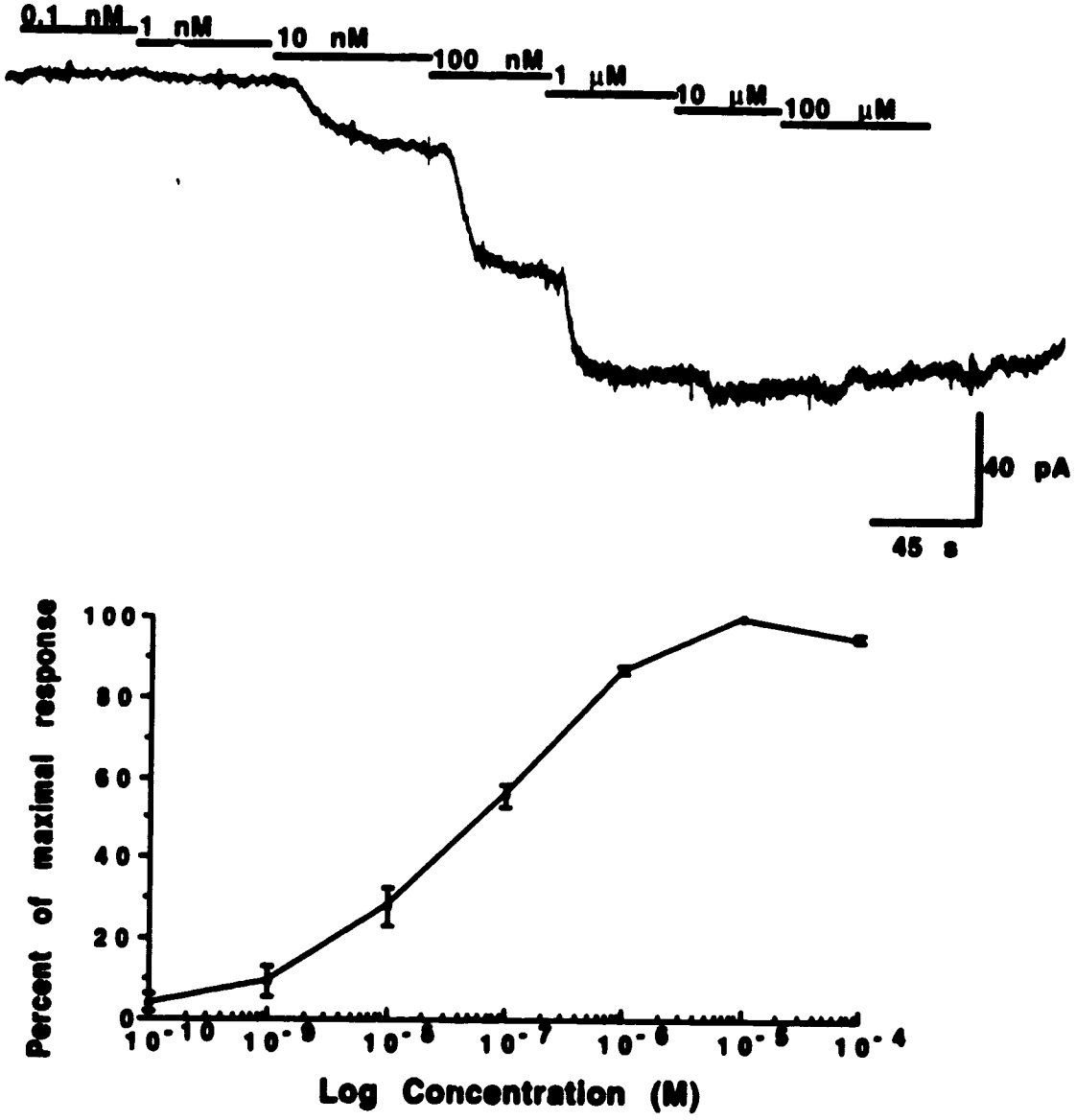

Figure VI-1: Dose-response relationship for 5-HT activation of inward current. Upper trace: Exposure of neuron B19 to increasing doses of 5-HT resulted in the dose-dependent activation of inward current. Holding potential -70 mV; bars indicate duration of exposure to a given concentration of 5-HT. Lower panel: Dose-response curve showing the mean percentage of inward current activated as a function of 5-HT concentration (n=9).

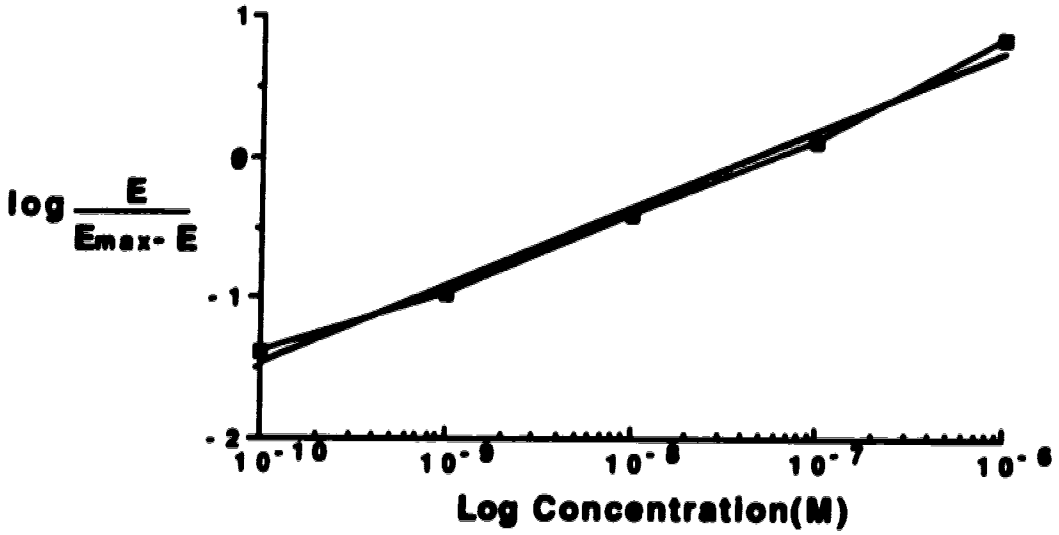

Figure VI-2: Hill plot for 5-HT activation of inward current. By plotting the value obtained from the formula:

$$\log \frac{E}{E_{max} - E}$$

where E represents the amplitude of the effect at a given concentration and Emax the maximal effect, against the log of the concentration, a Hill plot was generated (Cooper et al., 1978). The resulting plot was linear, and had a slope of 0.55.

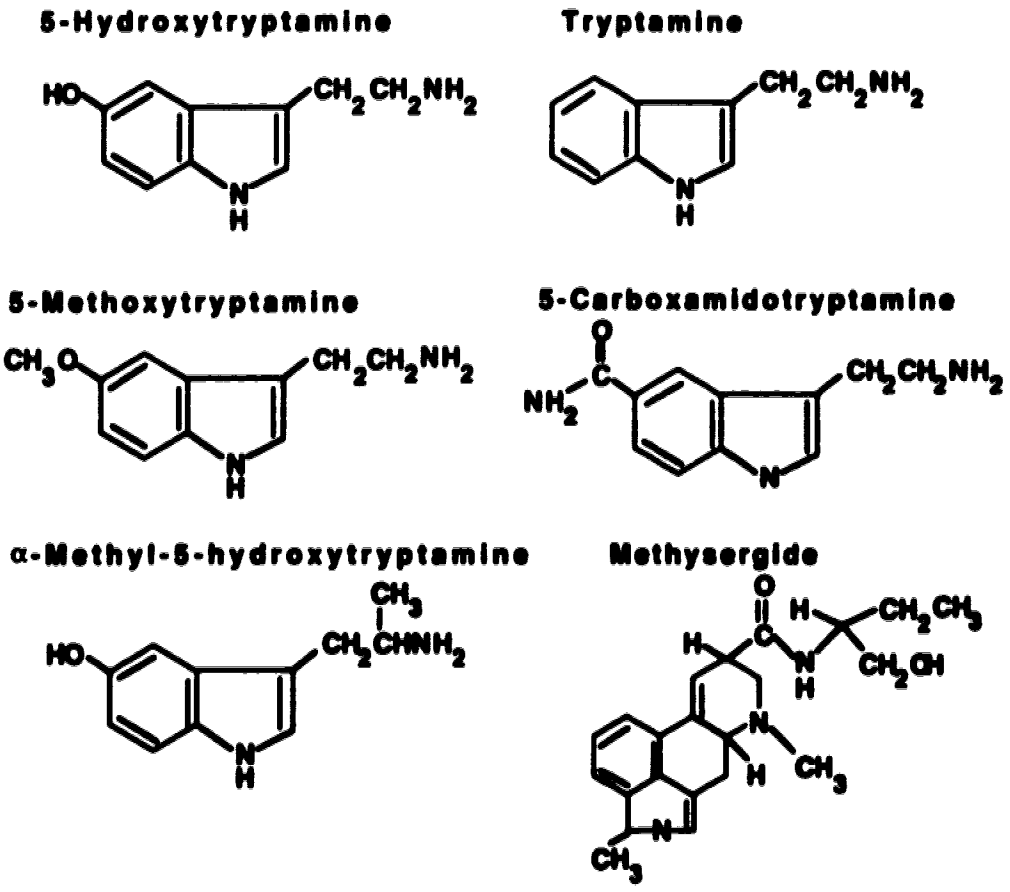

Figure VI-3: Chemical structures of compound having agonist activities at the B19 5-HT receptor. In pharmacological tests, agonist activity was observed with four indolylalkylamines: tryptamine, 5-methoxytryptamine, 5-carboxamidotryptamine and α-methyl serotonin, as well as with one egoline, methysergide.

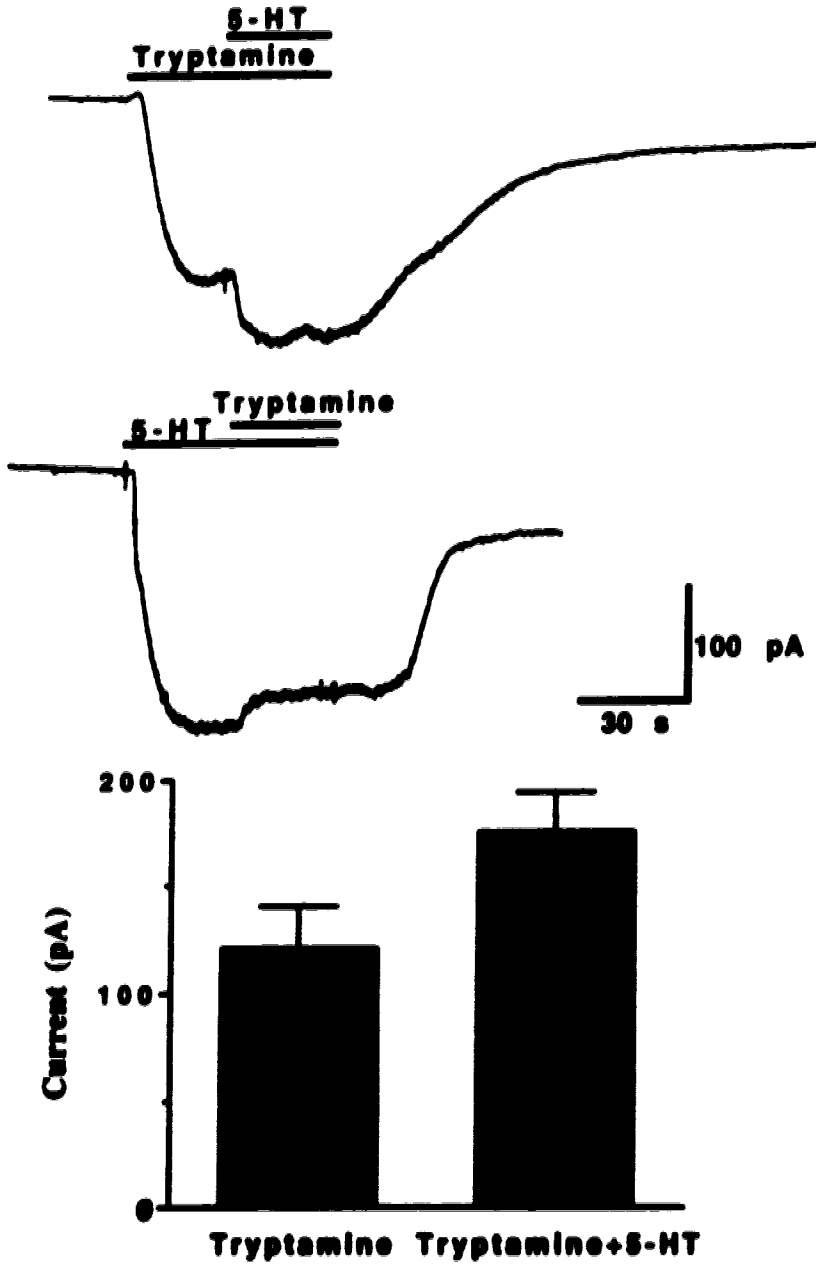

Figure VI-4: Tryptamine activation of inward current. Upper trace: Bath exchange for saline containing 100 μM tryptamine resulted in activation of a sustained inward current. Subsequent exchange containing 25 μM 5-HT and 100 μM tryptamine resulted in additional inward current activation. Lower trace: Upon washing with fresh saline, reapplication of tryptamine, following initial 5-HT application, did not result in additional inward current. Both traces were from the same cell, with the experiment carried out in the order of presentation. Holding potential was -70 mV; bars indicate duration of exposure to each compound. Bottom panel: Mean inward current activated by exposure to tryptamine and by subsequent exposure to 5-HT (n=7).

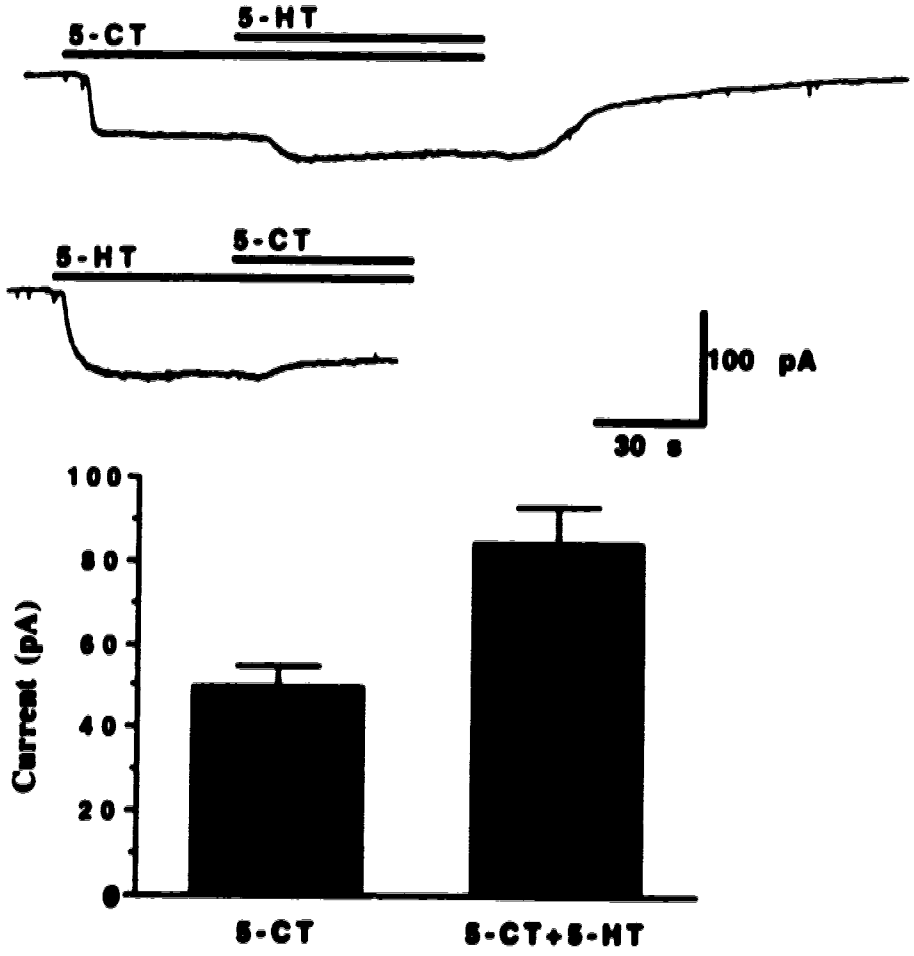

Figure VI-5: 5-carboxamidotryptamine (5-CT) activation of inward current. **Upper trace:** Bath exchange for saline containing 100 μM 5-CT resulted in activation of a sustained inward current. Subsequent exchange for saline containing both 5-CT and 25 μM 5-HT resulted in the activation of additional inward current. **Lower trace:** Upon washing with fresh saline, reapplication of 5-CT, following initial exposure to 5-HT, did not result in additional inward current activation. Both traces were from the same cell with the experiment performed in the order of presentation. Holding potential was -70 mV; bars indicate duration of exposure to each compound. **Bottom panel:** Mean inward current activated by exposure to 5-CT and subsequent exposure to 5-HT (n=6).

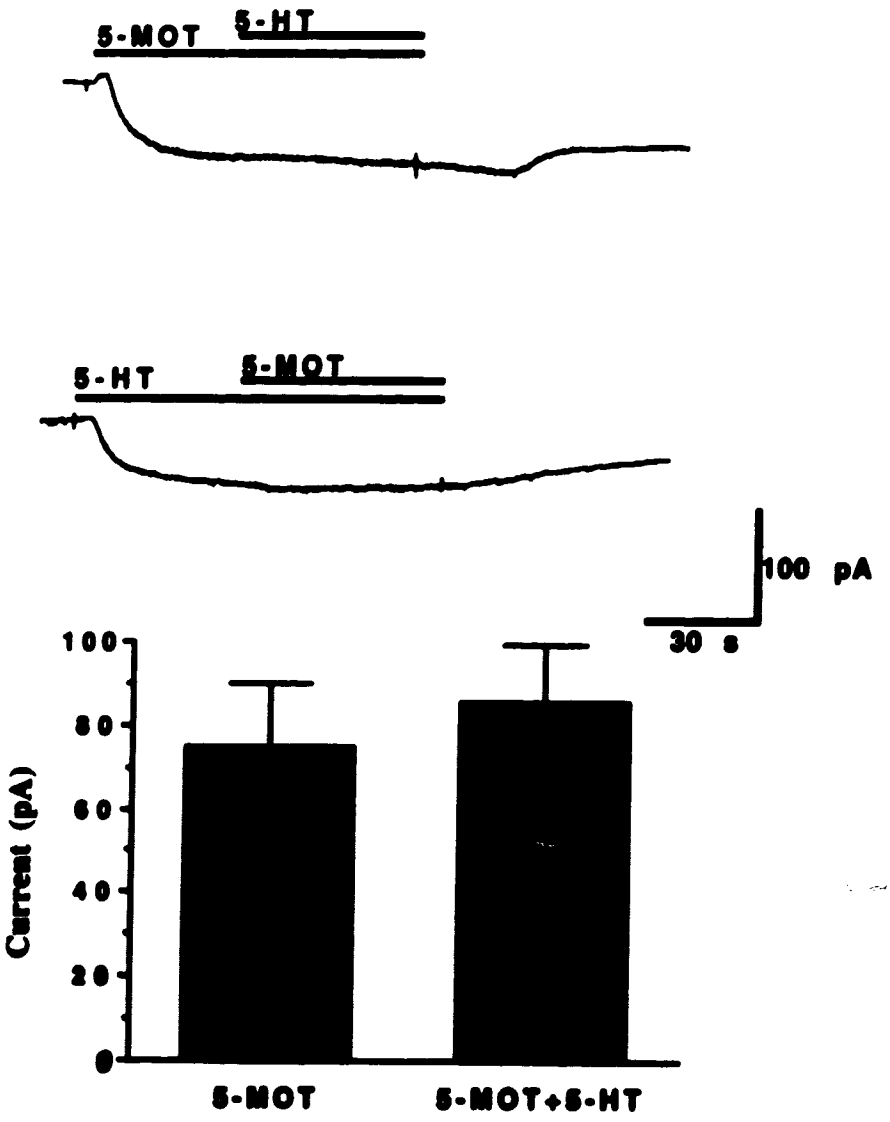

Figure VI-6: 5-methoxytryptamine (5-MOT) activation of inward current. **Upper trace:** Bath exchange for saline containing 100 μM 5-MOT resulted in activation of a sustained inward current. Subsequent exchange for saline containing 5-MOT and 25 μM 5-HT did not result in any additional inward current. **Lower trace:** Upon washing with fresh saline, reapplication of 5-MOT, following initial exposure to 5-HT, did not result in additional inward current. Both traces were from the same cell, with the experiment performed in the order of presentation. Holding potential was -70 mV; bars indicate duration of exposure to each compound. **Bottom panel:** Mean inward current activated by exposure to 5-MOT and by subsequent exposure to 5-HT (n=5).

Figure VI-7: α-methyl serotonin (αm-5-HT) activation of inward current. **Upper trace:** Bath exchange for saline containing 100 μM αm-5-HT resulted in activation of a sustained inward current. Subsequent exchange for saline containing both αm-5-HT and 25 μM 5-HT resulted in activation of additional inward current. **Lower trace:** Upon washing with fresh saline, reapplication of αm-5-HT, following initial exposure to 5-HT, did not result in additional inward current. Both traces were recorded from the same cell with the experiment performed in the order of presentation. Holding potential was -70 mV; bars indicate duration of exposure to each compound. **Bottom panel:** Mean inward current generated following αm-5-HT exposure and following subsequent exposure to 5-HT (n=4). A version of this figure has been published previously (Price and Goldberg, 1993).

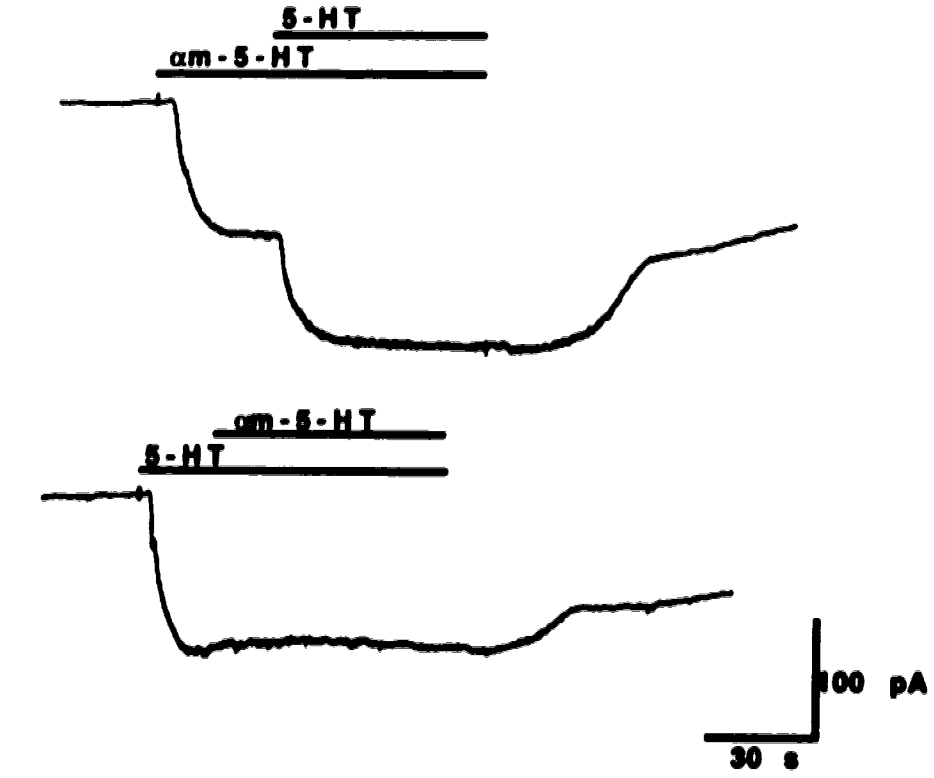
5-HT
αm-5-HT
αm-5-HT
5-HT
100 pA
30 s

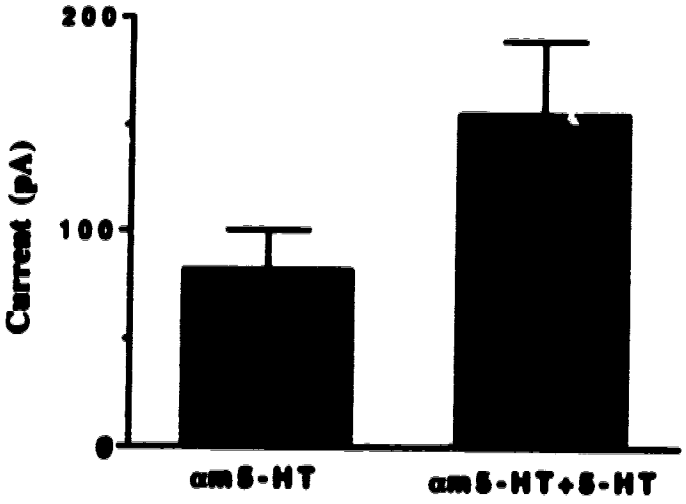
200
100
0
Current (pA)
αm5-HT
αm5-HT+5-HT

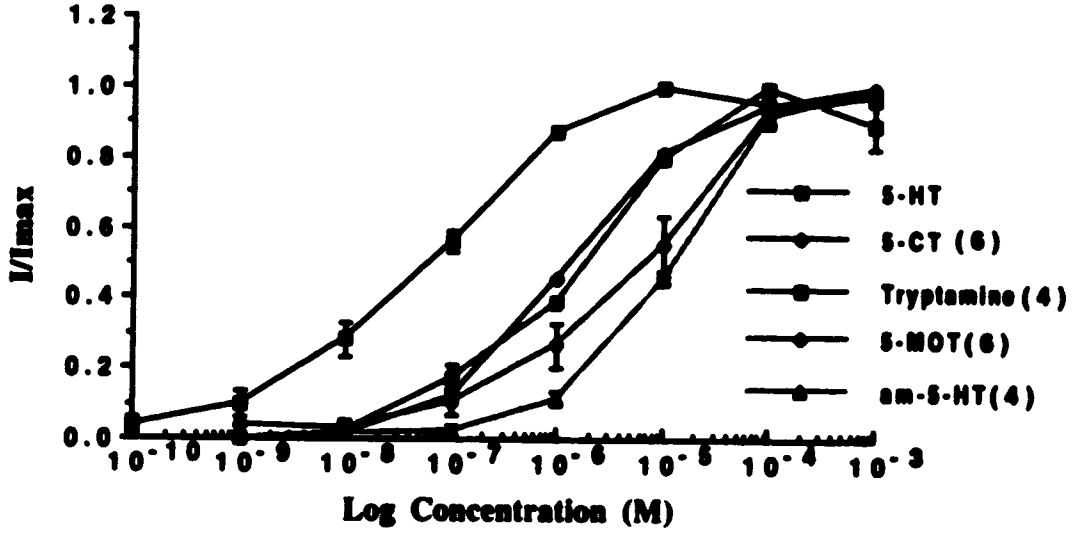

Figure VI-8: Dose-response curves for activation of inward current by indolylalkylamines. Shown are means describing the relative fraction of current activated at each concentration, normalized to the maximum current, for each agonist and for 5-HT. Experiments were performed as in Figure VI-1. Numbers in brackets indicate the number of cells used to obtain dose-response data.

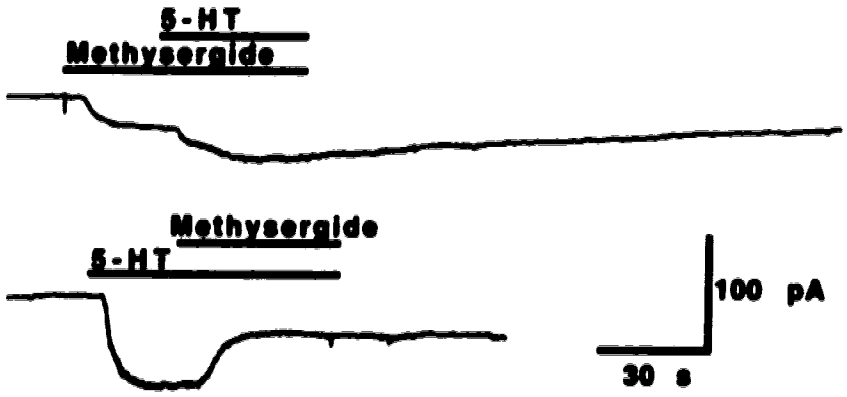

Figure VI-9: Mixed agonist/antagonist activity of methysergide. Upper trace: Bath exchange for saline containing 25 μM methysergide resulted in the weak activation of sustained inward current. Subsequent exchange for saline containing methysergide and 25 μM 5-HT resulted in additional inward current activation. Lower trace: Upon washing with fresh saline 5-HT was reapplied resulting in inward current activation. Upon reapplication of methysergide, the 5-HT activated current markedly decreased in amplitude. Both traces were from the same cell, with the experiment performed in the order of presentation. Holding potential was -70 mV; bars indicate duration of exposure to each compound. A version of this figure has been published previously (Price and Goldberg, 1993).

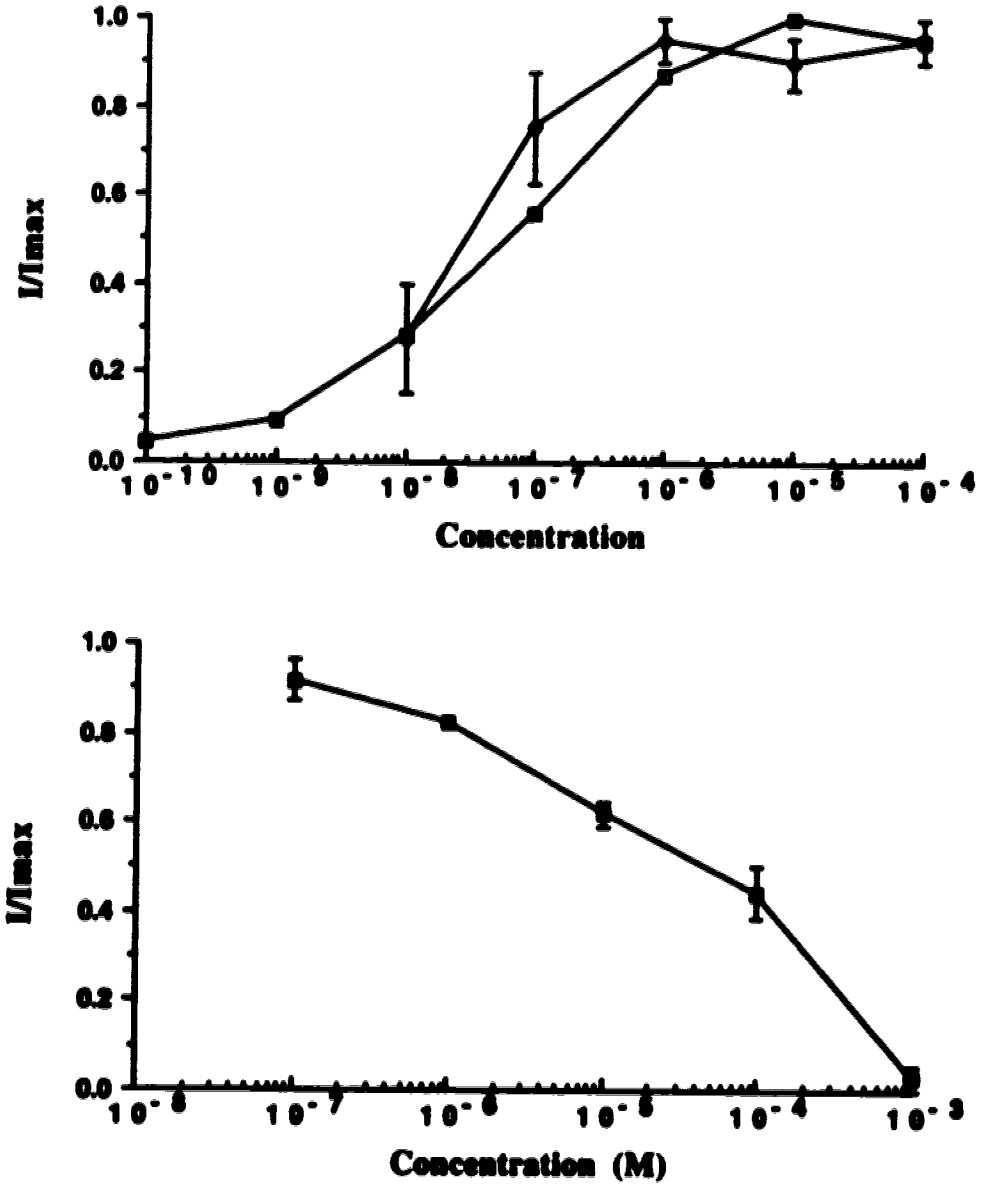

Figure VI-10: Methysergide dose-response curves. Top panel: Mean amount of inward current activated at each concentration of methysergide (closed symbols; n=4) and, for comparison, 5-HT (open symbols). Bottom panel: Mean fraction of inward current activated by 25 μM 5-HT remaining as a function of methysergide concentration (n=3).

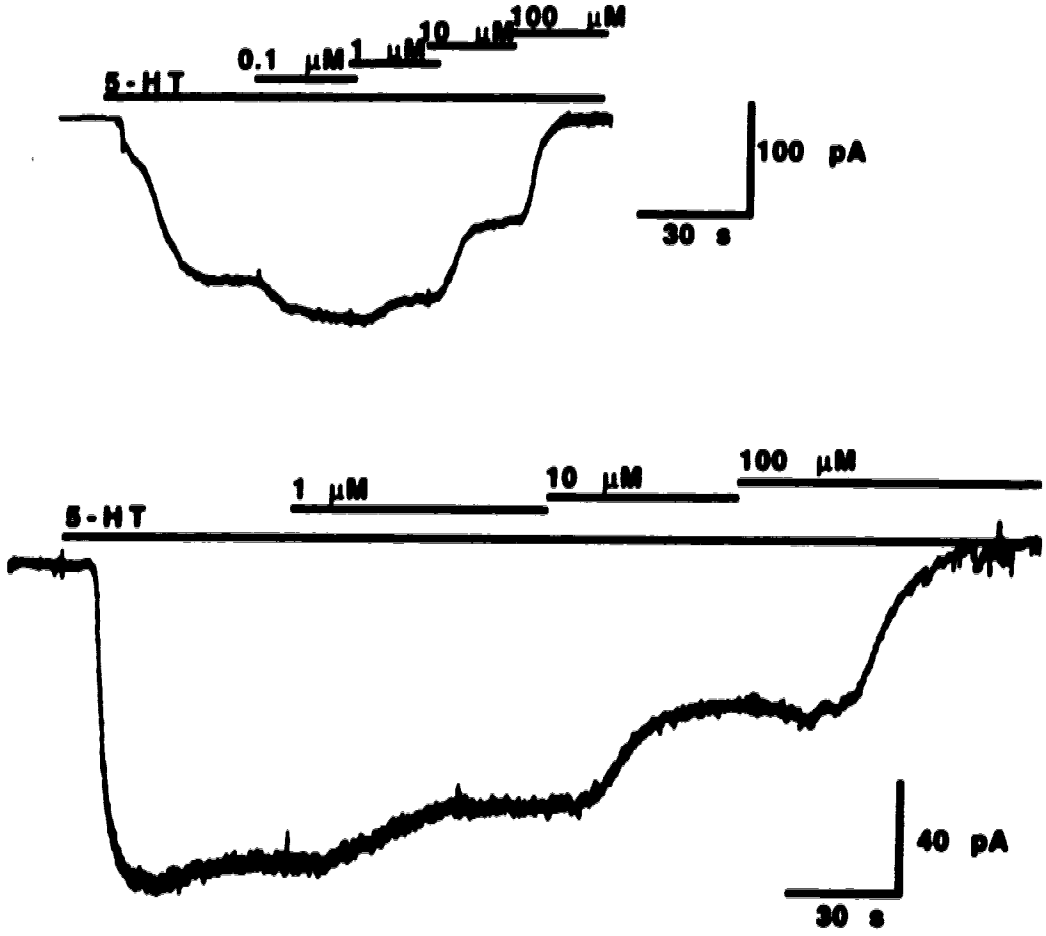

Figure VI-11: Apparent antagonism of 5-HT-dependent inward current. The response to 25 µM 5-HT was antagonized in a dose-dependent fashion by either cyproheptadine (Upper trace) or mianserin (Lower trace). Holding potential was -70 mV in both recordings; bars indicate duration of exposure to each compound.

Figure VI-12: Mianserin and cyproheptadine inhibition of voltage-gated ion currents. **Upper trace:** Voltage-gated currents elicited by 10 ms voltage steps from -90 to +10 mV before, during and after exposure to 100 μM mianserin (Mian.). **Lower trace:** Voltage-gated currents elicited by 10 ms voltage steps from -70 to 0 mV before, during and after exposure to 100 μM cyproheptadine (cyp). In both instances the compound indiscriminantly decreased the amplitude of all visible voltage-gated currents. Recordings were made under 50% sodium recording conditions to ensure good voltage control and keep currents within the current-passing range of the patch clamp amplifier.

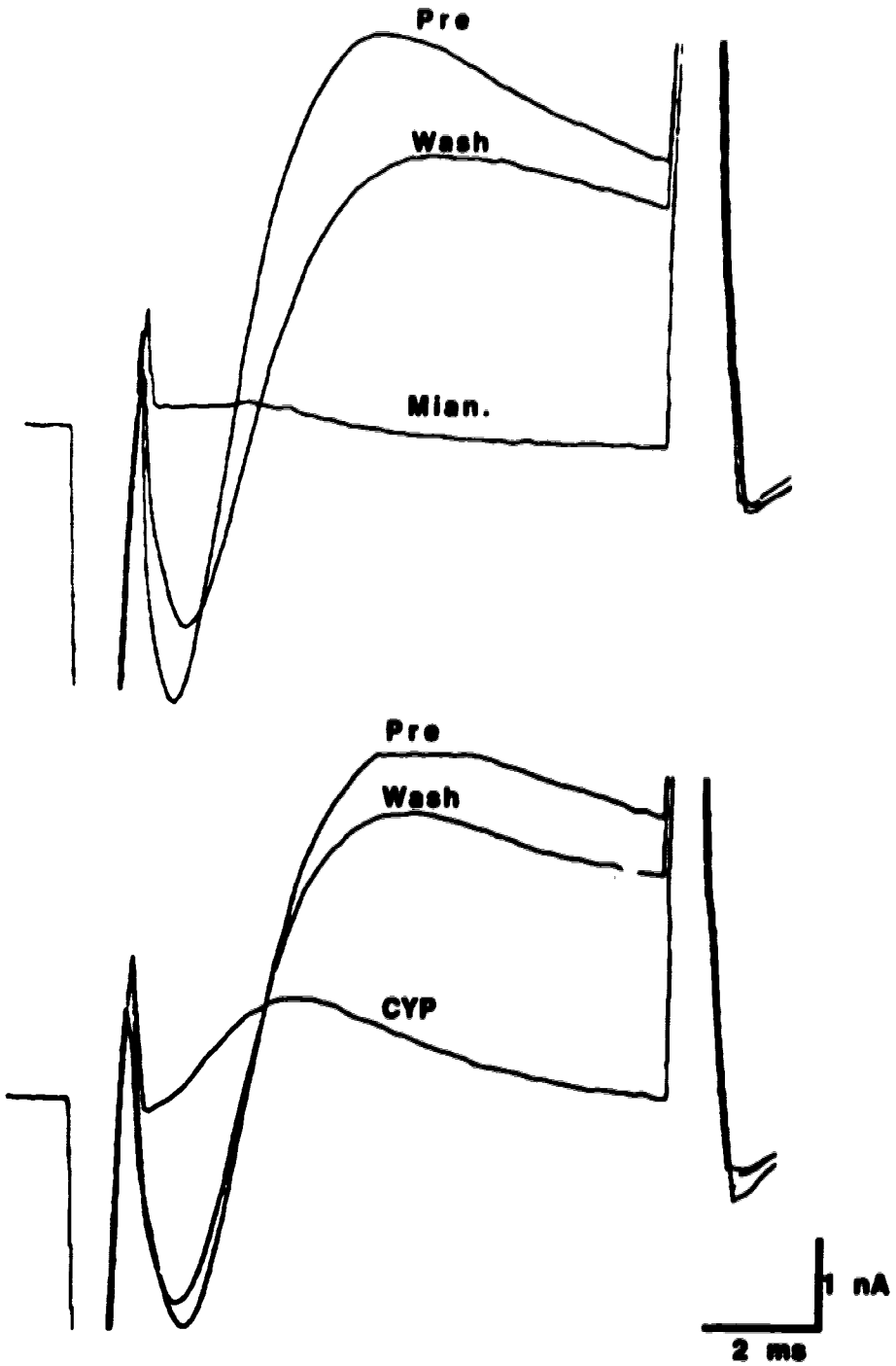
Pre
Wash
Mian.
Pre
Wash
CYP
1 nA
2 ms

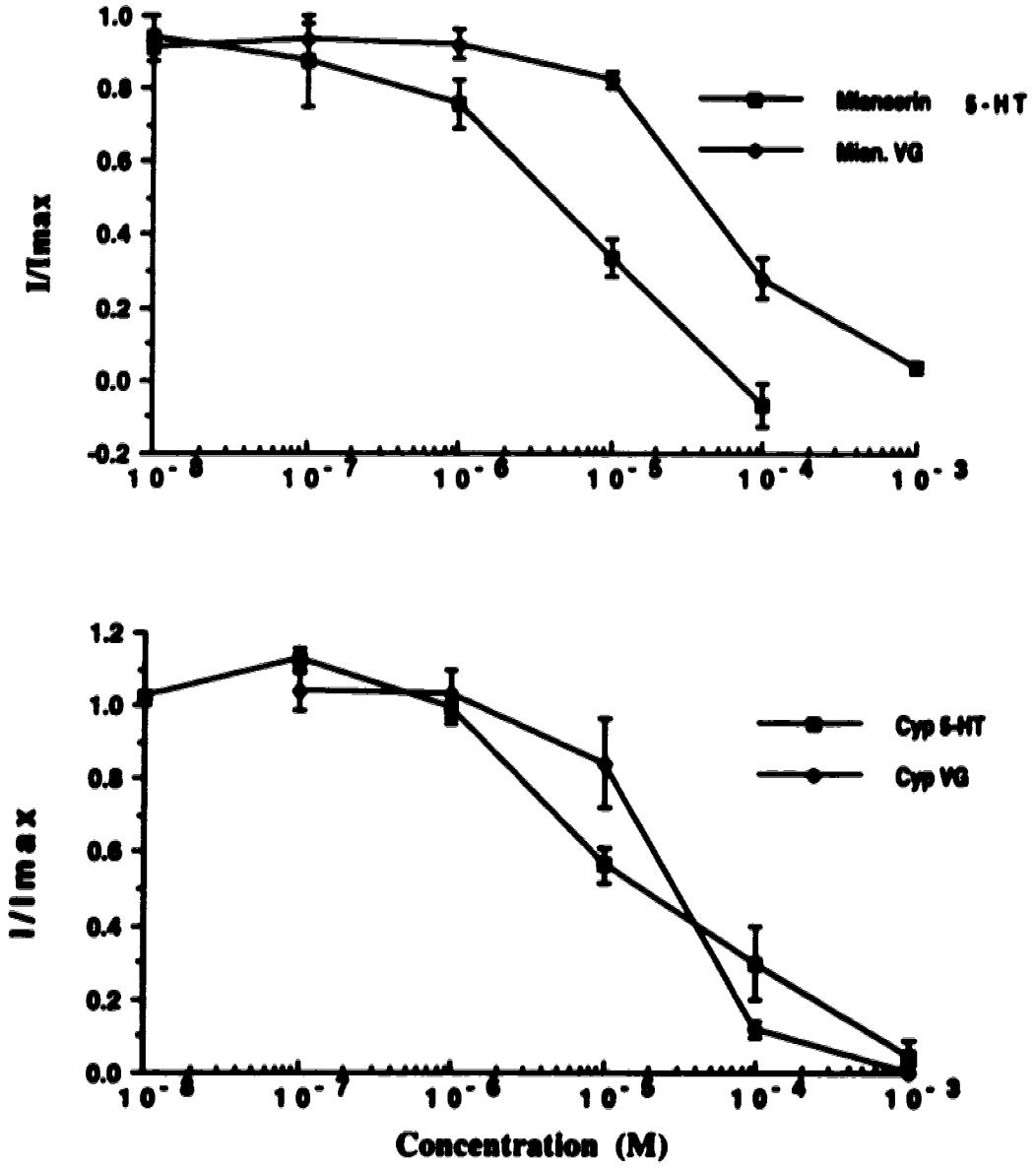

Figure VI-13: Dose-response relationships for antagonism of 5-HT-dependent inward current and voltage-gated sodium current. Top panel: Mianserin; Bottom panel: Cyproheptadine. Numbers in brackets indicate the number of cells contributing data to each mean.

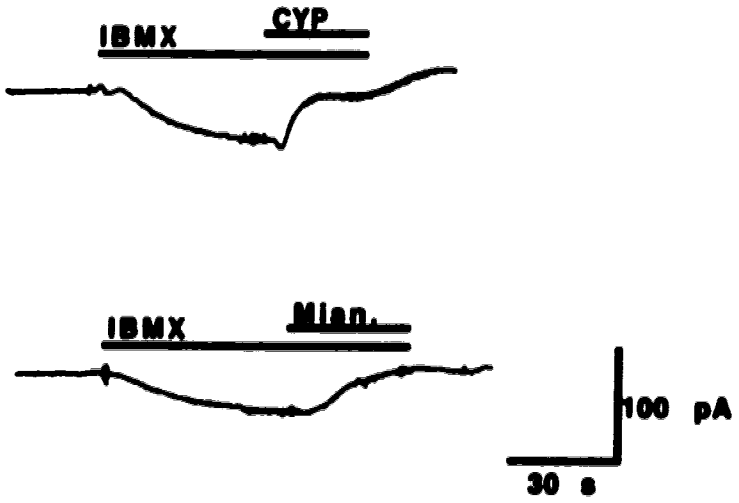

Figure VI-14: Antagonism of inward current induced by IBMX. Bath exchange for saline containing 0.5 mM IBMX resulted in inward current activation. Subsequent exposure to either 100 μM cyproheptadine (Cyp, Upper trace) or 100 μM mianserin (Mian, Lower trace) inhibited the inward current. Holding potential in both cases was -70 mV; bars indicate duration of exposure to each compound.

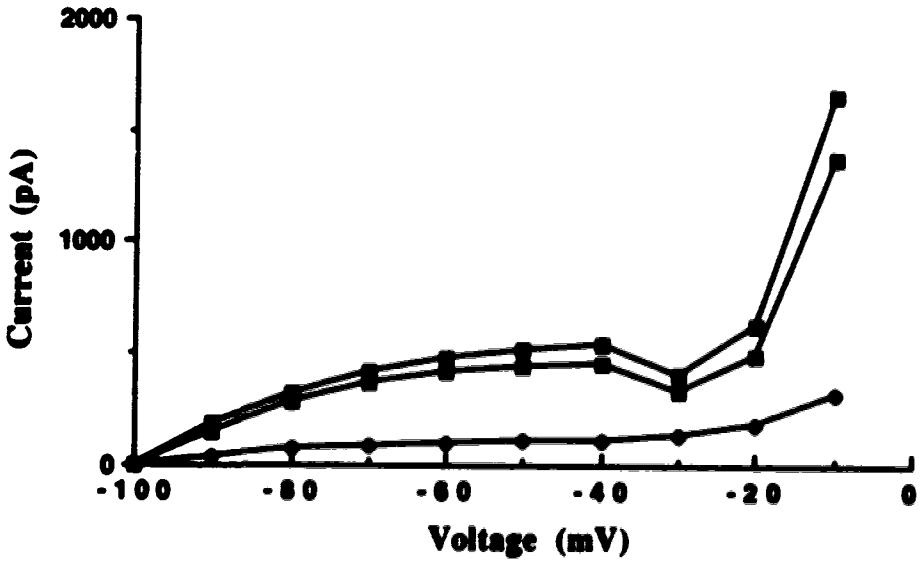

Figure VI-15: Cyproheptadine inhibition of neuron B19 steady-state currents. Using the staircase protocol, steady-state I/V curves were obtained before (open symbols), during (closed diamonds) and after (solid squares) exposure to 100 μM cyproheptadine. Note the reversible inhibition of negative slope current as well as the overall decrease in slope of the steady-state I/V curve associated with cyproheptadine exposure.

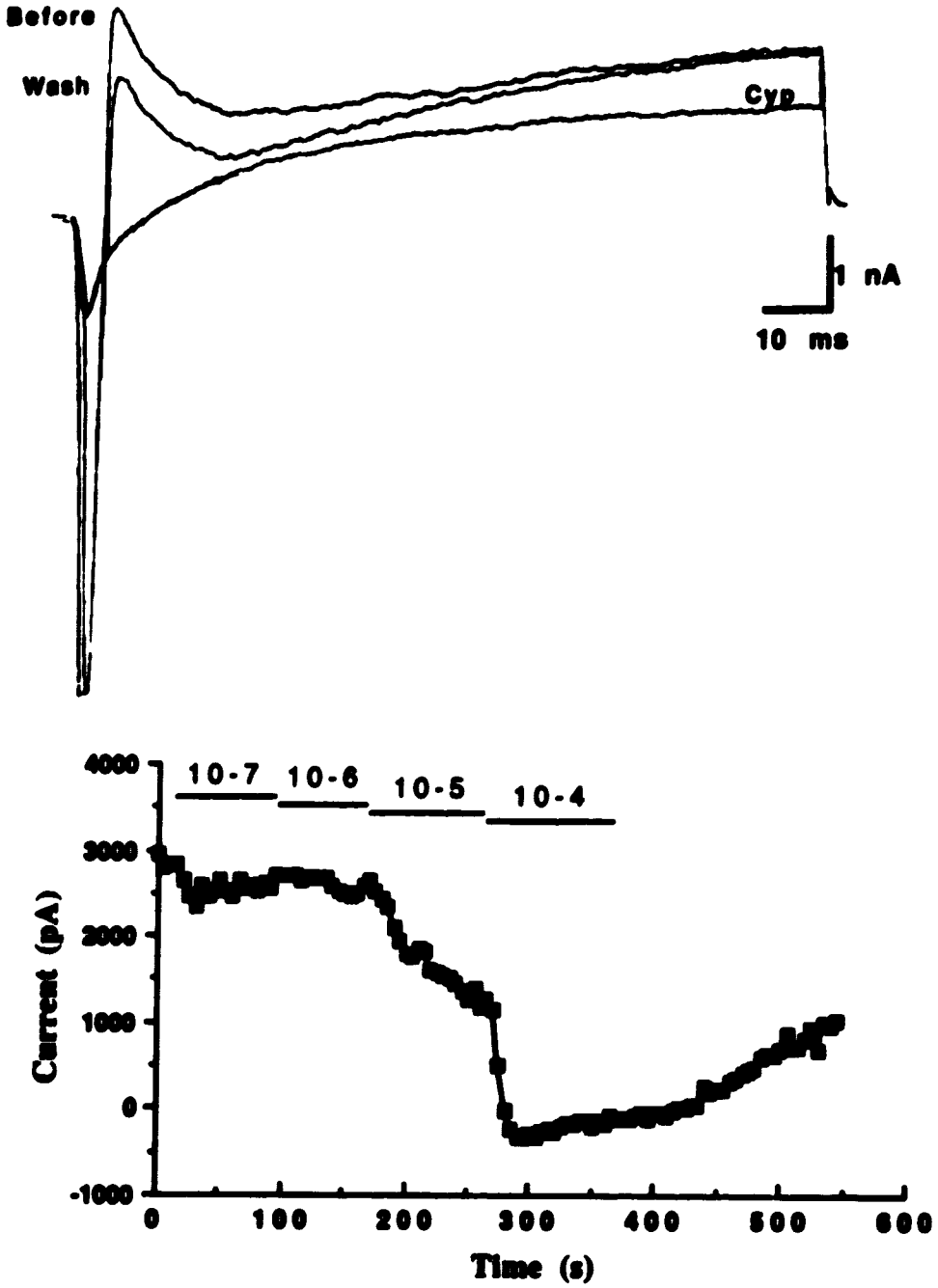

Figure VI-16: Cyproheptadine inhibition of voltage-gated currents in *Aplysia* sensory neurons. Upper trace: Whole-cell currents elicited with 100 ms voltage steps to 0 mV from -70 mV before, during and after exposure to 100 μM cyproheptadine. Bottom panel: From a different sensory neuron, the amplitude of the transient outward current was reduced in a dose-dependent fashion with cyproheptadine exposure. Measurements were taken from whole-cell recordings of voltage steps to 0 mV from -70 mV delivered every 5 s.

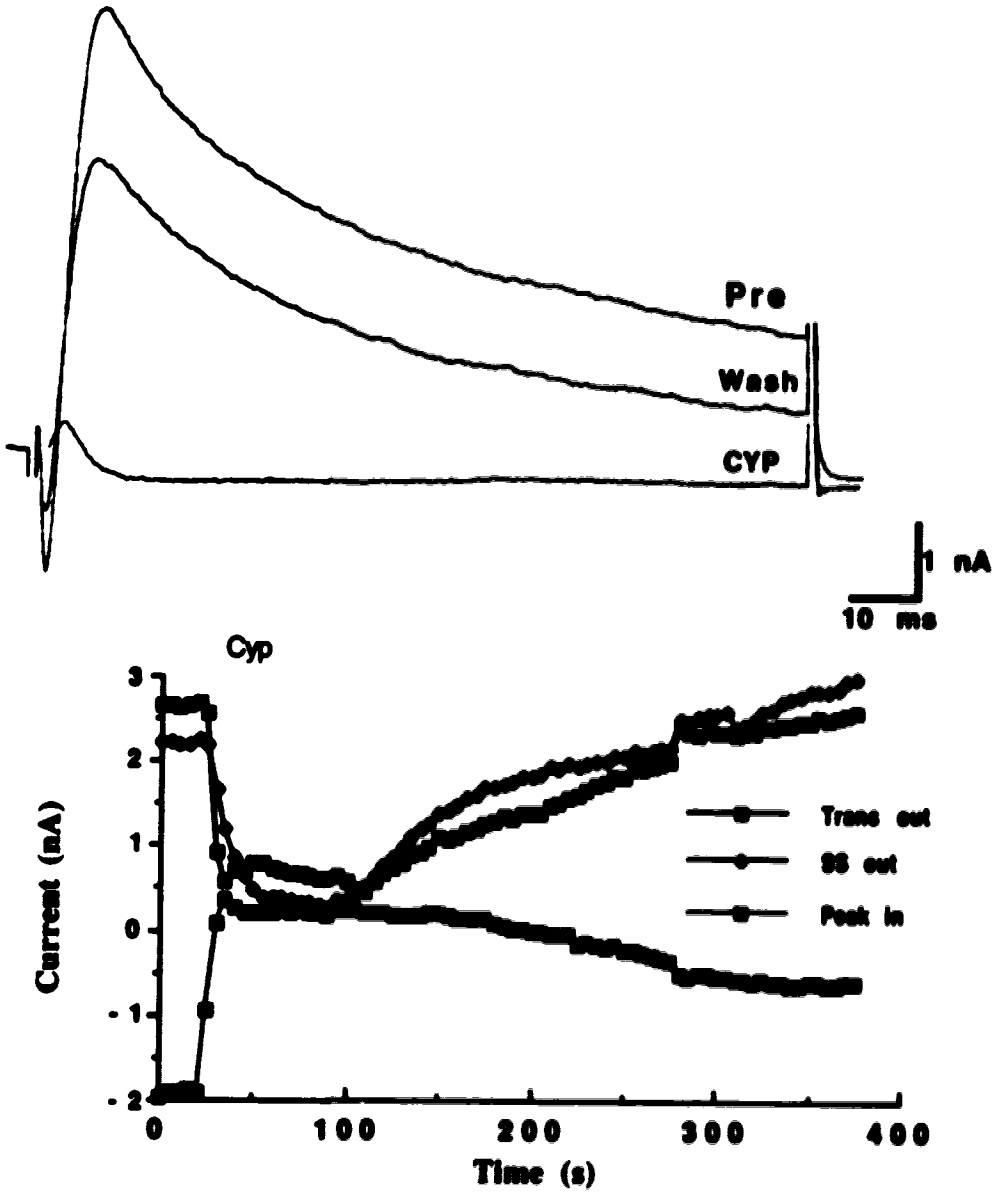

Figure VI-17: Cyproheptadine inhibition of *Lymnaea* voltage-gated currents. Upper trace: In an unidentified *Lymnaea* neuron, whole-cell currents were elicited with 100 ms voltage steps to -10 mV from -70 mV before, during and after exposure to 100 μM cyproheptadine. Bottom panel: In a different cell, amplitudes of the peak inward, transient outward and steady-state outward currents were obtained from 100 ms voltage steps from -70 mV to +10 mV at 5s intervals. Bar indicates duration of exposure to 100 μM cyproheptadine.

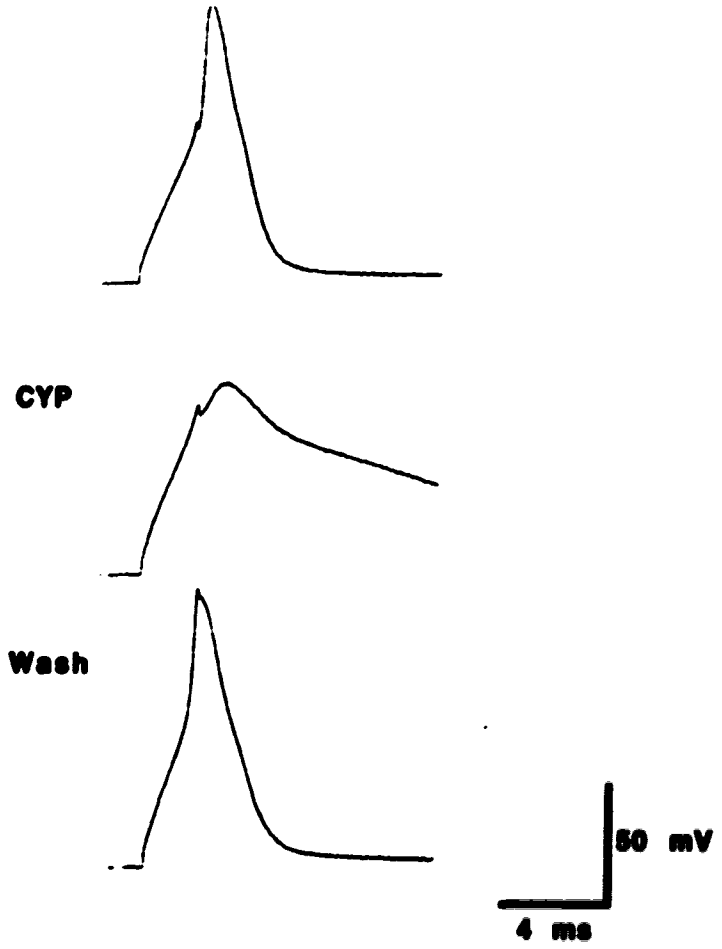

Figure VI-18: Cyproheptadine inhibits action potential firing in *Aplysia* sensory neurons. Current clamp traces demonstrating action potentials elicited in an sensory neuron by a 2 ms current pulse of 2.5 nA in amplitude. Current pulses were delivered before, during and after exposure to 100 μM cyproheptadine. The cell's membrane potential was maintained near -60 mV.

VII) Excitable properties of embryonic *Helisoma* neurons

From the *in vivo* experiments of Goldberg and Kater (1989), it is clear that 5-HT is important for the normal development of neuron B19. Moreover, the results from *in vitro* experiments show that the state of neurite outgrowth and intracellular calcium concentrations are influenced by 5-HT in some, but not all, embryonic cells which possess neuronal morphologies (Goldberg et al., 1988; Goldberg et al., 1991). To determine if these results reflect a similar mechanism controlling neurite outgrowth in developing embryonic and regenerating adult neurons, embryonic neurons must meet three conditions. First, embryonic neurons must be excitable. Second, embryonic neurons must possess voltage-gated calcium channels. Finally, embryonic neurons must respond electrophysiologically to 5-HT. Therefore, a study was made to test whether cultured embryonic neurons meet these three conditions.

i) Embryonic neurons are electrically excitable

As a first step in examining the excitable nature of embryonic neurons, whole-cell voltage and current clamp recordings were performed to test for the presence of voltage-gated currents and the ability to generate action potentials. The cells used for this study were obtained from primary cultures of embryos that were dissociated at a stage of development when the nervous system is just starting to differentiate (McKinney and Goldberg, 1989). The cells used represent a heterogeneous population of cells that were both unidentified and were likely of differing states of differentiation. Their common feature was the possession of neuronal morphology.

When cells with neuronal morphologies were voltage clamped, steps to positive potentials typically resulted in the activation of voltage-gated currents (Figure VII-1). The whole-cell current profiles usually showed the presence of an inward current that activated quickly in response to the voltage pulse and then inactivated. This likely represents a voltage-

gated sodium current, although a calcium component to this current can not be ruled out, and was seen in 46 of 54 cells tested. A second current routinely seen was an outward current, that remained active throughout the duration of the depolarizing voltage pulse. This current likely represents a delayed rectifier potassium current. In addition to this non-inactivating outward current, most whole-cell profiles possessed an inactivating component to their outward current. This likely corresponds to an A-like potassium current and was seen in 33 of 44 cells tested.

The mean maximal amplitude for the voltage-gated inward current was 57.8 ± 7.9 pA, and ranged from 8 to 188.5 pA (n=43). For the delayed rectifier current the mean amplitude measured from voltage steps to +40 mV was 56.9 ± 6.5 pA, and ranged from 5.5 to 189 pA. Recordings were performed on cells that had been in cell culture for between one and three days. To determine if the length of time spent in cell culture influenced the expression of these two currents, the mean amplitudes of currents recorded on each day were compared (Figure VII-2). A trend towards a reduction in current amplitude with time in culture existed, especially for the steady-state outward current. However one way analysis of variance comparison indicated this trend was not significant at a 95% confidence interval for inward current ($p=0.2764$), but was almost significant for outward current ($p=0.0622$).

To examine the voltage-dependent properties of the currents seen in whole cell recordings, I/V relationships were determined. For the voltage-gated inward current, the threshold voltage for activation was between -20 and -10 mV, while the current reached maximal amplitude at +20 mV (Figure VII-3). I/V curves were also generated for the outward currents. While no attempt was made to isolate the various components of the outward current, measurements of the steady-state current over the last 10 ms and of the peak outward current over the first 20 ms of each voltage pulse allowed these two components to be differentiated. I/V curves for the delayed rectifier current indicated that this current activates at more positive potentials than the voltage-gated sodium

current, with threshold lying near 0 mV (Figure VII-4). I/V curves for the A-like current revealed this current to activate at less positive voltages than the delayed rectifier, with a threshold for activation of between -20 and -10 mV (Figure VII-5).

To determine how the expression of these voltage-gated currents was translated into a cell's electrical excitability current clamp recordings were performed. Three types of stimuli were used to achieve this. The first involved a long duration depolarizing current pulse to directly evoke an action potential. The second involved a 50 pA hyperpolarizing current pulse to induce an anode-break action potential. If necessary the cells were hyperpolarized to -60 mV in order to limit steady-state inactivation of voltage-dependent ion channels. In addition to these experiments examining the active responses of cells, small amplitude hyperpolarizing current pulses were also delivered to estimate cell input resistance. For 43 cells in which this was tested, the mean input resistance was 17.1 ± 3.0 GΩ, and ranged from 2.3 to 125 GΩ.

Using the two stimulus protocols described above to examine excitability, embryonic neurons were grouped into four excitable states (Figure VII-6). Excitable state 1 cells, when challenged with a long duration depolarizing current pulse, had a voltage response that showed no evidence of inward current activation on the upward going phase. However, they did show some degree of rectification, indicated by the voltage response reaching its apex and then decreasing before the current pulse was turned off. Eleven of 35 cells were included in this group. In contrast, the 14 cells grouped into excitable state 2 showed inward current activation on the upward phase of their voltage responses, evidenced by a steepening of the positive-going voltage response. However, like the state 1 cells, they demonstrated a limited ability for rectification. The six cells grouped into excitable state 3 , on the other hand, were characterized by both a steepening of the upward phase of the voltage response and a markedly improved ability to rectify.

Excitable state 4 consisted of four cells that generated fast action potentials upon recovery from the anode break stimulus, leaving no doubt that these cells were completely electrically excitable (Figure VII-7). In fact one of these cells generated spontaneous action potentials, the only cell in this study that demonstrated this ability. In addition to these four cells that gave fast anode break action potentials, two cells gave slower anode-break depolarizing responses (Figure VII-7). Interestingly, however, when these two cells were tested for their response to a long duration depolarizing current, they gave responses more typical of excitable state 2 cells (Data not shown). Therefore, these two cells were not included in the state 4 grouping.

To further analyze the relationship between voltage-gated currents and excitability, a comparison of the amplitudes of the voltage-gated sodium and the delayed rectifier currents was made between cells displaying the various excitable states (Figure VII-8). One way analysis of variance comparison revealed that the mean maximal inward current became significantly larger from excitable state 1 to 2 to 3 ($p < 0.0001$, 95% confidence interval). No difference was noted between states 3 and 4. However, quite surprisingly, no significant difference was seen between groups regarding the amplitude of the delayed rectifier current ($p=0.2155$). Therefore, cells in states 3 and 4 are both likely to be fully excitable, while those in 1 and 2 are in a pre-excitable condition.

ii) Voltage-gated calcium currents in embryonic neurons

The previous experiments demonstrated that embryonic cells with neuronal morphologies possess the required voltage-gated sodium and potassium currents for basic cellular excitabililty. To determine if these cells fulfill the second condition stated above, voltage-clamp recordings were made under ionic conditions that favored the recording of calcium currents. When choline chloride replaced external sodium and cesium chloride replaced potassium aspartate in the electrode solution, the rapidly activating and inactivating inward current and the outward

currents were eliminated. This uncovered an inward current that showed little inactivation over the duration of a 100 ms voltage pulse (Figure VII-9). Since calcium was the only carrier of inward current remaining, this likely represents a voltage-gated calcium current. This calcium current was seen in all six cells recorded from under these ionic conditions and in all 10 cells where only cesium chloride was used.

To help characterize this voltage-dependent calcium current I/V relationships were determined. The embryonic calcium current was of the high-voltage activated variety, with a threshold for activation more positive than -30 mV, while maximum current was seen at approximately +30 mV. The threshold for activation described here corresponds well with that for the non-inactivating calcium current previously described in the cell bodies and growth cones of the identified *Helisoma* neuron B5 (Haydon and Man-Son-Hing, 1988). These results provide clear evidence that the second criterion, the presence of voltage-gated calcium currents, is met by embryonic *Helisoma* neurons.

iii) Electrophysiological responsiveness of embryonic neurons to 5-HT

The final criterion that must be met is that embryonic neurons respond to 5-HT in a manner that would lead to depolarization of the cell. To test for this, perforated patch recordings were performed using amphotericin B as the pore forming molecule. Perforated patch recordings were chosen because the small size of the embryonic neurons could facilitate the wash out of cellular constituents that are necessary for second messenger mediated responses to occur. To evaluate if adequate electrical access was attained using the perforated patch method, the ability to record voltage-gated currents was tested. Perforated patch recordings always gave voltage-gated currents comparable to those seen under standard whole cell recording conditions (Figure VII-10).

To examine for electrophysiological responses to 5-HT, 5-HT was bath applied (25 μM final concentration) to 14 voltage clamped cells, and voltage staircase stimuli were delivered before and after application. Current clamp recordings were not used since they were not stable enough to obtain an adequate baseline. In two instances, bath applied 5-HT yielded promising results (Figure VII-11). In one cell, 5-HT application resulted in a maintained, inwardly directed shift in holding current that was accompanied by a dramatic increase in baseline noise. The overall size of this shift was very small, approximately 1 pA. The difference current obtained from staircases delivered before and in 5-HT were not useful since control curves displayed an unacceptable amount of fluctuation around 0 pA. In a second cell a maintained, outward shift in holding current was seen, accompanied by an increase in baseline noise level. Again, the control difference current demonstrated an unacceptable amount of fluctuation. From these two results it appears that to obtain an unambiguous answer as to whether embryonic neurons respond electrophysiologically to 5-HT, a different approach must be used, probably using single channel recordings. While 1 pA currents may be physiologically significant in these high input resistance-possessing cells, this size current is below the resolving power of whole-cell recordings to allow adequate study.

From these experiments two of the three criteria were met supporting the hypothesis that developing embryonic neurons use similar mechanisms to regulate neurite outgrowth as do regenerating neurons. Embryonic neurons possess the voltage-dependent sodium, potassium and calcium currents that would allow action potential generation and calcium influx. Moreover, while no conclusive evidence was obtained regarding 5-HT-induced depolarization, two promising results suggest 5-HT may result in a variety of electrophysiological effects, including membrane depolarization. Therefore, it is possible that the 5-HT-transduction system seen in regenerating adult neurons is also expressed developmentally.

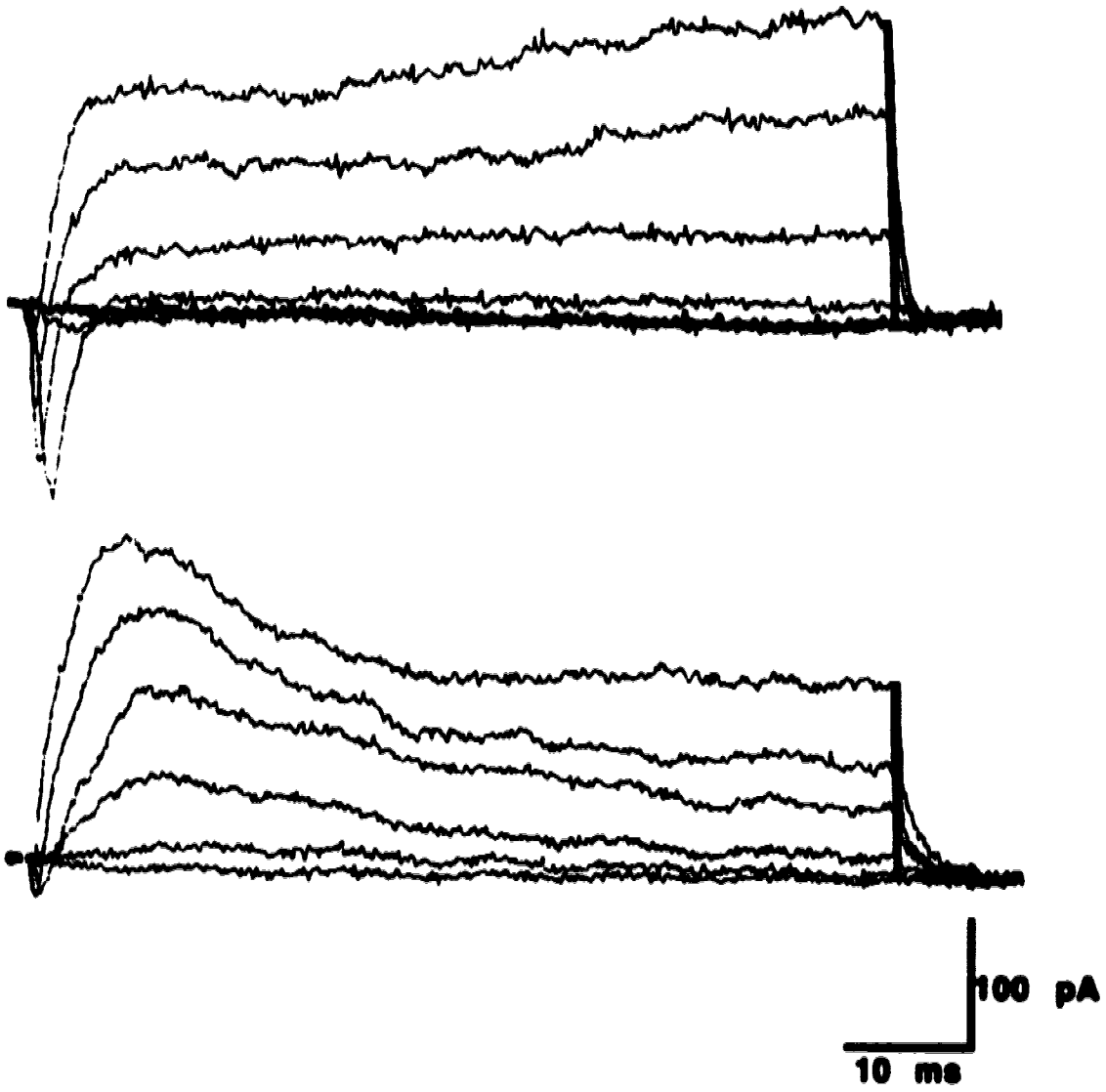

Figure VII-1: Whole-cell voltage-clamp currents of embryonic neurons. Shown are currents elicited from two cells with neuronal morphologies in response to 100 ms voltage steps to -30, -10, 10, 30, 50 and 70 mV from a holding potential of -60 mV. A full range of voltage-gated currents were generally seen, including rapidly activating and inactivating inward currents (Top traces), transiently activated outward currents (Lower traces) and maintained outward currents. A version of this figure has been published previously (Goldberg and Price, 1991).

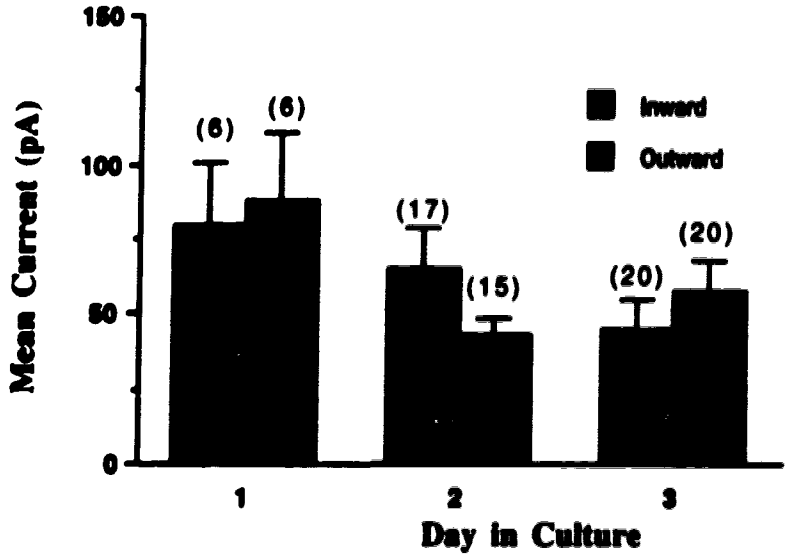

Figure VII-2: Comparison of the amplitudes of voltage-gated currents recorded from embryonic neurons in cell culture for between one and three days. Values plotted are for the mean peak inward current, measured at the potential that gave maximal current, and the mean steady-state outward current elicited with voltage steps to +40 mV. One way analysis of variance comparison revealed no significant differences at the 95% confidence interval in the amplitudes of these currents with the number of days in cell culture (inward: p=0.2764; outward: p=0.0822). Numbers in brackets refer to the number of cells contributing to each mean.

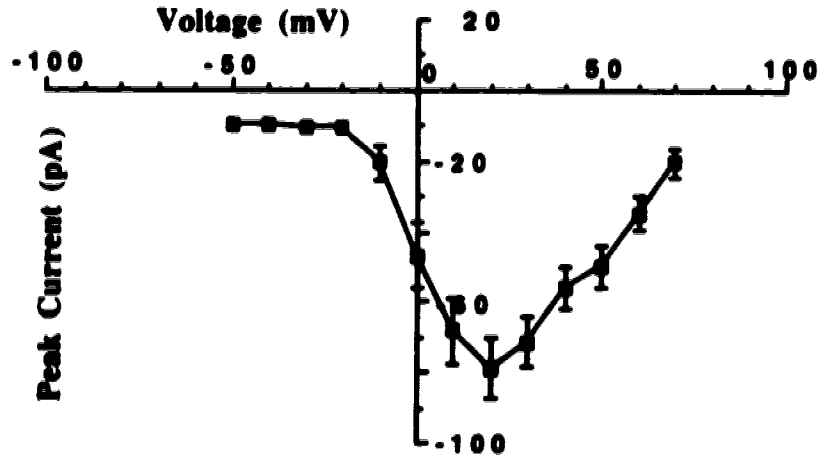

Figure VII-3: *I/V* **relationship for embryonic voltage-gated inward current. Mean peak inward current for 30 embryonic cells possessing voltage-gated inward current. Current activation occurred near -20 mV and was maximal at approximately +20 mV. The holding potential was -60 mV for all cells.**

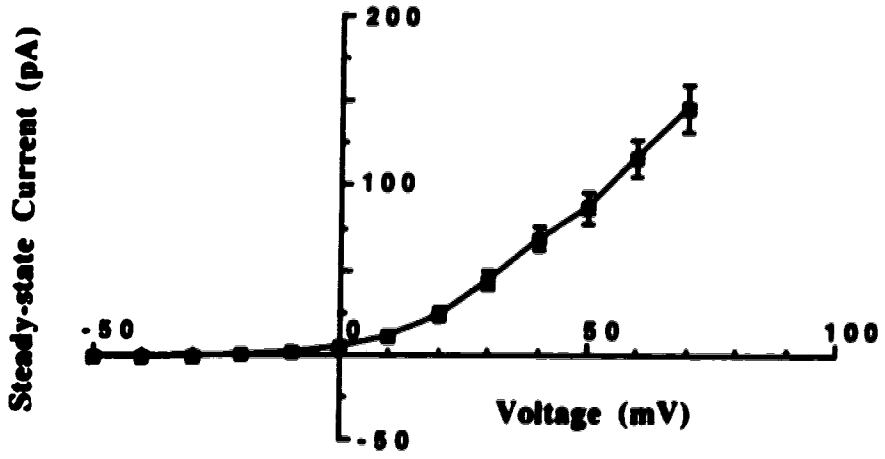

Figure VII-4: I/V relationship for embryonic steady-state outward current. Mean steady-state outward I/V curve for 33 embryonic cells. Steady-state values were obtained by measuring and averaging the current over approximately the last 10 ms of a 100 ms voltage step. The holding potential was -60 mV for all cells.

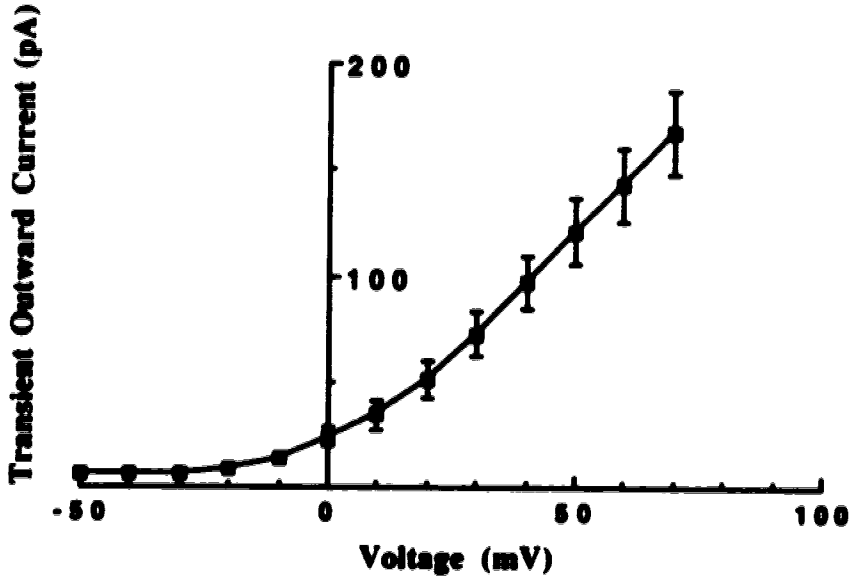

Figure VII-5: I/V relationship for the embryonic transient outward current. Values used for calculation of the means were the peak outward current measured during approximately the first 20 ms of each voltage step. Holding potential was -60 for all cells (n=16). To better visualize the amplitudes of currents at the threshold activation potential, only cells which possessed maximal inward currents of under 50 pA were used.

Figure VII-6: Excitable states of embryonic neurons. **Upper trace:** Cells in excitable state 1, when stimulated with depolarizing current pulses, showed no steepening of the upward-going voltage response, but did show rectification. **Middle trace:** Cells in excitable state 2 showed a marked inflection in the upward-going voltage response. However, rectification was present but not substantial. **Lower trace:** Cells in excitable state 3 showed a well developed inflection in the upward-going voltage response and showed substantial rectification and repolarization. The current stimulus pattern used is indicated above the three traces. The initial hyperpolarizing current pulse was necessary to remove any steady-state inactivation of voltage-gated currents.

+40 pA
0 pA
-10 pA
1
2
3
15 mV
40 ms

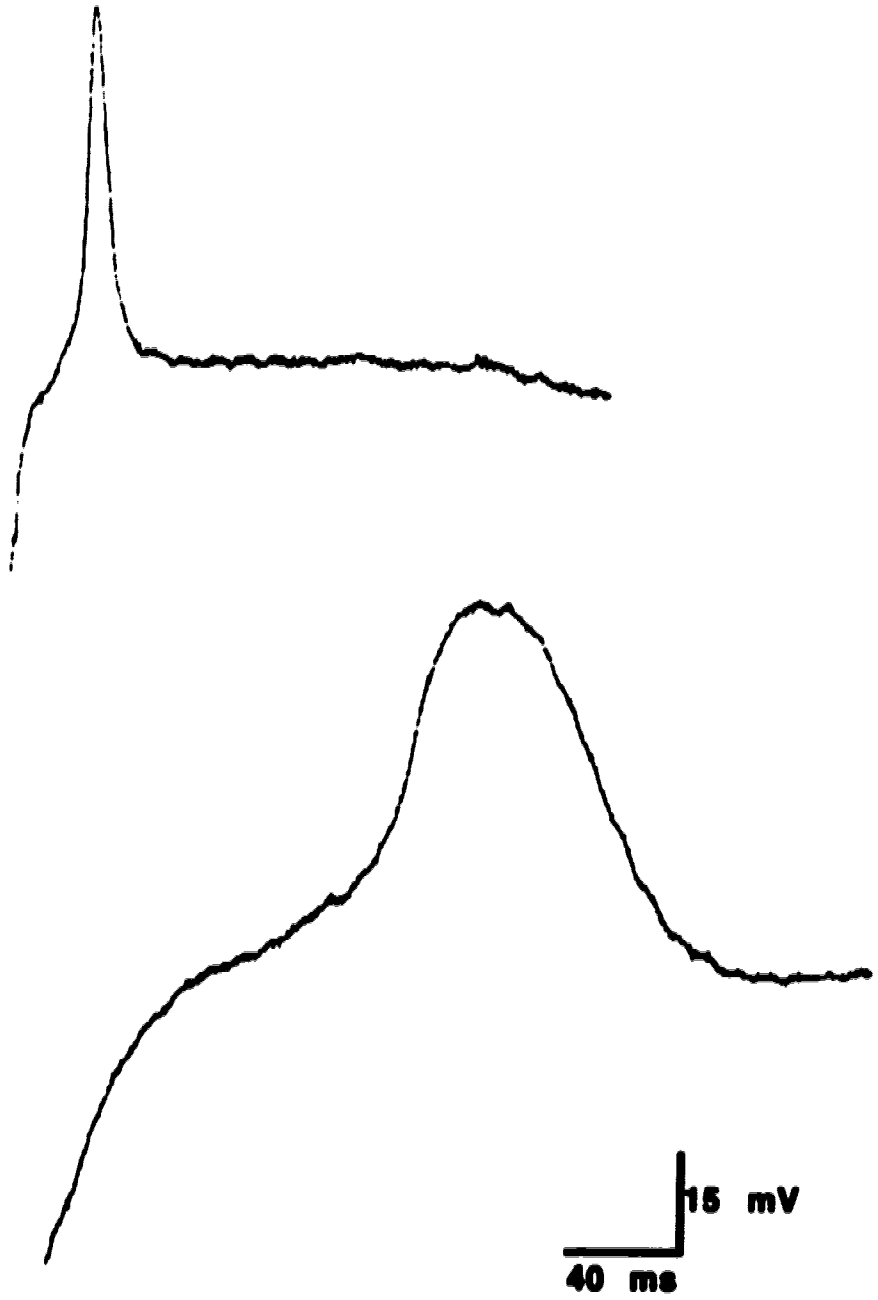

Figure VII-7: Anode-break responses of embryonic cells. Upper trace: When challenged with a large (50 pA for 100 ms) hyperpolarizing current pulse, four cells fired fast action potentials upon termination of the pulse. These cells were grouped as excitable state 4. Lower trace: Two additional cells responded to the anode-break test with a much slower "action potential". Both these cells showed responses to depolarizing current typical of excitable state 2 cells, therefore they were not included as belonging to excitable state 4.

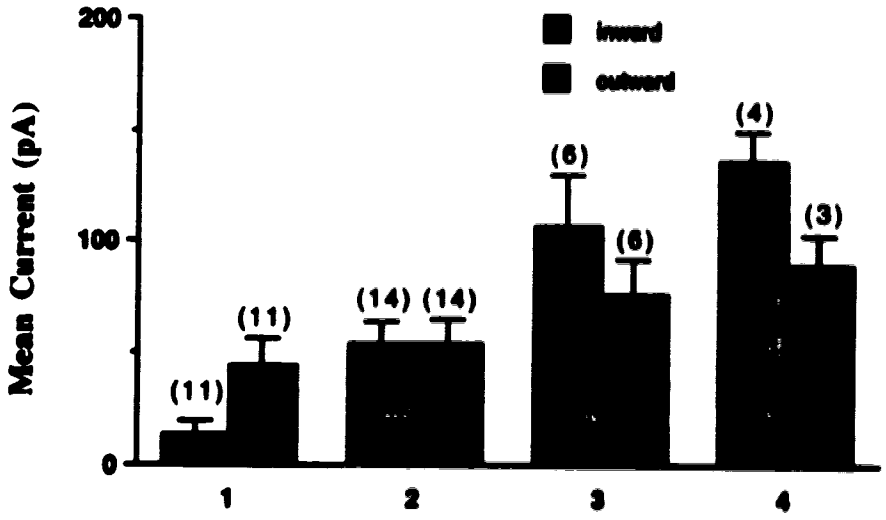

Figure VII-8: Current amplitudes vs. excitable states of embryonic neurons. For each of the four excitable state that embryonic neurons were grouped into, means for the maximal inward current and for the steady-state outward current recorded with a voltage step to +40 mV were obtained. Analysis of variance comparison revealed that the differences seen in the amplitude of inward current were significant ($p < 0.0001$, 95% confidence interval) between all groups, except for state 3 vs. state 4. No significant difference was noted between groups in the amplitude of the steady-state outward current. Numbers in brackets indicate the number of cells used for calculation of each mean.

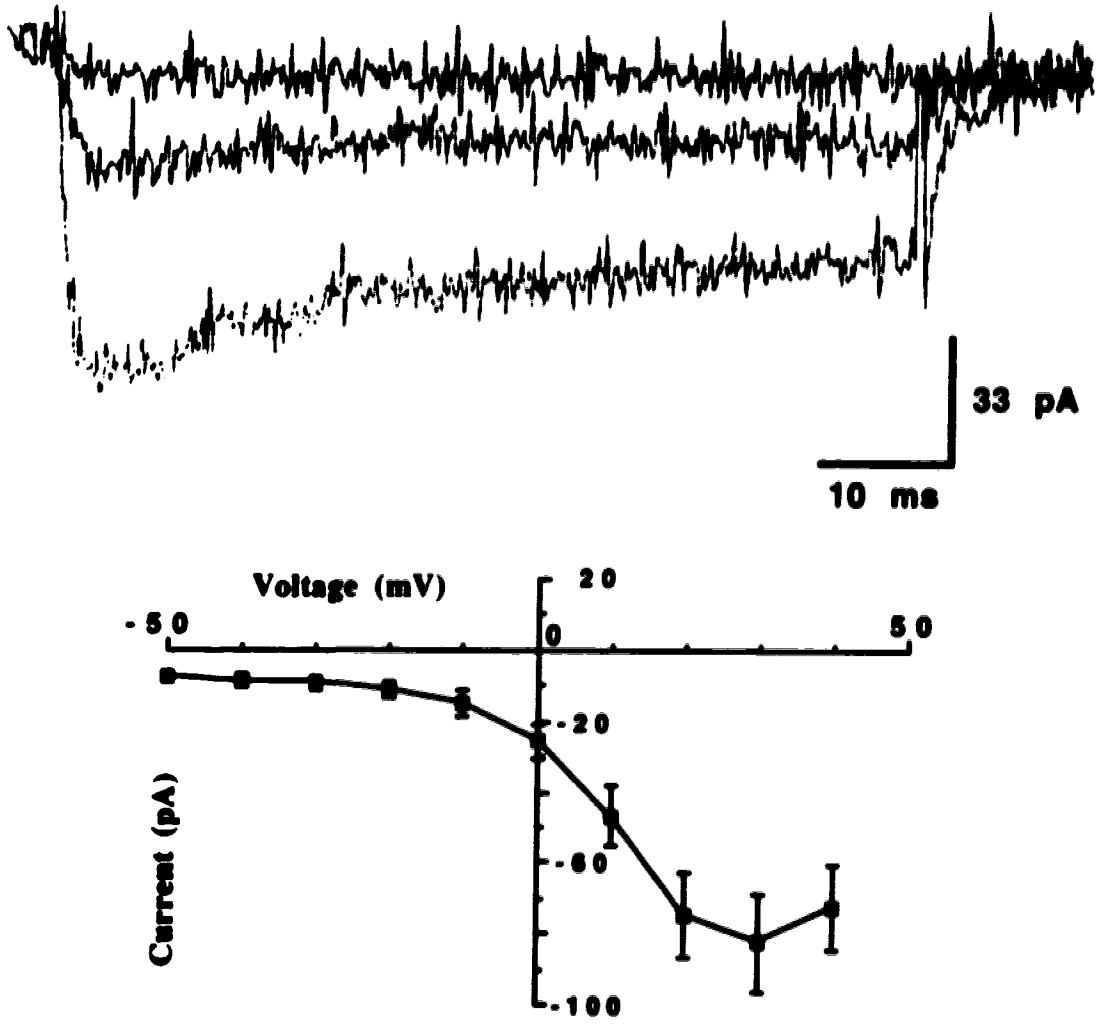

Figure VII-9: Voltage-gated calcium current. Upper trace: Using sodium-free, choline saline and an electrode solution in which potassium aspartate was replaced by cesium chloride, voltage-gated calcium currents were observed in embryonic neurons. Shown are calcium currents recorded with 100 ms voltage steps to -30, -10 and +10 mV from a holding potential of -60 mV. Bottom panel: The I/V relationship for the embryonic calcium current revealed this current to be a high voltage activated calcium current. Values used to contruct means represent the peak inward current amplitude (n=6).

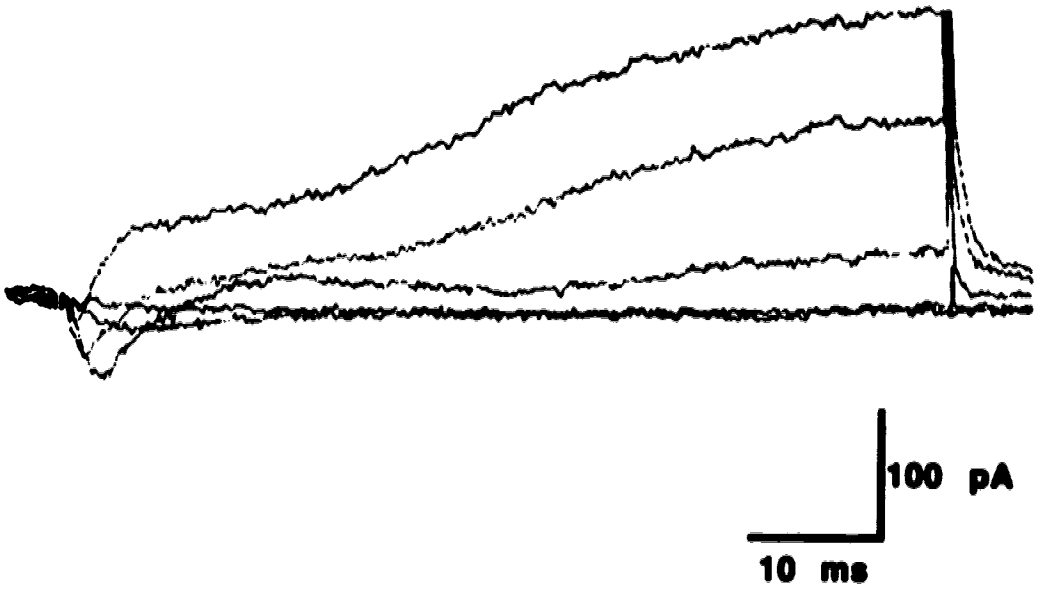

Figure VII-10: Voltage-gated currents obtained from perforated patch recordings. Shown are the currents elicited during 100 ms voltage steps to -50, -30, -10, +10 and +30 mV from a holding potential of -70 mV. The same variety of voltage-gated currents seen with standard whole-cell recordings was routinely seen in perforated patch recordings.

Figure VII-11: Possible responses of embryonic neurons to 5-HT. Upper trace: Voltage clamp, perforated patch recording showing a very small inward shift in holding current and an increase in the baseline noise level from an embryonic neuron following bath application of 5-HT. Lower trace: Perforated patch recording from a different cell that responded to bath application of 5-HT with a small outward shift in holding current and an increase in baseline noise. Holding potential was -70 mV for both cells; final 5-HT concentration was 25 μM. 5-HT was applied at the beginning of each trace.

VIII) Discussion

The results that I have presented contribute significantly towards understanding how 5-HT leads to the depolarization of neuron B19. In analyzing these results, several characteristics of the cyclic nucleotide-gated ion channel that carries the depolarizing current and the 5-HT receptor that mediates the responses activation have been identified. This permits the comparison of the neuron B19 cyclic nucleotide-gated ion channel and 5-HT receptor with those that mediate similar responses in other molluscan species and in the well studied vertebrates. By taking this comparative approach, a better understanding of the biological relevance of the neuron B19 5-HT response will be acquired.

i) Neuron B19 5-HT/cyclic nucleotide response: comparison to similar molluscan responses

In neuron B19, 5-HT exposure led to the activation of an inward current. This was mediated through cyclic nucleotides and was devoid of rapid desensitization. Two different mechanisms have been identified in molluscs where 5-HT has led to such a depolarization, the closure of the potassium carrying S-channel (Klein et al., 1982) and the opening of a sodium conductance (Gerschenfeld and Paupardin-Tritsch, 1974a and b). Owing to the sodium dependence of the neuron B19 response and the general lowering of input resistance following 5-HT exposure, it was safe to conclude that the principal 5-HT response observed was not an S-current response.

5-HT activation of a sodium conductance lacking rapid desensitization has been known for many years to occur in molluscan neurons. The A'-response described by Gerschenfeld and Paupardin-Tritsch (1974a) in *Helix* and *Aplysia* neurons had these properties. Unfortunately, their study did not address the question of second messenger mediation of the response and they have not followed this up. Therefore, no further conclusions linking the two responses can be made. However, more

recent studies have demonstrated A'-like responses to 5-HT in the identified buccal ganglion neurons B15 and B16 from *Aplysia* (Kirk et al., 1988; Taussig et al., 1989). These responses were mimicked by exposure of the cells to cAMP analogues. while 5-HT increased intracellular levels of cAMP in these cells. In addition to these two studies, several studies have been reported that describe the activation of sodium conductances in identified neurons from a wide variety of molluscan species following direct intracellular injection of cAMP (Aldenhoff et al., 1983; Connor and Hockberger, 1984; Green and Gillette, 1987; Kehoe, 1990).

Several characteristic properties of the current underlying 5-HT-dependent depolarization of neuron B19 include its ion selectivity and sensitivity to calcium ions. Based on ion substitution experiments, the 5-HT-dependent inward current was found to be carried primarily by sodium ions. However the reversal potential measured for the whole-cell current was approximately -20 mV, well below the reversal potential for sodium ions. This suggests that the channel may conduct cations nonselectively. Further support for this idea is that the reversal potential shifted towards the potassium equilibrium potential with zero sodium in the saline, and a prominent outward current was observed positive to the reversal potential. In the studies involving *Aplysia* neurons B15 and B16, the reversal potentials ranged from -20 to -10 mV (Kirk et al., 1988; Taussig et al., 1989). Moreover, in anterior and medial cells of *Aplysia* pleural ganglia the inward current seen following cAMP injection had a reversal potential of +25 mV and current could still conduct if all external sodium was replaced with potassium ions (Kehoe, 1990). Therefore, based on the lack of ion selectivity, these *Aplysia* responses resemble that of neuron B19.

A second characteristic of the neuron B19 5-HT-dependent inward current is its sensitivity to calcium ions. On average, the amplitude of the 5-HT-dependent inward currents was greater under recording conditions in which saline calcium concentrations were reduced to 100 μM. The inhibitory activity of calcium ions is also a common feature of

the sodium conductance activated following cAMP injection. Enhancement of current amplitude under calcium-free recording conditions was observed in *Helix* neurons, *Pleurobranchea* ventral white cells, and in anterior and medial *Aplysia* pleural ganglia neurons (Aldenhoff et al., 1983; Green and Gillette, 1987; Kehoe, 1990). In only one report was reduction of extracellular calcium found not to have an effect on current amplitude. This was in a study of the responses of various *Aplysia* and *Archidoris* neurons to cAMP injection (Connor and Hockberger, 1984). However, in general calcium sensitivity is likely a common feature of the sodium current activated by cAMP in molluscs.

A third interesting and, in light of the above discussion, contradictory characteristic of the neuron B19 5-HT-dependent inward current is its apparent ability to conduct calcium ions. Under sodium-free conditions, a small amount of inward current was usually evident. This residual current was especially evident when potentiated by IBMX. The fact that the residual current potentiated by IBMX was smaller when recordings were made under 100 μM calcium recording conditions suggests that at least a portion of the residual current was carried by calcium ions. A similar situation was also evident in the cAMP-dependent sodium current recorded from *Helix* cells (Aldenhoff et al., 1983). It was observed that under sodium-free conditions, an increasing amount of inward current was recorded as external calcium concentrations were increased, despite the inhibitory influence of calcium under normal sodium recording conditions. In contrast, using Arsenazo III imaging of intracellular calcium levels Connor and Hockberger (1984) found no evidence of increased calcium concentration accompanying cAMP activation of inward current in *Aplysia* and *Archidoris* cells. However, if calcium was rapidly buffered in these cells, the low calcium permeability evident in the *Helisoma* and *Helix* currents might not register a change in intracellular calcium levels.

Another characteristic of the neuron B19 5-HT-dependent inward current is an apparent voltage sensitivity. From the results of staircase experiments to establish the steady-state I/V relationship of the

response, two distinct phases were evident for the 5-HT difference current. At very hyperpolarized membrane potentials the current was inwardly directed and gradually decreased in amplitude as the membrane potential was brought to more positive values. However, at around -40 mV the current gained amplitude in the inward direction. As demonstrated in the steady-state I/V relationship for neuron B19, -40 to -20 mV is a region of negative slope conductance where some voltage-dependent current is active. Voltage sensitivity of the neuron B19 cyclic nucleotide-gated current over this range of potentials would therefore enhance the negative slope conductance.

In studies of cAMP activation of sodium current in other molluscs, two general situations are encountered regarding voltage sensitivity. In the *Aplysia* neurons B15 and B16, the I/V curves for the 5-HT and cAMP-activated sodium current resemble very closely that seen in *Helisoma* neuron B19 (Kirk et al., 1988; Taussig et al., 1989). Moreover, a similar situation was also observed in the *Aplysia* neurons recorded by Connor and Hockberger (1984) and the *Pleurobranchea* white cells recorded by Gillette and Green (1987) where inward currents induced by cAMP injection were larger at -30 mV than at more hyperpolarized membrane potentials, contrary to what was expected considering the reversal potential of the response. Conversely, in the anterior and medial cells of *Aplysia* pleural ganglia, *Helix* neurons, *Archidoris* neurons and buccal ganglion neurons from *Lymnaea*, the I/V curve for the cAMP-activated current was flat between -20 and -80 mV (Kehoe, 1990; Aldenhoff et al., 1983; Connor and Hockberger 1984; McCrohan and Gillette, 1988). In these latter reports there was no indication whether a negative slope region existed for the cells studied.

These divergent findings suggest that there are two subclasses of channels influenced by cyclic nucleotides in molluscan neurons; one that is strongly voltage sensitive and another that appears to be quite non-ohmic over a wide range of membrane potentials. An interesting explanation for this non-ohmic behavior is that these channels are not

lacking voltage-sensitivity, but are simply less voltage sensitive. In this scenerio, the increase in open probability accompanying more positive membrane potentials completely balances the decrease in driving force expected at those potentials (Connor and Hockberger, 1984; McCrohan and Gillette, 1988). The two classes can not be attributed to species differences, since both situations have been observed in *Aplysia*. Therefore, the possibility exists that two closely related channels, differing only in their voltage sensitivity, are expressed in different neurons according to some functional criterion.

A possible complicating factor in the interpretation of the 5-HT enhancement of the negative slope conductance result concerns how well the neurons used in experiments were space clamped. In cells deviating from a true spherical morphology, the access resistance to remote parts of the cell becames an important factor that can lead to those areas not being at the same potential as that at the electrode tip while voltage clamping. This is of particular importance if the intracellular solution has low ionic concentrations. In poorly space clamped cells, the voltage from poorly clamped regions can influence the voltage at the electrode tip, to which the recording electronics will respond to in the appropriate manner. Therefore, depolarization, associated with the activation of voltage-gated currents, invading from poorly clamped regions could result in an increase in the perceived inward current during the application of the staircase protocol.

To limit space clamp artifact in generation of I/V relationships for the neuron B19 5-HT-activated current, only neurons that lacked processes contributed data at potentials where voltage-gated currents would activate. Infact in process-bearing cells, unclamped action potential activity made measurement impossible at potentials more positive than -50 mV. However even in cells lacking processes, their well developed lamellipodia and overall large size could still present a problem for adequate space clamping. To obtain a definite answer regarding the question of voltage sensitivity of the neuron B19 cyclic nucleotide-gated

channel, experiments testing this property at the single channel level would be required.

Another characteristic of the 5-HT-dependent activation of sodium current in neuron B19 is that it does not require a phosphorylation-dependent step to cause channel opening. Two sources of evidence lead to this conclusion: (1) high concentrations of protein kinase inhibitors failed to eliminate current activation following 5-HT application; (2) more significantly, cAMP application to inside-out membrane patches reversibly activated ion channels that resembled those activated in cell attached patches following bath application of 5-HT. Failure of protein kinase inhibitors to inhibit cAMP activation of sodium current has also been demonstrated in *Aplysia* neuron B15 by Taussig et al. (1989), and in the anterior and medial cells of *Aplysia* pleural ganglia by Kehoe (1990). However, in the PON neuron from *Achatina*, 5-HT and cAMP-enhancement of a negative slope conductance and stimulation of a second negative slope was sensitive to the protein kinase inhibitor H8 (Funase et al., 1993). It should be remembered that H7 at concentrations high enough to inhibit all kinase activity did not inhibit the enhancement of the negative slope by 5-HT in neuron B19. Therefore, the possibility exists that the ion channels responsible for 5-HT- and cAMP-dependent sodium current in many molluscs belong to the family of ion channels that are directly gated by cyclic nucleotides.

A final characteristic for comparison among molluscs concerns the specificity of sodium current activation for various cyclic nucleotides. From single channel studies involving application of cyclic nucleotides to neuron B19 inside-out membrane patches, both cAMP and cGMP stimulated channel activity over a similar concentration range. In experiments using 8-bromo cGMP, Kirk et al. (1988) found it to be as effective as 8-bromo cAMP in activating sodium current in *Aplysia* neuron B16. Similarly, cGMP injection was equally as effective as cAMP in activating sodium current in other *Aplysia* neurons and in *Archidoris* neurons (Connor and Hockberger, 1984). However, in *Helix* neurons,

cGMP was found to be ineffective in mimicking cAMP-dependent current activation (Aldenhoff et al., 1983). While the situation that appears to be most common in molluscs is that 5-HT leads to the stimulation of cAMP synthesis, there is a report of cGMP mediating 5-HT's effects on high voltage-activated calcium currents in *Helix* neurons (Paupardin-Tritsch et al., 1986). Therefore, the specific nucleotide system that 5-HT activates in neuron B19 remains unknown. Only by using cAMP- or cGMP-specific phosphodiesterase inhibitors, or through direct biochemical measurements of cyclic nucleotide concentrations can this issue be resolved.

ii) Comparison with vertebrate cyclic nucleotide-gated ion channels

Within recent years a significant amount of research has gone towards characterizing the ion channels in vertebrates that are directly gated open by cyclic nucleotides. In vertebrate photoreceptors, the electrophysiological response to light consists of the reduction of a steady-state inward current and subsequent hyperpolarization of the photoreceptor membrane potential (Pugh and Cobbs, 1986). The ion channels that underlie the steady-state "dark current" are directly gated by cGMP, as evidenced through studies using excised inside-out membrane patches (Fesenko et al., 1985; Haynes et al., 1986; Zimmerman and Baylor, 1986). In the olfactory epithelium of vertebrates, channels directly gated by cyclic nucleotides also provide one mechanism through which odors are perceived. Here, odorant binding can stimulate the synthesis of cyclic nucleotides which then result in membrane depolarization (Ronnett and Snyder, 1992). Single channel recording experiments have revealed that cyclic nucleotides directly gate the ion channels that are responsible for this depolarization (Firestein et al., 1991; Zufall et al., 1991).

Owing to the availability of large amounts of bovine retinal tissue, the first cyclic nucleotide-gated ion channel to be purified was the rod cGMP-

dependent channel (Kaupp, 1991). Using partial amino acid sequences obtained from this 63K peptide, synthetic nucleotide probes were constructed and used to screen a cDNA library. With this approach, Kaupp et al. (1989) isolated a clone. When RNA synthesized from this clone was injected into *Xenopus* oocytes functional cGMP-gated ion channels were expressed. Moreover, clones for the cyclic nucleotide-gated channel from rat and catfish olfactory epithelia have been isolated using probes obtained from the bovine rod channel sequence (Dhallan et al., 1990; Goulding et al., 1992). Studies of the cloned channels, as well as of the native channels, have generated a considerable amount of information regarding the nature of vertebrate cyclic nucleotide-gated ion channels which could provide insight into the nature of the neuron B19 cyclic nucleotide-gated channel.

Examination of the amino acid sequences obtained from the cloned channels produced some surprising conclusions. Despite being "ligand-gated" ion channels, the sequence information and hydropathy analysis indicated that they were more similar to the voltage-gated family of ion channels rather than the traditional family of ligand-gated ion channels (Jan and Jan, 1992). Each peptide possesses six potential transmembrane segments plus another region that likely forms a hairpin turn into the membrane between the fifth and sixth transmembrane segments to form a portion of the pore. This is the situation generally associated with voltage-gated potassium channels (Mackinnon, 1991). However, unlike the voltage-gated channels the cyclic nucleotide-gated channels possess in their cytoplasmic C-terminus a cyclic nucleotide recognition site that is structurally similar to the nucleotide binding domains of other cyclic nucleotide binding proteins (Kaupp et al., 1989; Dhallan et al., 1990).

Like the voltage-gated channels, the cyclic nucleotide-gated channels possess a positively charged amino acid in every third position for a certain distance along the fourth transmembrane segment (S4; Papazian et al., 1991). In the voltage-gated channels this arrangement is thought

to be important in voltage sensing (Stumer et al., 1989; Papazian et al., 1991). Studies with vertebrate cyclic nucleotide-gated channels generally conclude that they are only weakly voltage sensitive at best (Kaupp, 1991). However, the cyclic nucleotide-gated channels recorded in many molluscan preparations, including *Helisoma* neuron B19, may be relatively more voltage sensitive. This results in or contributes to the negative slope region of the steady-state I/V curve. Two possible explanations for the lack of voltage sensitivity in the vertebrate channels are: 1) that they lack the leucine heptade motif found in the voltage-gated potassium channels; 2) they have a smaller total charge on the S4 segment (Goulding et al., 1992). These may reflect adaptations for the vertebrate channels becoming voltage independent and acquiring a sensory role, while the neuronal molluscan channels retained these features.

One characteristic that is common to all cyclic nucleotide-gated ion channels is their sensitivity to divalent cations. For both the molluscan and the vertebrate channels, the presence of divalent cations in recording solutions results in smaller amplitude currents. However, in all examples where it was tested, including neuron B19, divalent cations could also permeate the channels giving rise to measurable currents. The simplest explanation for this apparently contradictory phenomenon is that a cation binding site exists within the channel. Given their greater charge, divalent cations bind to the site more strongly and for longer periods of time, consequently slowing conduction through the channel (Colamartino et al., 1991; Zimmerman and Baylor, 1992).

The function of cyclic nucleotide-gated ion channels appears to be under the control of several intracellular regulatory systems. Calcium-dependent regulation provides an interesting example. In catfish olfactory neurons intracellular calcium ions shift the cAMP dose-response relationship to higher doses (Kramer and Siegelbaum, 1992). This effect is independent of normal divalent blockade at the channel pore since it is achieved with micromolar calcium levels while millimolar levels are

needed for blockade. Moreover, the effect washed out with excision of macropatches and was not seen in channels expressed in *Xenopus* oocytes. Kramer and Siegelbaum concluded that this effect of micromolar calcium likely involved a separate calcium binding protein that reduced the channel's affinity for cAMP when activated by calcium. Similarly in rods, the sensitivity of the rod channel for cGMP decreases through a calmodulin-dependent process that involves a 240K protein (Hsu and Molday, 1993). In *Pleurobranchea*, Green and Gillette (1988) have shown that responses to cAMP injection decrease in cells that display spiking activity. This depression is reduced if extracellular calcium is lowered and can be blocked with calmodulin blockers. Coupled with the calcium sensitivity of certain phosphodiesterase and cyclase molecules, the calcium permeability of the cyclic nucleotide gated ion channels may be physiologically important in negative feedback systems controlling the channel's activity (Kaupp, 1991). In my recordings, 5-HT responses were maintained which suggests such negative feedback systems may not be active in neuron B19. However, the use of EGTA in the electrode solution wouid have precluded any negative feedback mechanisms that may be important in effecting the duration of the neuronB19 5-HT response.

In addition to the above calcium-dependent pathways, cyclic nucleotide-gated ion channel function can be modified by phosphorylation. The rod cGMP channel can exist in one of two states in excised patches, with one state being three orders of magnitude less sensitive to cGMP than the other (Gordon et al., 1992). Treatment with serine/threonine specific phosphatase inhibitors prevented the shift to the less sensitive state, whereas it could be induced with protein phosphatase 2A. This suggested that an endogenous serine/threonine phosphatase, and likely a kinase, is localized near the channels to regulate the channel's phosphorylation state and modulate its affinity for cGMP. A second site regulated by phosphorylation was also identified by Gordon et al. (1992) based on the finding that protein phosphatase 1 treatment increased the affinity of the channel for cGMP. The results of IBMX experiments

revealed that neuron B19 had considerably more ion channels available than were activated with a saturating dose of 5-HT. However, the possibility that a similar phosphorylation-dependent regulatory mechanism is responsible for these extra channels is unlikely since H7 experiments did not result in larger currents.

iii) Pharmacology of the neuron B19 5-HT receptor

Despite the wide use of molluscan preparations as models for 5-HT activities in nervous systems and other tissues, very little is known about the identity of the receptors that mediate these actions. Therefore, experiments were performed to initiate a pharmacological description of the neuron B19 5-HT receptor. The response to 5-HT diminished if the interior of the cell was perfused with a GTPγS-containing solution. This suggested the neuron B19 5-HT receptor was a G-protein coupled receptor. Furthermore, the amplitude of the current evoked by exposure to the phosphodiesterase inhibitor IBMX was greater if the cell was initially exposed to 5-HT. This suggested that receptor activation was positively coupled to the synthesis of cyclic nucleotides. In molluscs, little pharmacological information is available for 5-HT receptors positively linked to cyclase activation. Therefore, the data gathered here is particularly useful.

One of the disappointments of this study was the inability to identify pharmacological agents with specific antagonistic activities at the neuron B19 5-HT receptor. Several known serotonin receptor antagonists were tested for this activity and all that showed apparent antagonistic activities also had non-specific effects on voltage-gated ion currents. Dose response relationships for apparent antagonism and non-specific effects for two of these agents were obtained. For both cyproheptadine and mianserin, the lack of a several log-unit separation in the dose-responses for apparent antagonism and non-specific effects indicates that their use as functional antagonists is not appropriate.

While experiments with antagonists were disappointing, experiments using serotonin agonists were very useful, especially for determining relationships between the neuron B19 5-HT receptor and other known 5-HT receptors. The indolylalkylamines tryptamine, 5-carboxyamidotryptamine, α-methyl 5-HT and 5-methoxytryptamine all displayed lower receptor activation abilities and/or affinities than 5-HT. The ergoline methysergide displayed high affinity, partial agonist activity, where at low concentrations methysergide gave weak activation of inward current but at high concentrations it completely opposed 5-HT activation of inward current. Both tryptamine and 5-carboxamidotryptamine also caused a reduction of inward current when applied following initial 5-HT exposure, which is not surprising because of their partial agonist behavior. However, dose-response experiments were not performed on these two compounds to determine if they could give complete reduction 5-HT-activated inward current. Finally, the traditional 5-HT_{1A} agonist 8-OH DPAT possessed no agonist activity at the neuron B19 5-HT receptor.

Using this combination of functional and pharmacological data, a meaningful comparison between the neuron B19 5-HT receptor and known 5-HT receptors can be pursued. The best known 5-HT receptors are the vertebrate receptors. In the vertebrates a multitude of 5-HT receptors have been described and many of these have been cloned. Therefore, a great wealth of information is available concerning their functional and pharmacological properties. From functional information, the vertebrate 5-HT_3 receptor group can be eliminated as a source of useful comparison. These receptors exist as a receptor/ion channel complex similar to the nicotinic acetylcholine receptors, GABA receptors, glycine receptors and the non-metabotropic glutamate receptors (Betz, 1990; Maricq et al, 1991). 5-HT_3 receptors are not sensitive to treatment with GTPγS and demonstrate rapid desensitization in the continued presence of the ligand.

The receptors in the 5-HT_1 group, like the neuron B19 5-HT receptors, are high affinity binding sites for 5-HT. In contrast, indolylalklyamine analogues generally have lower affinities to these receptors (Glennon, 1987). An exception to this is 5-carboxamidotryptamine, which is a high affinity ligand for all 5-HT_1 sites, save for 5-HT_{1E} sites (Glennon, 1987; Beer et al., 1993). 5-HT_1 receptors are generally negatively coupled to cAMP synthesis, including 5-HT_{1E} sites. The lack of functional correlation and deviations in pharmacology suggest, not surprisingly, that there is no obvious relationship between the neuron B19 5-HT receptor and the 5-HT_1 group of receptors.

Another vertebrate 5-HT receptor group that demonstrates no obvious relationship to the neuron B19 receptor are the 5-HT_2 receptors. This includes the 5-HT_{1c} receptors, based on structural and functional criteria (Humphrey et al., 1993). These receptors are functionally linked to phospholipase C activation and result in the liberation of the second messengers diacylglycerol and inositol trisphosphate. 5-HT_2 receptors have a relatively low affinity for 5-HT compared to 5-HT_1 sites and alpha methylation of 5-HT does not result in a reduction of activity, differentiating this receptor from the neuron B19 receptor (Ismaiel et al., 1990). Unfortunately, the ligands best suited for comparison with the 5-HT_2 receptors are the classical serotonin antagonists such as mianserin and cyproheptadine (Glennon, 1987; Zifa and Fillion, 1992). Ligand binding assays would have to be performed to better evaluate the question of similarity.

5-HT receptors demonstrating positive coupling to adenylate cyclase activation have also been identified in vertebrates. The first of these to be described was the 5-HT_4 receptor of embryonic mouse colliculi neurons (Dumuis et al., 1988). Subsequent studies have identified similar receptors in neuroblastoma NCB.20 cells and in cells of the human frontal cortex (Connor and Mansour, 1990; Monferini et al., 1993). Like the neuron B19 receptor the indolylalkylamine analogues 5-carboxamidotryptamine and tryptamine both show lower activity at 5-

HT_4 sites, while 8-OH DPAT showed no activity. However, the relative effectiveness of 5-methoxytryptamine and the inactivity of methysergide as agonists were characteristics not shared with the neuron B19 receptor. A second 5-HT receptor pharmacologically distinct from the 5-HT_4 receptor, but which is also positively coupled to adenylate cyclase activity in vertebrates, has recently been cloned and labeled the 5-HT_7 receptor (Lovenberg et al., 1993). With the exception of sensitivity to methysergide, the 5-HT_7 receptor is quite dissimilar pharmacologically from the neuron B19 receptor. These receptors show high affinity binding for 5-carboxamidotryptamine and modest affinity for 8-OH DPAT.

With these results, it appears that the neuron B19 5-HT receptor is dissimilar to both of the vertebrate 5-HT receptors that are positively coupled to adenylate cyclase activity. However a recent example of how pharmacological data can be misleading in determining phylogenetic relationships between receptors suggests that an open mind must be kept when trying to determine relationships. The rat 5-HT_{1B} and human 5-$HT_{1D\beta}$ receptors share 93% amino acid sequence homology, however, they are pharmacologically quite different, in that the rat receptor has greater sensitivity for β-adrenergic antagonists (Beer et al., 1993). Interestingly, a single amino acid accounts for the pharmacological difference, where if threonine 355 on the human receptor is replaced with the asparagine found at the same location on the rat receptor, the pharmacology of the mutant becomes largely similar to the rats (Oksenberg et al., 1992). Final conclusions regarding the phylogenetic relationship of the neuron B19 5-HT receptor and the vertebrate receptors would require cloning of the neuron B19 receptor and determination of its primary structure.

A phylogenetically more logical source of comparison for the neuron B19 5-HT receptor are the arthropods. The best studied of the arthropod 5-HT receptors are those that have been cloned from *Droeophila*. So far three clones have been isolated, two that are negatively linked to adenylate cyclase activity and one that is positively linked. Of the two

negatively linked receptors, dro2A and dro2B, both have micromolar affinities for serotonin, methysergide and 8-OH DPAT. The dro2B receptor generally has higher affinities for these compounds than the dro 2A receptor (Saudou et al., 1992). The receptor positively linked to adenylate cyclase activity, dro1, has many features in common with the neuron B19 receptor. The dro1 has similar 5-HT and 5-methoxytryptamine sensitivities as the neuron B19 receptor based on functional measurements of cAMP accumulation (Witz et al., 1990). Moreover, dro1 is antagonized by high concentrations of methysergide and 8-OH DPAT demonstrated only very weak agonist activity.

A receptor with similar properties to dro1 has also been observed in preparations of mandibular closer muscle from the cricket *Gryllus domestica* (Baines and Downer, 1991). Here a receptor with submicromolar sensitivity for 5-HT has been found to increase intracellular cAMP levels. 5-methoxytryptamine was a less effective agonist at this site while 8-OH DPAT did not raise cAMP concentrations significantly above basal levels. Therefore, in the insects serotonin receptors occur that are positively linked to adenylate cyclase activity and methoxy substitution of the five hydroxyl group leads to decreased activity of the ligand, unlike what was observed with the 5-HT$_4$ receptor (Dumuis et al., 1988).

Despite the common use of molluscan systems as models for 5-HT activity, molluscan 5-HT pharmacology is at best rudimentary. However, from the few studies where pharmacological testing has been performed, it is clear that a variety of 5-HT receptor subtypes exist. In the early study of Gerschenfeld and Paupardin-Tritsch (1974a), the responses A, A', B and C could each be antagonized with specific pharmacological agents. 7-methyltryptamine specifically blocked the A response, 5-methoxygramine specifically blocked the B response and neostigmine specifically blocked the C response. The A' response was only blocked by bufotenine, which blocked the other three responses as well. Since A' was the response that most resembled the neuron B19

response, it would have been worth while to test neuron B19's sensitivity to bufotenine. Unfortunately, this controlled substance was not readily available and therefore was not tested.

The above pharmacological experiments were performed on both *Helix* and *Aplysia* neurons. A more recent report by Mercer et al. (1991) has identified another apparent antagonist of a molluscan 5-HT receptor using *Aplysia* sensory neurons. In this report, 200 μM cyproheptadine inhibited the broadening of action potentials that is normally seen following exposure of these cells to 5-HT. This experiment provided the impetus for examination of this drug as an antagonist of the neuron B19 5-HT response, since both responses involve cyclase stimulation. 100 μM cyproheptadine was found to be very effective at antagonizing the neuron B19 5-HT response. However, it was also effective at reversibly inhibiting voltage-gated ion currents. Cyproheptadine also reduced steady-state currents including the current carried by the negative slope conductance and could inhibit the current activated by IBMX alone. Similar results were also obtained for mianserin.

The above results suggest that cyproheptadine can act as a non-specific ion channel blocker of molluscan ion currents. To test this hypothesis further, current and voltage clamp recordings were also performed on *Lymnaea* and *Aplysia* neurons. Here too, voltage-gated inward and outward currents were reversibly inhibited. This suggests that the results seen by Mercer et al. (1991) may have been misinterpreted, where cyproheptadine had already blocked the S-channels prior to 5-HT exposure. These results demonstrate that cyproheptadine and mianserin are not suitable drugs for electrophysiological experiments employing molluscan systems. Interestingly, calcium currents in guinea pig taenia coli also show sensitivity to cyproheptadine (Lowe et al., 1981).

The best pharmacological data for a molluscan 5-HT receptor comes from the only one that has been cloned. Using a cDNA library from the

central nervous system mRNA of *Lymnaea*, a clone was isolated, sequenced and expressed in COS-7 cells (Sugamori et al., 1993). The receptor shares 61% homology with the dro2B receptor which may indicate that it is negatively coupled to adenylate cyclase activation. This hypothesis is supported by the observation that it possesses a large third cytoplasmic loop and a short C-terminus, which are features shared by receptors that are negatively linked to adenylate cyclase activity. Pharmacologically, the *Lymnaea* receptor has a fairly weak affinity for 5-HT and demonstrates higher affinity for 5-carboxamidotryptamine, methysergide and 8-OH DPAT. Therefore, pharmacologically and perhaps functionally the *Lymnaea* receptor is quite different from the neuron B19 receptor.

iv) The neuron B19 5-HT response and its role in the biology of neuron B19

5-HT plays a very important role in the biology of neuron B19, being involved in determining its morphology and synaptic interactions during embryonic development and regulating its electrical activity in the adult. Of the two roles, study of the first has generated the most interest. From the studies of Goldberg and Kater (1989) it is clear that 5-HT does influence the morphology and synaptogenesis in neuron B19. However, do the results from the present study which describe a response seen in adult cultured cell bodies have any developmental relevence? There is evidence suggesting that this response may indeed be an element of the mechanism through which 5-HT regulates growth cone motility. Depolarization is an important element in the mechanism since injection of hyperpolarizing current inhibits 5-HT's effects on growth cone motility (McCobb and Kater, 1988). The ability of forskolin and db cAMP to inhibit neurite outgrowth is also consistent with the involvement of a cyclic nucleotide-gated ion channel in the mechanism (Mattson et al., 1988D). This demonstration that a cyclic nucleotide-gated ion channel is involved in 5-HT signalling would then identify at least one previously unknown role for cyclic nucleotides in this process.

Evidence that would confirm the developmental significance of this 5-HT response awaits discovery. The most telling line of evidence would come from cloning the receptor and ion channel and examining embryos for their expression. The basic knowledge obtained from this study would facilitate the process of selecting probes for screening a cDNA library and provide a set of characteristics to ensure that the clones isolated correspond to the right entities. Alternatively, electrophysiological recordings could be performed on growth cones of adult cells and on embryonic cells to examine for these responses. I did perform some single channel recordings from growth cones, however, unambiguous evidence for cyclic nucleotide-gated channels was not obtained. This may not be too surprising given the recent report by Davenport et al. (1993), which demonstrated that growth cone filopodia alone can respond to 5-HT with increases in intracellular calcium. Therefore, the channels may be preferentially concentrated there, rather than in the more experimentally accessible "body" of the growth cone. Similar to the growth cone recordings, no concrete evidence for 5-HT responses in embryonic neurons was obtained. While my recordings demonstrate that embryonic cells definitely possess excitable characteristics, and experiments by Goldberg and his collegues show that some of these cells must possess 5-HT receptors (Goldberg et al., 1991;1992), no link between the two could be demonstrated with the recording configuration used. Single channel recordings appear to be the best assay to use here.

One interesting aspect of the cyclic nucleotide-gated ion channel transduction system is the permeability of the channel to calcium. At a localized level, the calcium that penetrates the channel could generate a sizable increase in intracellular concentration with physiological significance. This is seen in the vertebrate rod where calcium feeds back to inhibit cGMP synthesis (Kaupp, 1991). In reports describing calcium-mediated 5-HT inhibition of growth cone motility, calcium is thought to enter via voltage-gated ion channels, based on divalent cation blockade of the calcium channels and the requirement for membrane depolarization

(Mattson and Kater, 1987). However, considering these results and that large divalent cations would have difficulty getting through cyclic nucleotide-gated ion channels (Colamartino et al, 1991), the contribution of these channels to increasing intracellular calcium concentrations may have been obscured.

A second interesting aspect of a cyclic nucleotide transduction system is the possibility of stimulating cAMP-response elements in the nucleus. cAMP-dependent kinase can be translocated to the nucleus where it interacts with a binding protein that controls the activity of cAMP-response elements (Montminy et al., 1990). cAMP response elements control the expression of certain genes and thereby provide a mechanism through which environmental cues can influence the genes expressed by a certain cell. For a neuron, this could be a signal for the cell to undergo the transition from a neuron with actively growing processes to one with stable processes. In *Aplysia* sensory neurons the opposite has been shown to occur. cAMP response elements are stimulated and gene products synthesized that underlie part of the morphological changes that occur during longterm behavioral sensitization (Kaang et al., 1993).

While 5-HT regulation of neurite outgrowth receives greater attention, the mechanism underlying 5-HT regulation of neuron B19 motor output is interesting in its own right. Neuron B19 displays a characteristic pattern of in situ electrical activity with periods of spiking activity broken up by large amplitude hyperpolarizations. Two hypothesis have been developed to describe this burst-hyperpolarization-burst pattern of electrical activity. Origionally it was thought a single cluster of interneurons coordinated the activity (Kater, 1974). Termed the cyberchron network, these interneurons would result in a large hyperpolarization of neuron B19, which terminated spiking activity. The next burst phase would then be initiated via an anode break spike on recovery from this hyperpolarization. An alternative hypothesis describing the control of the feeding rhythm involves interneurons that coordinate each of three phases of the feeding rhythm (Murphy, 1991). Here, B19 receives input

from three interneurons; one inhibitory that generates the large hyperpolarization that is characteristic of *in situ* B19 recordings, and two excitatory that drive the spiking activity between hyperpolarizations.

When neuron B19 is exposed to 5-HT *in situ*, one of two things occurs: 1) in a quiet preparation, patterned motor output is initiated; 2) in an active preparation, the frequency of bursts is increased (Granzow and Kater, 1977). As we have seen, 5-HT induces the activation of an inward current which can result in the initiate of action potential activity. 5-HT may also enhance a negative slope conductance that may be present in neuron B19. Negative slope conductances are common features of molluscan cells that demonstrate bursting activity. They are thought to aid the onset of bursts by providing an inward current influence at the region of voltage instability that corresponds to the threshold for action potential firing (Wilson and Wachtel, 1974). 5-HT-enhancement of the negative slope conductance would augment this inward current influence and provide a stronger force to accelerate the ascent from the synaptically induced hyperpolarization,. As a result, the cell would spend less time in the hyperpolarized state and the frequency of bursting would increase.

The conclusion that the neuron B19 cyclic nucleotide-gated channel may possess voltage sensitivity is interesting in light of the finding that vertebrate cyclic nucleotide-gated channels have an S4 transmembrane segment that still possesses charged amino acids at every third position for some portion of the segment (Goulding et al, 1992). It would be interesting to obtain the amino acid sequence for the neuron B19 channel and see how it differs from that of the vertebrate channels, especially with regard to structures that are thought to be involved in voltage sensing. It could provide an example of how ion channels have adapted to perform distinctly different roles.

One of the potential problems of this study that relates to both developmental and adult roles for 5-HT on neuron B19 concerns the use

of cell body recordings to describe events going on at peripheral synapses and growth cones. However, this may not be such a problem, considering the normal way that neuron B19 is exposed to 5-HT in the animal. Neuron B19's source for 5-HT is the giant serotonergic neuron C1, which appears to release 5-HT in a neurohumoral fashion. For an excitatory post synaptic potential to appear in neuron B19, multiple neuron C1 action potentials must be induced. However, the response persists in high calcium conditions indicating a polysynaptic mechanism is not involved (Granzow and Kater, 1977; Gadiotti et al., 1986). Moreover, the extensive elaboration of neuron C1 processes throughout the buccal ganglia suggests widespread release sites (Gadiotti et al., 1986). If neuron C1 release of 5-HT in the buccal ganglia is neurohumoral, then cell body responses would definitely be significant.

Despite the high success rate of getting multiple cyclic nucleotide-gated channels in membrane patches from cell bodies, overall whole-cell responses were rather small. This suggests that the response is highly regulated. The experimental results demonstrate two of these regulatory sources: divalent block of the channel and phosphodiesterase activity. Whole-cell recordings were performed under normal extracellular divalent cation-containing recording conditions, while inside-out single channel recordings were performed with no divalent cations in the pipette solution to avoid divalent cation block of inward currents. Divalent cation block reduces the rod channel conductance from 20-25 pS under divalent-free conditions to 0.1 pS with divalent cations present (Kaupp, 1991). Such a reduction in single channel conductance would increase the number of channels needed to obtain an average sized whole cell response in neuron B19. Additionally, phosphodiesterase activity appears to be quite significant in neuron B19 as indicated by experiments with IBMX.

In addition to intracellular regulation of the neuron B19 cyclic nucleotide-gated ion channel, the activity of this channel has the potential to be regulated by other important intercellular messengers. Besides 5-HT, both the monoamine dopamine and the neuropeptide small

cardioactive peptide$_B$ (SCP$_B$) can initiate patterned motor output in quiet preparations or accelerate it in active preparations (Murphy et al., 1985; Trimble and Barker, 1984). In addition, dopamine can induce inhibition of growth cone motility and neurite outgrowth in neuron B19 (McCobb et al., 1988). The transduction mechanism for neither dopamine, nor SCP$_B$ has been determined. However, since both cAMP and cGMP can activate the neuron B19 cyclic nucleotide-gated channel, either second messenger system could mediate the action of these transmitters. This underscores the potential importance of the cyclic nucleotide-gated channel to the function of neuron B19 as it may serve as a point of convergence for at least two other regulators of neuron B19 activity.

In conclusion, the results presented herein have significantly enhanced our understanding of how 5-HT results in the depolarization of neuron B19. Information on the ion channel responsible for the depolarizing current, its control by cyclic nucleotides and the receptor that initiates the response have been obtained. The receptor and ion channel described are likely to play important roles in the regulation of neuron B19 electrical activity and how this neuron behaves within the neuronal circuit underlying feeding. It is possible that this 5-HT receptor and cyclic nucleotide-gated ion channel play important roles in the development of neuron B19, and perhaps other neurons. This makes the study of their expression during embryonic development a logical extension of this study.

IX) Literature Cited

Aldenhoff, J.B., Hofmeier, G., Lux. H.D. and Swandulla, D. 1983. Stimulation of a sodium influx by cAMP in *Helix* neurons. Brain Research 276: 289-296.

Bailey, C.H. and Chen, M. 1983. Molecular basis of long-term habituation and sensitization in *Aplysia*. Science 220: 91-93.

Baines, R.A. and Downer, R.G.H. 1991. Pharmacological characterization of a 5-hydroxytryptamine-sensitive receptor/adenylate cyclase complex in the mandibular closer muscles of the cricket, *Gryllus domestica*. Archives of Insect Biochemistry and Physiology 16: 153-163.

Beer, M.S., Middlemiss, D.N. and McAllister, G. 1993. 5-HT1-like receptors: six down and still counting. Trends in Pharmacological Science 14: 228-231.

Betz, H. 1990. Ligand-gated ion channels in the brain: The amino acid receptor superfamily. Neuron 5: 383-392.

Blumenfeld, H., Spira, M.E., Kandel, E.R. and Siegelbaum, S.A. 1990. Facilitatory and inhibitory transmitters modulate calcium influx during action potentials in *Aplysia* sensory neurons. Neuron 5: 487-499.

Budnik, V., Wu, C.-F. and White, K. 1989. Altered branching of serotonin-containing neurons in *Drosophila* mutants unable to synthesize serotonin and dopamine. Journal of Neuroscience 9: 2866-2877.

Bulloch, A.G.M. and Dorsett, D.A. 1979. The integration of the patterned output of buccal motoneurones during feeding in *Tritonia hombergi*. Journal of Experimental Biology 79: 23-40.

Castellucci, V.F., Kandel, E.R., Schwartz, J.H., Wilson, F.D., Nairn, A.C. and Greengard, P. 1980. Intracellular injection of the catalytic subunit of cyclic AMP-dependent kinase simulates facilitation of transmitter release underlying behavioral sensitization in *Aplysia*. Proceedings of the National Academy of Science USA 77: 7492-7496.

Castellucci, V.F., Nairn, A., Greengard, P., Schwartz, J.H. and Kandel, E.R. 1982. Inhibitor of adenosine 3', 5'- monophosphate-dependent protein kinase blocks presynaptic facilitation in *Aplysia*. Journal of Neuroscience 2: 1673-1681.

Cohan, C.S. and Kater, S.B. 1986. Suppression of neurite elongation and growth cone motility by electrical activity. Science 232: 1638-1640.

Cohan, C.S., Connor, J.A. and Kater, S.B. 1987. Electrically and chemically mediated increases in intracellular calcium in neuronal growth cones. Journal of Neuroscience 7: 3588-3599.

Cohen, J.L., Weiss, K.R. and Kupfermann, I. 1978. Motor control of buccal muscles in *Aplysia*. Journal of Neurophysiology 41: 157-180.

Colamartino, G., Menini, A. and Torre, V. 1991. Blockage and permeation of divalent cations through the cyclic GMP-activated channel from tiger salamander retinal rods. Journal of Physiology 440: 189-206.

Colquhoun, D. and Hawkes, A.G. 1983. The principles of the stochastic interpretation of ion-channel mechanisms. in Single Channel Recording. B. Sakmann and E. Neher eds., Plenum Press, New York: pp 135-175.

Colquhoun, D. and Sigworth, F.J. 1983. Fitting and statistical analysis of single-channel recordings. in Single Channel Recording. B. Sakmann and E. Neher eds., Plenum Press, New York: pp 191-263.

Connor, D.A. and Mansour, T.E. 1990. Serotonin receptor-mediated activation of adenylate cyclase in the neuroblastoma NCB.20: A novel 5-hydroxyt yptamine receptor. Molecular Pharmacology 37: 742-751.

Connor, J.A. and Hockberger, P. 1984. A novel membrane sodium current induced by injection of cyclic nucleotides into gastropod neurones. Journal of Physiology 354: 139-162.

Cooper, J.R., Bloom, F.E. and Roth, R.H. 1978. The Biochemical Basis of Neuropharmacology. Oxford University Press, New York, New York. pp327.

Cottrell, G.A. and Macon, J.B. 1974. Synaptic connexions of two symmetrically placed giant serotonin-containing neurones. Journal of Physiology 236: 435-464.

Davenport, R.W., Dou, P., Rehder, V. and Kater, S.B. 1993. A sensory role for neuronal growth cone filopodia. Nature 361: 721-724.

Dhallan, R.S., Yau, K.-W., Schrader, K.A. and Reed, R.R. 1990. Primary structure and functional expression of a cyclic nucleotide-activated channel from olfactory neurons. Nature 347: 184-187.

Dumuis, A., Bouhelal, R., Sebben, M., Cory, R. and Bockaert, J. 1988. A nonclassical 5-hydroxytryptamine receptor positively coupled with adenylate cyclase in the central nervous system. Molecular Pharmacology 34: 880-887.

Fesenko, E.E., Kolesnikov, S.S. and Lyubarsky, A.L. 1985. Induction by cyclic GMP of cationic conductance in plasma membrane of retinal rod outer segment. Nature 313: 310-313.

Firestein, S., Zufall, F. and Shepherd, G.M. 1991. Single odor-sensitive channels in olfactory receptor neurons are also gated by cyclic nucleotides. Journal of Neuroscience 11: 3565-3572.

Funase, K., Watanabe, K. and Onozuka, M. 1993. Augmentation of bursting pacemaker activity by serotonin in an identified *Achatina fulica* neurone: an increase in sodium- and calcium-activated negative slope resistance via cyclic-AMP-dependent protein phosphorylation. Journal of Experimental Biology 175: 33-44.

Gadotti, D., Bauce, L.G., Lukowiak, K. and Bulloch, A.G.M. 1986. Transient depletion of serotonin in the nervous system of *Helisoma*. Journal of Neurobiology 17: 431-447.

Gelperin, A. 1981. Synaptic modulation by identified serotonin neurons. in Serotonin Neurotransmission and Behavior. B.L. Jacobs and A.Gelperin eds., MIT Press Cambridge, Mass.: pp 288-304.

Gerschenfeld, H.M. and Paupardin-Tritsch, D. 1974a. Ionic mechanisms and receptor properties underlying the responses of molluscan neurones to 5-hydroxytryptamine. Journal of Physiology 243: 427-456.

Gerschenfeld, H.M. and Paupardin-Tritsch, D. 1974b. On the transmitter function of 5-hydroxytryptamine at excitatory and inhibitory monosynaptic junctions. Journal of Physiology 243: 457-481.

Gillette, R. and Davis, W.J. 1977. The role of the metacerebral giant neuron in the feeding behavior of *Pleurobranchaea*. Journal of Comparative Physiology 116: 129-159.

Gillette, R. and Green, D.J. 1989. Calcium dependence of voltage sensitivity in adenosine 3',5'-cyclic phosphate-stimulated sodium current in *Pleurobranchaea*. Journal of Physiology 393: 233-245.

Gilman, A.G. 1987. G Proteins: Transducers of receptor-generated signals. Annual Review of Biochemistry 56: 615-649.

Glennon, R.A. 1987. Central serotonin receptors as targets for drug research. Journal of Medicinal Chemistry 30: 1-12.

Goldberg, J.I. and Kater, S.B. 1989. Expression and function of the neurotransmitter serotonin during development of the *Helisoma* nervous system. Developmental Biology 131: 483-495.

Goldberg, J.I., McCobb, D.P., Guthrie, P.B., Lawton, R.A., Lee, R.E. and Kater, S.B. 1988. Characterization of cultured embryonic neurons from the snail *Helisoma*. in Cell Culture Approaches to Invertebrate Neurosciences. D. Beadle, G. Lees and S.B. Kater eds., Academic Press Inc., London: pp.85-108.

Goldberg, J.I., Mills, L.R. and Kater, S.B. 1990. Novel effects of serotonin on neurite outgrowth in neurons cultured from embryos of *Helisoma trivolvis*. Journal of Neurobiology 22: 182-194.

Goldberg, J.I., Mills, L.R. and Kater, S.B. 1992. Effects of serotonin on intracellular calcium in embryonic and adult *Helisoma* neurons. International Journal of Developmental Neuroscience 10: 255-264.

Goldberg, J.I. and Price, C.J. 1991. Voltage-gated ionic currents in neurons isolated from *Helisoma trivolvis* embryos. in Molluscan Neurobiology. Kitts, K.S., Boer, H.H. and Joosse, J. eds. North Holland Publishing Company, Amsterdam. pp161-167.

Gordon, S.E., Brautigan, D.L. and Zimmerman, A.L. 1992. Protein phosphatases modulate the apparent agonist affinity of the light-regulated ion channel in retinal rods. Neuron 9: 739-748.

Goulding, E.H., Ngai, J., Kramer, R.H., Colicos, S., Axel, R., Siegelbaum, S.A. and Chess, A. 1992. Molecular cloning and single-channel properties of the cyclic nucleotide-gated channel from catfish olfactory neurons. Neuron 8: 45-58.

Granzow, B. and Kater, S.B. 1977. Identified higher-order neurons controlling the feeding motor program of *Helisoma*. Neuroscience 2: 1049-1063.

Granzow, B. and Rowell, C.H.F. 1981. Further observations on the serotonergic cerebral neurones of *Helisoma* (Mollusc, Gastropoda): The case for homology with the metacerebral giant cells. Journal of Experimental Biology 90: 283-305.

Green, D.J. and Gillette, R. 1988. Regulation of cAMP-stimulated ion current by intracellular pH, Ca^{2+}, and calmodulin blockers. Journal of Neurophysiology 59: 248-258.

Hadley, R.D. and Kater, S.B. 1983. Competence to form electrical connections is restricted to growing neurites in the snail, *Helisoma*. Journal of Neuroscience 3: 924-932.

Hamill, O.P., Marty, A., Neher, E., Sakmann, B. and Sigworth, F.J. 1981. Improved patch-clamp techniques for high-resolution current recording from cells and cell-free membrane patches. Pflugers Archive 391: 85-100.

Hansen, G.H., Meier, E., Abraham, J. and Schousboe, A. 1987. Trophic effects of GABA on cerebellar granule cells in culture. in Neurotrophic Activity of GABA During Development. Redburn, D.A.

and Schousboe, A. eds., Alan R. Liss, Inc., New York, New York: pp109-138.

Haydon, P.G. and Man-Son-Hing, H. 1988. Low- and high- voltage-activated calcium currents: Their relationship to the site of neurotransmitter release in an identified neuron of *Helisoma*. Neuron 1: 919-927.

Haydon, P.G. and Zoran, M.J. 1989. Formation and modulation of chemical connections: evoked acetylcholine release from growth cones and neurites of specific identified neurons. Neuron 2: 1483-1490.

Haydon, P.G., McCobb, D.P. and Kater, S.B. 1984. Serotonin selectively inhibits growth cone motility and synaptogenesis of specific identified neurons. Science 226: 561-564.

Haydon, P.G., Cohan, C.S., McCobb, D.P., Miller, H.R. and Kater, S.B. 1985. Neuron-specific growth cone properties as seen in identified neurons of *Helisoma*. Journal of Neuroscience Research 13: 135-147.

Haydon, P.G., McCobb, D.P. and Kater, S.B. 1987. The regulation of neurite outgrowth, growth cone motility, and electrical synaptogenesis by serotonin. Journal of Neurobiology 18: 197-215.

Haynes, L.W., Kay, A.R. and Yau, K.-W. 1986. Single cyclic GMP-activated channel activity in excised patches of rod outer segment membrane. Nature 321: 66-70.

Hille, B. 1992. Ionic Channels of Excitable Membranes. Sinauer Associates Inc., Sunderland, Mass., pp607.

Horn, R. and Marty, A. 1988. Muscarinic activation of ionic currents measured by a new whole-cell recording method. Journal of General Physiology 92: 145-159.

Hsu, Y.-T. and Molday, R.S. 1993. Modulation of the cGMP-gated channel of rod photoreceptor cells by calmodulin. Nature 361: 76-79.

Humphrey, P.P.A., Hartig, P. and Hoyer, D. 1993. A proposed new nomenclature for 5-HT receptors. Trends in Pharmacological Sciences 14: 233-236.

Ismaiel, A.M., Titeler, M., Miller, K.J., Smith, T.S. and Glennon, R.A. 1990. 5-HT_1 and 5-HT_2 binding profiles of the serotonergic agents α-methylserotonin and 2-methylserotonin. Journal of Medicinal Chemistry 33: 755-758.

Jan, L.Y. and Jan, Y.N. 1992. Tracing the roots of ion channels. Cell 69: 715-718.

Kaang, B.-K., Kandel, E.R. and Grant, S.G.N. 1993. Activation of cAMP-responsive genes by stimuli that produce long-term facilitation in *Aplysia* sensory neurons. Neuron 10: 427-435.

Kandel, E.R., Klein, M., Bailey, C.H., Hawkins, R.D., Castellucci, V.F., Lubit, B.W., and Schwartz, J.H. 1981. Serotonin, cyclic AMP, and the modulation of calcium current during behavioral arousal. in Serotonin Neurotransmission and Behavior. B.L. Jacobs and A.Gelperin eds., MIT Press Cambridge, Mass.: pp 211-254.

Kandel, E.R. and Schwartz, J.H. 1982. Molecular biology of learning: Modulation of transmitter release. Science 218: 433-443.

Kater, S.B. 1974. Feeding in *Helisoma trivolvis*: The morphological and physiological bases of a fixed action pattern. American Zoologist 14: 1017-1036.

Kater, S.B. and Rowell, C.H.F. 1973. Integration of sensory and centrally programmed components in generation of cyclical feeding activity of *Helisoma trivolvis*. Journal of Neurophysiology 36: 142-155.

Kaupp, U.B. 1991. The cyclic nucleotide-gated channels of vertebrate photoreceptors and olfactory epithelium. Trends in Neuroscience 14: 150-157.

Kaupp, U.B., Niidome, T., Tanabe, T., Terada, S., Bonigk, W., Stuhmer, W., Cook, N.J., Kangawa, K., Matsuo, H., Hirose, T., Miyata, T. and Numa, S. 1989. Primary structure and functional expression from complementary DNA of the rod photoreceptor cyclic GMP-gated channel. Nature 342: 762-766.

Katz, B. and Miledi, R. 1967. A study of synaptic transmission in the absence of nerve impulses. Journal of Physiology 192: 407-436.

Kehoe, J. 1990. Cyclic AMP-induced slow inward current in depolarized neurons of *Aplysia californica*. Journal of Neuroscience 10: 3194-3207.

Kirk, M.D., Taussig, R. and Scheller, R.H. 1988. Egg-laying hormone, serotonin and cyclic nucleotide modulation of ionic currents in the identified motoneuron B16 of *Aplysia*. Journal of Neuroscience 8: 1181-1193.

Klein, M., Camardo, J. and Kandel, E.R. 1982. Serotonin modulates a specific potassium current in the sensory neurons that show presynaptic facilitation in *Aplysia*. Proceedings of the National Academy of Science USA 79: 5713-5717.

Kramer, R.H. and Siegelbaum, S.A. 1992. Intracellular Ca^{2+} regulates the sensitivity of cyclic neucleotide-gated channels in olfactory receptor neurons. Neuron 9: 897-906.

Kupfermann, I. and Weiss, K.R. 1981. The role of serotonin in arousal of feeding behavior of *Aplysia*. in Serotonin Neurotransmission and Behavior. B.L. Jacobs and A.Gelperin eds., MIT Press Cambridge, Mass.: pp 255-287.

Lankford, K., De Mello, F.G. and Klein, W.L. 1987. A transient embryonic dopamine receptor inhibits growth cone motility and neurite outgrowth in a subset of avian retina neurons. Neuroscience Letters 75: 169-174.

Lauder, J.M. 1993. Neurotransmitters as growth regulatory signals: role of receptors and second messengers. Trends in Neuroscience 16: 233-240.

Lauder, J.M., Wallace, J.A., Krebs, H., Petrusz, P. and McCarthy, K. 1982. *In vivo* and *in vitro* development of serotonergic neurons. Brain Research Bulletin 9: 605-625.

Levitan, E.S. and Levitan, I.B. 1988. Serotonin acting via cyclic AMP enhances both the hyperpolarizing and depolarizing phases of bursting pacemaker activity in the *Aplysia* neuron R15. Journal of Neuroscience 8: 1152-1161.

Llinas, R. and Nicholson, C. 1975. Calcium role in depolarization-secretion coupling: An aequorin study in squid giant synapse. Proceedings of the National Academy of Science USA 72: 187-190.

Llinas, R., Steinberg, I.Z. and Walton, K. 1976. Presynaptic calcium currents and their relationship to synaptic transmission: Voltage

clamp study in squid giant synapse and theoretical model for the calcium gate. Proceedings of the National Academy of Science USA 73: 2918-2922.

Lotshaw, D.P., Levitan, E.S. and Levitan, I.B. 1986. Fine tuning of neuronal electrical activity: modulation of several ion channels by intracellular messengers in a single identified nerve cell. Journal of Experimental Biology 124: 307-322.

Lovenberg, T.W., Baron, B.M., de Lecea, L., Miller, J.D., Prosser, R.A., Rea, M.A., Foye, P.E., Racke, M., Slone, A.L., Siegel, B.W., Danielson, P.E., Sutcliffe, J.G. and Erlander, M.G. 1993. A novel adenylyl cyclase-activating serotonin receptor (5-HT7) implicated in the regulation of mammalian circadian rhythms. Neuron 11: 449-458.

Lowe, D.A., Matthews, E.K. and Richardson, B.P. 1981. The calcium antagonistic effects of cyproheptadine on contraction, membrane electrical events and calcium influx in the guinea-pig taenia coli. British Journal of Pharmacology 74: 651-663.

MacKinnon, R. 1991. New insights into the structure and function of potassium channels. Current Opinion in Neurobiology 1: 14-19.

Maricq, A.V., Peterson, A.S., Brake, A.J., Myers, R.M. and Julius, D. 1991. Primary structure and functional expression of the 5-HT3 receptor, a serotonin-gated ion channel. Science 254: 432-437.

Matt: on, M.P. and Hauser, K.F. 1991. Spatial and temporal integration of neurotransmitter signals in the development of neural circuitry. Neurochemistry International 19: 17-24.

Mattson, M.P. and Kater, S.B. 1987. Calcium regulation of neurite elongation and growth cone motility. Journal of Neuroscience 7: 4034-4043.

Mattson, M.P., Dou, P. and Kater, S.B. 1988A. Outgrowth-regulating actions of glutamate in isolated hippocampal pyramidal neurons. Journal of Neuroscience 8: 2087-2100.

Mattson, M.P., Guthrie, P.B. and Kater, S.B. 1988B. Intracellular messengers in the generation and degeneration of hippocampal neuroarchitecture. Journal of Neuroscience Research 21: 447-464.

Mattson, M.P., Lee, R.E., Adams, M.E., Guthrie, P.B. and Kater, S.B. 1988C. Interactions between Entorhinal axons and target hippocampal neurons: a role for glutamate in the development of hippocampal circuitry. Neuron 1: 865-876.

Mattson, M.P., Taylor-Hunter, A. and Kater, S.B. 1988D. Neurite outgrowth in individual neurons of a neuronal population is differentially regulated by calcium and cyclic AMP. Journal of Neuroscience 8: 1704-1711.

Mattson, M.P., Murrain, M., Guthrie, P.B. and Kater, S.B. 1989. Fibroblast growth factor and glutamate: opposing roles in the generation and degeneration of hippocampal neuroarchitecture. Journal of Neuroscience 9: 3728-3740.

McCobb, D.P. and Kater, S.B. 1988. Membrane voltage and neurotransmitter regulation of neuronal growth cone motility. Developmental Biology 130: 599-609.

McCobb, D.P., Cohan, C.S., Connor, J.A. and Kater, S.B. 1988. Interactive effects of serotonin and acetylcholine in neurite elongation. Neuron 1: 377-385.

McCrohan, C.R. and Gillette, R. 1988. Cyclic AMP-stimulated sodium current in identified feeding neurons of *Lymnaea stagnalis*. Brain Research 438: 115-123.

McKenny, K. and Goldberg, J.I. 1989. Embryonic development of the pulmonate snail *Helisoma trivolvis*. Society of Neuroscience Abstract 15: 404.8.

Mercer, A.R., Emptage, N.J. and Carew, T.J. 1991. Pharmacological dissociation of modulatory effects of serotonin in *Aplysia* sensory neurons. Science 254: 1811-1813.

Michler-Stuke, A. and Wolff, J.R. 1989. Facilitation and inhibition of neurite elongation by GABA in chick tectal neurons. in Neurotrophic Activity of GABA During Development. Redburn, D.A. and Schousboe, A. eds., Alan R. Liss, Inc., New York, New York: 253-266.

Monerini, E., Gaetani, P., Rodriguez y Baena, R., Giraldo, E., Parenti, M., Zocchetti, A. and Rizzi, C.A. 1993. Pharmacological characterization of the 5-hydroxytryptamine receptor coupled to adenylyl cyclase stimulation in human brain. Life Sciences 52: 61-65.

Montminy, M.R., Gonzalez, G.A. and Yamamoto, K.K. 1990. Regulation of cAMP-inducible genes by CREB. Trends in Neuroscience 13: 184-188.

Murphy, A.D. 1991. The *Helisoma* cyberchron network revisited: what is its role in feeding. in Molluscan Neurobiology. Kitts, K.S., Boer, H.H. and Joosse, J. eds. North Holland Publishing Company, Amsterdam. pp. 25-29.

Murphy, A.D., Lukowiak, K. and Stell, W.K. 1985. Peptidergic modulation of patterned motor activity in identified neurons of *Helisoma*. Proceedings of the National Academy of Sciences USA 82: 7140-7144.

Murrain, M., Murphy, A.D., Mills, L.R. and Kater, S.B. 1990. Neuron-specific modulation by serotonin of regenerative outgrowth and intracellular calcium within the CNS of *Helisoma trivolvis*. Journal of Neurobiology 21: 611-618.

Oksenberg, D., Marsters, S.A., O'Dowd, B.F., Jin, H., Havlik, S., Peroutka, S.J. and Ashkenazi, A. 1992. A single amino-acid difference confers major pharmacological variation between human and rodent 5-HT_{1B} receptors. Nature 360: 161-163.

Papazian, D.M., Timpe, L.C., Jan, Y.N. and Jan, L.Y. 1991. Alteration of voltage-dependence of *Shaker* potassium channel by mutations in the S4 sequence. Nature 349: 305-310.

Paupardin-Tritsch, D. and Gerschenfeld, H.M. 1973. Transmitter role of serotonin in identified synapses in *Aplysia* nervous system. Brain Research 58: 529-534.

Paupardin-Tritsch, D., Hammond, C. and Gerschenfeld, H.M. 1986. Serotonin and cyclic GMP both induce an increase of the calcium current in the same identified molluscan neurons. Journal of Neuroscience 6: 2715-2723.

Polak, K.A., Edelman, A.M., Wasley, J.W.F. and Cohan, C.S. 1991. A novel calmodulin antagonist, CGS 9343B, modulates calcium-dependent changes in neurite outgrowth and growth cone movements. Journal of Neuroscience 11: 534-542.

Price, C.J. and Goldberg, J.I. 1993. Serotonin activation of a cyclic AMP-dependent sodium current in an identified neuron from *Helisoma trivolvis*. Journal of Neuroscience 13: 4979-4987.

Pugh Jr., E.N. and Cobbs, W.H. Visual transduction in vertebrate rods and cones: a tale of two transmitters, calcium and cyclic GMP. Vision Research 26: 1613-1643.

Rae, J., Cooper, K., Gates, P. and Watsky, M. 1991. Low access resistance perforated patch recordings using amphotericin B. Journal of Neuroscience Methods 37: 15-26.

Rashid, N.A. and Cambray-Deakin, M.A. 1992. N-methyl-D-aspartate effects on the growth, morphology and cytoskeleton of individual neurons in vitro. Developmental Brain Research 67: 301-308.

Ronnett, G.V. and Snyder, S.H. 1992. Molecular messengers of olfaction. Trends in Neuroscience 15: 508-513.

Saudou, F., Boschert, U., Amlaiky, N., Plassat, J.-L. and Hen, R. 1992. A family of *Drosophila* serotonin receptors with distinct intracellular signalling properties and expression patterns. The EMBO Journal 11: 7-17.

Shemer, A.V., Azmitia, E.C. and Whitaker-Azmitia, P.M. 1991. Dose-related effects of prenatal 5-methoxytryptamine (5-MT) on development of serotonin terminal density and behavior. Developmental Brain Research 59: 59-63.

Siegelbaum, S.A., Camardo, J.S. and Kandel E.R. 1982. Serotonin and cyclic AMP close single K^+ channels in *Aplysia* sensory neurones. Nature 299: 413-417.

Sikich, L., Hickok, J.M. and Todd, R.D. 1990. 5-HT_{1A} receptors control neurite branching during development. Developmental Brain Research 56: 269-274.

Stuhmer, W., Conti, F., Suzuki, H., Wang, X., Noda, M., Yahagi, N., Kubo, H. and Numa, S. 1989. Structural parts involved in activation and inactivation of the sodium channel. Nature 339: 597-603.

Sugamori, K.S., Sunahara, R.K., Guan, H.-C., Bulloch, A.G.M., Tensen, C.P., Seeman, P., Niznik, H.B. and Van Tol, H.H.M. 1993. Serotonin receptor cDNA cloned from *Lymnaea stagnalis*. Proceedings of the National Academy of Science USA 90: 11-15.

Tauc, L. 1962a. Site of origin and propagation of spike in the giant neuron of *Aplysia*. Journal of General Physiology 45: 1077-1097.

Tauc, L. 1962b. Identification of active membrane areas in the giant neuron of *Aplysia*. Journal of General Physiology 45: 1099-1115.

Taussig, R., Sweet-Cordero, A. and Scheller, R.H. 1989. Modulation of ionic currents in *Aplysia* motor neuron B15 by serotonin, neuropeptides, and second messengers. Journal of Neuroscience 9: 3218-3229.

Weiss, K.R., Cohen, J.L. and Kupfermann, I. 1978. Modulatory control of buccal musculature by serotonergic neuron (Metacerebral cell) in *Aplysia*. Journal of Neurophysiology 41: 181-203.

Whitaker-Azmitia, P.M. 1991. Role of serotonin and other neurotransmitter receptors in brain development: basis for developmental pharmacology. Pharmacological Reviews 43: 553-561.

Wilson, W.A. and Wachtel, H. 1974: Negative resistance characteristic essential for the maintainance of slow oscillations in bursting neurons. Science 186: 932-934.

Witz, P., Amlaiky, N., Plassat, J.-L., Maroteaux, L., Borrelli, E. and Hen, R. 1990. Cloning and characterization of a *Drosophila* serotonin receptor that activates adenylate cyclase. Proceedings of the National Academy of Science USA 87: 8940-8944.

Wong, R.G., Barker, D.L., Kater, S.B. and Bodnar, D.A. 1984. Nerve growth-promoting factor produced in culture media conditioned by specific CNS tissues of the snail *Helisoma*. Brain Research 292: 81-91.

Zifa, E. and Fillion, G. 1992. 5-Hydroxytryptamine receptors. Pharmacological Reviews 44: 401-458.

Zimmerman, A.L. and Baylor, D.A. 1986. Cyclic GMP-sensitive conductance of retinal rods consists of aqueous pores. Nature 321: 70-72.

Zimmerman, A.L. and Baylor, D.A. 1992. Cation interactions within the cyclic GMP-activated channel of retinal rods from the tiger salamander. Journal of Physiology 449: 759-783.

Zufall, F., Firestein, S. and Shepherd, G.M. 1991. Analysis of single cyclic nucleotide-gated channels in olfactory receptor cells. Journal of Neuroscience 11: 3573-3580.